ABSTRACT

WIESELQUIST, WILLIAM A. The New Nuclear Data Sensitivity Analysis and Uncertainty Propagation Tool in NESTLE. (Under the direction of Assistant Professor D.Y. Anistratov). In support of the need for better design and evaluation tools for reactor-based transmutation systems we have upgraded NESTLE, the 2/4 energy group thermal reactor physics code of the Nuclear Engineering Department at North Carolina State University with: i) the ability to perform nuclide transmutation calculations for a general, user-defined field of nuclei and transmutation paths and ii) the ability to analyze sensitivities and propagate uncertainties in the end-of-cycle (EOC) nuclide inventory with respect to nuclear data and beginning-of-cycle (BOC) nuclide inventory. We present two methods of sensitivity analysis: i) direct perturbation and recalculation (DPAR) and ii) sensitivity analysis utilizing an adjoint system (AS). With DPAR, we simply perturb data and recalculate solutions of our system and thus may analyze sensitivity of all responses to perturbations in one data parameter per solution of the perturbed forward problem. With the AS, we form a system of equations, the solution of which may be used to estimate the first variation of a response with respect to any data parameters. For the AS, we have developed the equations for both the predictor and predictor-corrector neutron/nuclide field coupling methods in NESTLE. To our knowledge, the AS for the predictor-corrector coupling has never been presented.

Then we used the tools we have developed to evaluate the sensitivity of EOC nuclide concentrations and SNF hazard measures with respect to nuclear data for a cycle 1 pressurized water reactor (PWR) core. In our study, we found that the nuclear data crucial to modelling US reactors' once-through cycle (fission cross sections of ^{235}U and ^{239}Pu, the main fuel nuclei, and capture cross sections for ^{238}U) also has the highest impact on EOC nuclide inventory of so-called "problem nuclei" (e.g. Am, Cm, etc.) Note that these results only apply to cycle 1, in which fresh fuel is irradiated for the first time. Because most fuel assemblies are present in the core for three cycles, two more cycles should be considered to analyze sensitivity of spent nuclear fuel (SNF)—the fuel for transmutation systems—with respect to nuclear data. Although, NESTLE has the capability to perform sensitivity analysis over multiple cycles, NESTLE does not have the capability to determine loading patterns and the benchmark case we used [1] did not include cycle 2 or cycle 3 data.

The New Nuclear Data Sensitivity Analysis and Uncertainty Propagation Tool in NESTLE

by

William A. Wieselquist

A thesis submitted to the Graduate Faculty of
North Carolina State University
in partial satisfaction of the
requirements for the Degree of
Masters of Science

Department of Nuclear Engineering

Raleigh

2004

Approved By:

Dr. Mansoor Haider	
Dr. D.Y. Anistratov Chair of Advisory Committee	Dr. Paul J. Turinsky

This project is dedicated to my favorite person, Liz—in addition to my mother, K.D.; father, Roy; and siblings, Andrew and Grace.

Biography

William Wieselquist was born in Washington D.C. on October 18, 1979. His family moved to North Carolina when William was 5, currently residing in Winston-Salem. In 1998, William graduated second in his class at Parkland High School and then moved to Raleigh to attend North Carolina State University. In 2002, he graduated *summa cum laude* with a B.S. in Nuclear Engineering from North Carolina State University. He received a fellowship from the Advanced Fuel Cycle Initiative (AFCI) University Program for graduate work on sensitivity analysis for reactor-based transmutation systems, completed in 2004. Academics aside, in the summer of 2001, William worked at Idaho National Engineering and Environmental Laboratory benchmarking Computational Fluid Dynamics software for planned coupling to reactor safety code RELAP5-3D and in the summer of 2002, he worked at Brookhaven National Lab testing loading patterns for Thorium cycles. In 2005, William will begin his Ph.D. work on transport methods for unstructured grids.

Acknowledgements

I would like to thank Dr. Dmitriy Y. Anistratov and Dr. Paul J. Turinsky for their numerous helpful and insightful comments, as well as the Advanced Fuel Cycle Initiative of the US Department of Energy for the main funding of this project, Dr. Michael Todosow of Brookhaven National Lab for additional funding, and the University Research Alliance of Amarillo, Texas for their excellent administration of funds.

Contents

List of Figures

List of Tables

Chapter 1

Introduction

Recently, mostly due to the Advanced Fuel Cycle Initiative (AFCI) program sponsored by the Department of Energy (DOE), researchers have begun investigating various systems for their potential to reduce the inventory of various "problem nuclei" in spent nuclear fuel (SNF) by *transmuting* them into less problematic nuclei. The so-called "problem nuclei" are those which make SNF difficult to transport, store, or those nuclei in storage which pose a hazard to the environment and humans in the vicinity of the repository. Reducing the inventory of problem nuclei in SNF reduces the size, cost, and complexity of containment—thus we can fit more SNF in our first repository at Yucca Mountain, Nevada, *and* possibly avoid the need for a second repository, at least a second repository of the incredible size and exhaustive design considerations of Yucca Mountain, which was designed to handle SNF in its current, unprocessed, un-transmuted state. No doubt, processing is extremely important in reducing the size of the repository, for example, if all ^{238}U was separated the rest of the nuclei, SNF volume would be reduced by greater than 95%! But to reduce the design considerations required for the repository, the inventory of some nuclei in SNF must be reduced (transmuted). Researchers have proposed two types of transmutation systems to reduce problem nuclei in SNF: i) accelerators and ii) reactors.

1.1 Accelerator-based Transmutation

Initially, accelerators were favored for the lack of coupling between the SNF and the source of neutrons. However, after some preliminary research, accelerators seemed prohibitively expensive, at least to employ en masse on our current stores of SNF.

1.2 Reactor-based Transmutation

Currently, researchers are looking more toward reactors as SNF transmutation systems. From one perspective, reactor-based transmutation is trickier than accelerator-based transmutation because if the SNF could still be used as fuel, it would still be in the reactor! Therefore, some separations and reprocessing of SNF appears essential for efficient, commercially-viable reactor-based transmutation with our current fleet of reactors. But the wide variation in optimal destruction environments for different problem nuclei appears to require a number of different reactor systems to process different stages of SNF, with accelerators used sparingly to "deep-burn" small volumes of SNF. But right now things are much less complicated because we can assume that the initial fuel for any multi-reactor transmutation system will be the fuel discharged from a Pressurized Water Reactor (PWR) or Boiling Water Reactor (BWR), currently sitting in spent fuel storage pools at reactor sites around the country awaiting Yucca Mountain's completion. And for these systems, nuclei which play a major role in the system (e.g. ^{235}U, ^{238}U,^{239}Pu, etc.) have very accurate nuclear data—but to design and/or evaluate these reactors as transmutation systems, additional (and possibly poorly measured) nuclear data may be important. For example, some of the nuclear data for minor actinides Am and Cm have been estimated only crudely, with uncertainties of 50% in some cases, and in most SNF, these nuclei are considered problem nuclei because of their long half-lives and the high heat load some of the isotopes put on their storage casks. But if the amount of these nuclei present in the SNF is dependent on some nuclear data with high uncertainty, then the amount of the problem nuclei may also be highly uncertain, which poses a difficulty to the design and evaluation of reactor-based transmutation systems.

Our research supports the need for better design and evaluation tools for reactor-based transmutation systems by adding new tools to NESTLE, a reactor simulator code developed by the Electric Power Research Center (EPRC) in the Department of Nuclear

Engineering at North Carolina State University [2].

1.2.1 Generalized Nuclide Field Solver

The first tool is a *generalized nuclide field solver*, used to solve the nuclide field equations which describe change in concentrations of nuclei over time for a user-defined field of nuclei and transmutation paths that describe how nuclei change into other nuclei. The two solvers implemented in NESTLE as a result of this research are

1. a 2^{nd} order Rosenbrock method with complex coefficients [3, 4] and
2. a matrix exponential method (like that used by ORIGEN) [5].

Mathematically, the nuclide field equations form a *stiff system of first order ODEs*. Earlier versions of NESTLE tracked concentrations of 12 nuclei with about 30 transmutation paths [2]. These nuclei and transmutation paths were "hard-coded", but it is well-known that only these nuclei are needed to accurately model a thermal reactor (PWR or BWR) system with a once-through cycle. The solver for the hard-coded nuclei (heavy metals ^{234}U, ^{235}U, ^{236}U, ^{238}U, ^{239}Pu, ^{240}Pu, ^{241}Pu, ^{242}Pu, and ^{241}Am and fission products Sm and Xe) was an analytic linear chain solver [2], which can only be used on linear chains of nuclei—those in which nuclide A transmutes into nuclide B, nuclide B transmutes into nuclide C, C into D, and so on...

1.2.2 Sensitivity Analysis Methods

The second tool is two *sensitivity analysis methods* to help users analyze the sensitivity of the various aspects of the system (responses) with respect to nuclear data and initial conditions. The two sensitivity analysis methods are

1. direct perturbation and recalculation (DPAR) and
2. first-order perturbation theory for the forward system of reactor cycle equations using a "physical" adjoint system (AS) [6].

The term "physical" adjoint refers to the adjoint equations realized when perturbation theory is applied to the *differential form of the forward equations*. Alternatively, the term "mathematical" adjoint refers to the adjoint equations realized when perturbation theory

is applied to a *completely discretized forward system.* One of the nice characteristics of the "physical" adjoint is that usually the methods used to solve the forward system (with inclusion of a special source term) may be used to solve the adjoint system. Under certain circumstances the mathematical and physical adjoint produce identical adjoint functions—but this is the exception, not the rule.

1.2.3 Sensitivity Analysis of Cycle 1 PWR

Finally, we apply our tool to analyze sensitivity in the EOC nuclide inventory and two SNF hazard measures—Hazard Index (HI) and Total Cancer Dose (TCD)—of a cycle 1 PWR core with attributes and loading pattern given by CASE 10 of an Argonne National Lab (ANL) benchmark source book [1].

Chapter 2

Notation

From the preface of Richard Bellman's *Introduction to Matrix Analysis* [7]:

> It follows that at the very beginning a determined effort must be made to devise a useful, sensitive, and perceptive notation. Although it would certainly be rash to attempt to assign a numerical value to the dependence of successful research upon well-conceived notation, it is not difficult to cite numerous examples where the solutions become apparent when the questions are appropriately formulated. Conversely, a major effort and great ingenuity would be required were a clumsy and unrevealing notation employed. Think, for instance, of how it would be to do arithmetic or algebra in terms of Roman numerals. A well-designed notation attempts to express the essence of the underlying mathematics without obscuring or distracting.

When dealing with operators, functions, and functionals in both continuous and discrete space, adopting a good notation is especially important. Therefore we adopt the following rules concerning notation, some of which are standard, some of which are not.

2.1 Original Space

Our original (continuous) space has 6 independent variables: energy E, space $\hat{r}$, time t, and nuclide index k.

E energy (MeV)

$\hat{r}$	space (cm)
t	time (s)
k	nuclide index $k = 1, ..., N_k$

2.1.1 Function

1. A function is symbolized using any letter from the Greek alphabet or a lowercase letter from the English alphabet. Examples: η, ϕ, Φ, σ, f, g.

2. Use subscripts for extra descriptiveness. Examples: Σ_s, σ_f, f_1.

3. Use superscripts for even more descriptiveness. Examples: η^*, $\varphi^\dagger$, f_1^*.

4. Indicate the function's dependence on independent variables using parentheses `( )` to enclose the comma-separated list of independent variable symbols. Examples: $\eta = \eta\left(\hat{r}, t\right)$, $\Phi = \Phi\left(t\right)$, $\Sigma_s = \Sigma_s\left(\hat{r}, E, t\right)$, $f = f\left(\hat{r}, E, t\right)$.

5. Suppress unneeded independent variables to increase readability.

2.1.2 Integration

1. Indicate integration of a function over some or all independent variables by enclosing that function in brackets `[ ]` with limits of integration subscripting the brackets. Examples:

$$\Big[\circ \Big]_{V,\epsilon,\tau} \stackrel{\text{def}}{=} \int_{t_0}^{t_N} dt \int_{E_N}^{E_0} dE \int_V \circ \, d^3r$$

and

$$\Big[\circ \Big]_{V_i,\epsilon_g,\tau_j} \stackrel{\text{def}}{=} \int_{t_{j-1}}^{t_j} dt \int_{E_g}^{E_{g-1}} dE \int_{V_i} \circ \, d^3r \,,$$

where we introduce

   (a) V_i to reference the volume of node i, $V_i = \delta x_i \delta y_i \delta z_i$,

   (b) ϵ_g to reference the energy bounds of group g, $\epsilon_g = E_{g-1} - E_g$,

   (c) τ_j to reference the time across the j^{th} time step, $\tau_j = t_j - t_{j-1}$, and

   (d) V, ϵ, and τ to indicate integration over the entire domain.

2. To aid readability, include a small space between functions. Example:

$$\left[\nu\Sigma_f \ \phi \right]_{V_i,\epsilon_g} = \int_{E_g}^{E_{g-1}} dE \int_{V_i} d^3r \ \nu\Sigma_f(\hat{r},E,t) \ \phi(\hat{r},E,t).$$

2.1.3 Functional

1. A functional is symbolized like a function with a Greek or lowercase English letter with optional sub- and super- scripts. Examples: $\Sigma_{2\to1}$, r_ℓ.

2. Indicate the functional's dependence on other functions using brackets `[ ]` (as opposed to parentheses `( )` with functions) to enclose the list of function symbols. Examples: $r_\ell = r_\ell[\vec{\delta}_\ell, \vec{\eta}]$; $\Sigma_f(\hat{r},E,t) = \Sigma[\vec{\sigma}_f, \vec{\eta}]$; $\Sigma_s(\hat{r},E,t) = \Sigma_{2\to1}[\Sigma_s(E' \to E), \phi(E')]$.

3. The functional's symbol defines the limits of integration/summation. Examples: $r_\ell[\vec{\delta}_\ell, \vec{\eta}] \stackrel{\text{def}}{=} \left[\vec{\delta}_\ell \ \vec{\eta} \right]_{\tau,k}$; $\Sigma[\vec{\sigma}_f, \vec{\eta}] \stackrel{\text{def}}{=} \left[\vec{\sigma}_f \ \vec{\eta} \right]_k$; $\Sigma_{2\to1}[\Sigma_s(E' \to E), \phi(E')] \stackrel{\text{def}}{=} \left[\Sigma_s(E' \to E) \ \phi(E') \right]_{\epsilon'}$.

2.1.4 Operator

1. An operator is symbolized with an uppercase English letter. Examples: L, F, B, M.

2. Indicate the operator's dependence on functions, functionals, or other operators using parentheses `( )` to enclose the semicolon-separated list of symbols. Examples: $L = L(\Sigma_s, \Sigma_a, d_c)$; $F = F(\nu\Sigma_f, \chi_p, \beta_{tot})$; $B = B(k_e, L, F)$; $M = M(\sigma_a, \sigma_f, \sigma)$.

3. Suppress dependencies to increase readability.

4. The only exception is the uppercase English letter N. It is never used as an operator but used exclusively with a subscript to define a number of something.

   (a) N_g is the number of energy groups

   (b) N_k is the number of nuclei

   (c) N_i is the number of nodes/subregions

   (d) N_j is the number of time steps

2.2 Discrete Space

In our discrete space we only have 4 dimensions, as the 3 dimensional spatial location, $\hat{r}$, has been collapsed into 1 index, i. We will use the following indices in the discretized system.

g	energy group index , $g = 1, ..., N_g$
i	subregion/node index, $i = 1, ..., N_i$
j	time node index , $j = 0, ..., N_j$
k	nuclide index , $k = 1, ..., N_k$

2.2.1 Vector

1. A vector uses the super-symbol $\vec{}$ with a function symbol (Greek or lowercase English letter). Examples: $\vec{\eta}$, $\vec{\Phi}$, $\vec{\sigma}_f$, $\vec{f}$, $\vec{g}$.

2. Indicate the vector's dependence on the four indices with parentheses (see Subvector/Submatrix below for additional use of this notation for indicating subvectors and submatrices.) Examples: $\vec{f} = {}^{(g)}\{ \vec{f} \}_{(i)}^{(j)}$ for a discrete version of function, $f = f(\hat{r}, E, t)$; and a vector of functions, such as the nuclide concentration vector, $\vec{\eta}$, using both notations, $\vec{\eta} = {}_{(k)}\{ \vec{\eta}(\hat{r}, t) \}$.

3. As alluded to above, a vector of functions is allowed. Examples: $\vec{\eta}(t)$, $\vec{\sigma}_f(\hat{r}, E, t)$.

4. δ_{mn} is the Kronecker delta.

$$\delta_{mn} = \begin{cases} 1 & m = n \\ 0 & m \neq n \end{cases} \tag{2.1}$$

5. $\vec{\delta}_n$ is a vector of Kronecker deltas.

$$\{ \delta_n \}_m = \begin{cases} 1 & m = n \\ 0 & m \neq n \end{cases} \tag{2.2}$$

2.2.2 Matrix

1. A matrix is a special kind of operator for linear systems and uses boldface type and the super-symbol $\widetilde{\ }$ with an operator symbol (uppercase English letter). Examples: $\widetilde{\mathbf{L}} = \widetilde{\mathbf{L}}(\vec{\Sigma}_s\,, \vec{\Sigma}_a\,, \vec{d}_c)$; $\widetilde{\mathbf{F}} = \widetilde{\mathbf{F}}(\nu\vec{\Sigma}_f\,, \vec{\chi}_p\ , \vec{\beta}_{tot})$; $\widetilde{\mathbf{B}} = \widetilde{\mathbf{B}}(\vec{k}_e\,, \widetilde{\mathbf{L}}\,, \widetilde{\mathbf{F}})$; $\widetilde{\mathbf{M}} = \widetilde{\mathbf{M}}(\vec{\sigma}_a\,, \vec{\sigma}_f\,, \vec{\sigma})$.

2. As alluded to above, a matrix of functions and operators is allowed, however the mapping of dependencies to entries in the matrix should be clear.

3. The identity matrix is noted without super-symbol as $\mathbf{E}$.

4. The super-symbol $\widetilde{\ }$ is non-standard for matrix notation but we give the following justifications.

   (a) It is good to have notation that may be easily produced by hand. Simply using boldface type for matrices, $\mathbf{L}$, is common in literature but difficult to represent easily by hand.

   (b) In some texts, the double line super-symbol is used for matrices, $\overline{\overline{L}}$, and sometimes the single line super-symbol is used for vectors, $\overline{f}$. I like these notations because they seem consistent but the requirement of a double line for matrices seems like too many pen-strokes when there are so many different single super-symbols that could be used. Also, I think it would be a shame to not use the vector symbol, $\vec{f}$, for vectors as it is such a universally recognized notation.

   (c) In other texts, the double line sub-symbol is used for matrices, $\underline{\underline{L}}$, and the single line sub-symbol is used for vectors, $\underline{f}$. I don't like these for the same reasons as the super-symbols mentioned above—plus sub-symbols sometimes crowd text, especially when using single-spacing.

   (d) So we will use the $\widetilde{\ }$ to denote a matrix. It is a single super-symbol and is easy to write, read, and recognize.

   (e) One possible problem with using the $\widetilde{\ }$ to indicate a matrix is it used frequently to denote a perturbed operator so we will use a prime superscript instead: if $L/\widetilde{\mathbf{L}}$ is the unperturbed operator/matrix then $L'/\widetilde{\mathbf{L}}'$ is the perturbed operator/matrix.

2.2.3 Elements of a Vector/Matrix

When working with vector or matrix quantities, it is important to be able to refer to certain elements of that vector or matrix, thus we adopt the following element notation system. It may appear clumsy at first but it has numerous advantages.

1. Refer to a single element of a vector or matrix by enclosing the matrix or vector in braces `{ }` and citing each fixed index.

2. When referring to the most basic element of a vector or matrix, the super-symbols are dropped.

3. To enhance readability, each phase space index lives in one of the four corners around the braces.

$$\begin{array}{ll} \text{matrix} & {}^{gg'}_{kk'}\{\quad\}^{j}_{ii'} \\ \text{vector} & {}^{g}_{k}\{\quad\}^{j}_{i} \end{array}$$

4. All vectors are considered column vectors.

5. With all matrices, the first index is a row index and the second is a column index.

6. Examples:

   - If the vector $\vec{\eta}$ is the number of various nuclei, in all subregions/nodes in the core, at all times; then ${}_{k}\{\,\eta\,\}^{j}_{i}$ is the concentration of nuclide k, in subregion/node i, at time nodes t_j, $j = 0, ..., N_j$. Note that when referring to the most basic element of a vector, such as ${}_{k}\{\,\eta\,\}^{j}_{i}$, the vector super-symbol is dropped.
   - If the vector $\vec{\phi}$ is the scalar flux for all energy groups, in all subregions/nodes in the core at all times, then ${}^{g}\{\,\phi\,\}^{j}_{i}$ is the scalar flux for energy group g in subregion/node i at time nodes t_j, $j = 0, ..., N_j$.
   - If the matrix $\widetilde{\mathbf{M}}$ describes the average rate of transmutation of nuclei into other nuclei in all subregions/nodes in the core at over all time steps τ_j, $j = 1, ..., N_j$, then ${}_{kk'}\{\,\mathbf{M}\,\}^{j}_{ii'}$ is rate of transmutation of nuclide k' into nuclide k in subregion/node i over time step τ_j, $j = 1, ..., N_j$.

2.2.4 Summation

1. Indicate a summation of a vector quantity over some indices by enclosing that vector in brackets `[ ]` with summation indices subscripting the brackets.

2. A set of weights w may be implicitly applied to any summation in order to approximate the original integration over continuous space.

3. Example:

$$\left[\vec{\phi} \right]_{V_i,\epsilon_g} = w_g \, w_i \, {}^{g}\{ \phi \}_i \approx \left[\phi \right]_{V_i,\epsilon_g} = \int_{E_g}^{E_{g-1}} dE \int_{V_i} d^3r \, \phi(\hat{r}, E, t).$$

   Here, for an integration of the scalar flux, the weights $w_i = V_i$ and $w_g = 1$.

2.2.5 Matrix Transpose Definition

The transpose is indicated by a T superscript.

$$\overset{gg'}{kk'}\{ \mathbf{A} \}^{j}_{ii'} \overset{\text{def}}{=} \overset{g'g}{k'k}\{ \mathbf{A}^T \}^{j}_{i'i} \tag{2.3}$$

Matrix-Vector Products

The resultant vectors $\vec{c}$ and $\vec{d}$ of the matrix-vector products,

$$\vec{c} = \widetilde{\mathbf{A}} \vec{b}$$

$$\vec{d} = \widetilde{\mathbf{A}}^T \vec{b}$$

are defined below.

$$\vec{c} = \widetilde{\mathbf{A}} \vec{b} \tag{2.4a}$$

$$\overset{g}{k}\{ c \}^{j}_{i} \overset{\text{def}}{=} \left[\widetilde{\mathbf{A}} \vec{b} \right]_{g',i',k'} = \sum_{g'} \sum_{i'} \sum_{k'} \overset{gg'}{kk'}\{ \mathbf{A} \}^{j}_{ii'} \, \overset{g'}{k'}\{ b \}^{j}_{i'} \tag{2.4b}$$

$$\vec{c}^{\,T} = \vec{b}^{\,T} \widetilde{\mathbf{A}}^T \tag{2.4c}$$

$$\overset{g}{k}\{ c^{\,T} \}^{j}_{i} \overset{\text{def}}{=} \left[\vec{b}^{\,T} \widetilde{\mathbf{A}}^{\,T} \right]_{g,i,k} = \sum_{g} \sum_{i} \sum_{k} \overset{g}{k}\{ b^T \}^{j}_{i} \, \overset{gg'}{kk'}\{ \mathbf{A}^T \}^{j}_{ii'} \tag{2.4d}$$

$$\vec{d} = \widetilde{\mathbf{A}}^T \vec{b} \tag{2.4e}$$

$$\overset{g}{k}\{ d \}^{j}_{i} \overset{\text{def}}{=} \left[\widetilde{\mathbf{A}}^T \vec{b} \right]_{g',i',k'} = \sum_{g'} \sum_{i'} \sum_{k'} \overset{gg'}{kk'}\{ \mathbf{A}^T \}^{j}_{ii'} \, \overset{g'}{k'}\{ b \}^{j}_{i'} \tag{2.4f}$$

$$\vec{d}^{\,T} = \vec{b}^{\,T}\widetilde{\mathbf{A}} \tag{2.4g}$$

$$\overset{g}{k}\{\, d^{\,T}\,\}_i^j \overset{\text{def}}{=} \left[\, \vec{b}^{\,T}\widetilde{\mathbf{A}}\,\right]_{g,i,k} = \sum_g \sum_i \sum_k \overset{g}{k}\{\, b^T\,\}_i^j \; \overset{gg'}{kk'}\{\, \mathbf{A}\,\}_{ii'}^j \tag{2.4h}$$

2.2.6 Block Diagonal Matrices

The block diagonal matrix is indicated by repeated subscripts,

$$\delta_{ii'\,kk'}\{\, \mathbf{A}\,\}_{ii'}^j = {}_{kk'}\{\, \mathbf{A}\,\}_{ii}^j \,.$$

2.2.7 Subvector/Submatrix

In many cases, one would rather refer to a *subset* of the elements of a vector or matrix.

1. Refer to a subvector or submatrix by suppressing indices.
2. Alternately, the suppressed indices may be enclosed in parentheses `( )`, like we indicated dependencies of a vector.
3. Examples:
   - If the vector $\vec{\eta}$ is the concentration of all nuclei in all subregions/nodes in the core at all times, then $\{\,\vec{\eta}\,\}_i^j$ (or ${}_{(k)}\{\,\vec{\eta}\,\}_i^j$) is the vector of nuclide concentrations in subregion/node i at time t_j.
   - If the vector $\vec{\phi}$ is the scalar flux for all energy groups in all subregions/nodes in the core at all times, then $\{\,\vec{\phi}\,\}^j$ (or ${}^{(g)}\{\,\vec{\phi}\,\}_{(i)}^j$) is the scalar flux vector at time t_j.
   - If the matrix $\widetilde{\mathbf{M}}$ describes the rate of transmutation of nuclei into other nuclei in all subregions/nodes in the core over all time steps, then $\{\,\widetilde{\mathbf{M}}\,\}_{ii}^j$ (or ${}_{(kk')}\{\,\mathbf{M}\,\}_{ii}^j$) is the transmutation matrix in subregion/node i over time step τ_j.

2.3 Inner Products

The concept of an inner product is fundamental to the development of the Adjoint System (AS) sensitivity analysis method. With our notation, the inner product for functions

$f_1 = f_1(\hat{r}, E, t)$, $f_2 = f_2(\hat{r}, E, t)$ is defined by

$$\left\langle f_1 \, , \, f_2 \right\rangle = \left[f_1 \, f_2 \right]_{V,\epsilon,\tau} = \int_{t_0}^{t_N} dt \int_{E_N}^{E_0} dE \int_V d^3r \; f_1(\hat{r}, E, t) \; f_2(\hat{r}, E, t)$$

and the inner product for vectors $\vec{f}_1 = {}^{(g)}\{ \vec{f}_1 \}_{(i)}^{(j)}$, $\vec{f}_2 = {}^{(g)}\{ \vec{f}_2 \}_{(i)}^{(j)}$ is defined analogously by

$$\left\langle \vec{f}_1 \, , \, \vec{f}_2 \right\rangle = \left[\vec{f}_1 \, \vec{f}_2 \right]_{V,\epsilon,\tau} = \sum_j w_j \sum_g w_g \sum_i w_i \, {}^g\{ f_1 \}_i^j \;\; {}^g\{ f_2 \}_i^j \, .$$

Note that when we have a vector of functions, like the nuclide concentrations, $\vec{\eta}_1 = {}_{(k)}\{ \vec{\eta}_1(\hat{r}, t) \}$ and $\vec{\eta}_2 = {}_{(k)}\{ \vec{\eta}_2(\hat{r}, t) \}$, we must use a combination of summation and integration,

$$\left\langle \vec{\eta}_1 \, , \, \vec{\eta}_1 \right\rangle = \left[\vec{\eta}_1 \, \vec{\eta}_2 \right]_{V,\tau,k} = \sum_k w_k \int_{t_0}^{t_N} dt \int_V d^3r \;\; {}_k\{ \eta_1(\hat{r}, t) \} \;\; {}_k\{ \eta_2(\hat{r}, t) \} \, .$$

2.3.1 Boundary Terms

The operator L^* adjoint to operator L is defined as

$$\left\langle L f_1 \, , \, f_2 \right\rangle = \left\langle f_1 \, , \, L^* f_2 \right\rangle .$$

If one considers differential operators, the definition of the operator consists of two parts: (i) definition of the differential operator and (ii) boundary conditions for functions. If the boundary conditions for functions are not homogeneous, then the equations for definition of the adjoint operator have the following form:

$$\left\langle L f_1 \, , \, f_2 \right\rangle = \left\langle f_1 \, , \, L_0^* f_2 \right\rangle + \left\langle \left\langle f_1 \, , \, f_2 \right\rangle \right\rangle .$$

Here the last term is a boundary term. It is defined by an integral over corresponding phase space at the boundary surface of the domain of definition of operators. In such case L_0^* is the so-called "formal" adjoint operator and the definition of the adjoint operator L^* will include delta functions. If the boundary condition for functions in both spaces are homogeneous, then the boundary term vanishes.

2.4 Final Thought

It is the author's hope that this notation will not be too burdensome to the reader; in the following sections, as much of it will be suppressed as possible, when possible.

Chapter 3

The Problem

Consider a set of responses we think are important in our reactor system (EOC inventory of Am-242, pin power distribution, etc.) These responses, r_s, may be expressed as functionals of the input data to our system, $\vec{\alpha}$, and the solution of our system, $\vec{x}$,

$$r_s = r_s\,[\,\vec{\alpha}\,,\vec{x}\,] = \left\langle\, \vec{h}_{s,\alpha}\,,\,\vec{\alpha}\,\right\rangle_{\alpha} + \left\langle\, \vec{h}_{s,x}\,,\,\vec{x}\,\right\rangle_{x}, \tag{3.1}$$

where we have chosen to represent the functional as two inner products, which describe two distinctly different effects: a direct effect, $\left\langle\ ,\ \right\rangle_{\alpha}$, and an indirect effect, $\left\langle\ ,\ \right\rangle_{x}$. The response, r_s, we seek determines the realization vector for the direct effect, $\vec{h}_{s,\alpha}$, and the realization vector for the indirect effect, $\vec{h}_{s,x}$. We may calculate the direct effect with just the value $\vec{\alpha}$. The indirect effect requires we solve a system of equations for $\vec{x}$. Our goal is to determine what happens to response, r_s, when some data parameters (e.g. ^{235}U thermal fission cross section, ^{237}Np decay constant, ^{241}Pu fission yields, etc.) in the set of parameters $\vec{\alpha}$ are perturbed. With most responses, perturbing $\vec{\alpha} \rightarrow \vec{\alpha}\,' = \vec{\alpha} + \Delta\vec{\alpha}$ also perturbs the system solution, $\vec{x} \rightarrow \vec{x}\,' = \vec{x} + \Delta\vec{x}$, yielding a perturbed response,

$$r_s{}' = r_s[\vec{\alpha}\,,\vec{x}\,'] = \left\langle\, \vec{h}_{s,\alpha}\,,\,\vec{\alpha}\,'\,\right\rangle_{\alpha} + \left\langle\, \vec{h}_{s,x}\,,\,\vec{x}\,'\,\right\rangle_{x}.$$

And in general, the degree of the perturbation (e.g. -1%, 1%, 5%, etc.) will nonlinearly impact the response so we actually have a perturbed response, $\{\,r_s{}'\,\}_p$, that depends on some perturbation index p,

$$\{\,r_s{}'\,\}_p = r_s\,[\,\{\,\vec{\alpha}\,'\,\}_p\,,\,\{\,\vec{x}\,'\,\}_p\,] = \left\langle\, \vec{h}_{s,\alpha}\,,\ \{\,\vec{\alpha}\,'\,\}_p\,\right\rangle_{\alpha} + \left\langle\, \vec{h}_{s,x}\,,\ \{\,\vec{x}\,'\,\}_p\,\right\rangle_{x}, \tag{3.2}$$

where we can represent the data perturbation as $\{\,\vec{\alpha}\,'\,\}_p = \vec{\alpha} + \{\,\Delta\vec{\alpha}\,\}_p$. The elements of $\{\,\Delta\vec{\alpha}\,\}_p$ are given by $\{\,\Delta\alpha\,\}_{m,p} = \{\,\mathrm{f}\,\}_{m,p}\,\{\,\alpha\,\}_m$, where $\{\,\mathrm{f}\,\}_{m,p}$ is the perturbation fraction of degree p (e.g. -1%, 1%, 5%, etc.) for parameter m. The most efficient manner in which to analyze sensitivity (i.e. how much responses change when data is perturbed) is dependent upon three factors:

1. the number of responses we are interested in, N_s,
2. the number of input data parameters we will perturb, N_m and
3. whether we are more interested in
   (a) sensitivities of responses to input data,
   (b) propagation of uncertainties in input data, or
   (c) exact changes in responses, $\{\,\Delta r_s\,\}_p = \{\,r_s\,'\,\}_p - \{\,r_s\,\}_p$, for perturbations of degree p in data parameter m.

Before we proceed, let us remark on the indices m and p we have introduced to deal with sensitivity analysis. These two indices live in the lower right corner, $\{\,\circ\,\}_{m,p}$, like the spatial index i, but we will only use them when it is absolutely necessary to refer to data parameter m or perturbation degree p.

Chapter 4

The Reactor Physics Equations

4.1 Neutron Field Equation

To model the field of neutrons in the reactor system, we use the time-dependent neutron diffusion equation which describes the neutron scalar flux, $\phi(\hat{r}, E, t)$, at all positions $\hat{r}$ in the reactor, for all neutron energies E, from BOC at t_0 to EOC at t_N is given by

$$\frac{1}{v}\frac{\partial \phi}{\partial t} + L\phi = F_p\phi + P_d\,\vec{\eta} + Q_{ext} \tag{4.1}$$

i. from $t_0 < t \leq t_N$ with initial conditions $\vec{\eta}(\hat{r}, t_0) = \vec{\eta}_0(\hat{r})$ and $\phi(\hat{r}, E, t_0) = \phi_0(\hat{r}, E)$

ii. and boundary conditions $\phi(\hat{r}_{bc}, E, t) = \phi_{bc}(\hat{r}, E, t)$ for $\hat{r} \in \hat{r}_{bc}$

with leakage/loss operator L, prompt fission operator F_p, and delayed neutron precursor operator P_d defined by

$$L\circ \stackrel{\text{def}}{=} -\nabla d_c \cdot \nabla \circ + \Sigma_t \circ - \Big[\, \Sigma_s(E' \to E)\circ \,\Big]_{\epsilon'} \,, \tag{4.2a}$$

$$F_p\circ \stackrel{\text{def}}{=} \chi_p(E)\Big[\, \nu\Sigma_f(E')\circ \,\Big]_{\epsilon'} \,, \tag{4.2b}$$

$$P_d\circ \stackrel{\text{def}}{=} \Big[\, \vec{\chi}_d(E)\,\vec{\lambda}_d\circ \,\Big]_k \,. \tag{4.2c}$$

We are also interested in the local fission power density, $p\,(\,\hat{r},t\,)$, produced in the reactor from BOC to EOC described by

$$p\,(\,\hat{r},t\,) \quad = \quad p\,[\,\kappa\Sigma_f(E')\,,\phi(E')\,] \stackrel{\text{def}}{=} \Big[\ \kappa\Sigma_f(E')\ \phi(E')\ \Big]_{\epsilon'}\,. \tag{4.2d}$$

For reference, the terms appearing in Eq. (4.1) are outlined below.

$\phi(\hat{r},E,t)$	scalar flux $\left(\frac{\text{neutrons}}{\text{MeV}\cdot\text{cm}^2\cdot\text{s}}\right)$
$v(E)$	velocity of neutrons with energy E $\left(\frac{\text{cm}}{\text{s}}\right)$
$d_c(\hat{r},E,t)$	diffusion coefficient (cm)
$\Sigma_t(\hat{r},E,t)$	macroscopic total cross section $\left(\frac{1}{\text{cm}}\right)$
$\Sigma_s(\hat{r},E'\rightarrow E,t)$	macroscopic scattering cross section $\left(\frac{1}{\text{MeV}\cdot\text{cm}}\right)$
$\chi_p(\hat{r},E,t)$	prompt neutrons energy spectrum $(-)$
$\nu\Sigma_f(\hat{r},E,t)$	macroscopic nu-fission cross section $\left(\frac{1}{\text{cm}}\right)$
$Q_{ext}(\hat{r},E,t)$	external source of neutrons $\left(\frac{\text{neutrons}}{\text{MeV}\cdot\text{cm}^2\cdot\text{s}}\right)$
${}_k\{\,\chi_d(E)\,\}$	delayed neutron energy spectrum for nuclide k $(-)$
${}_k\{\,\lambda_d\,\}$	production rate of delayed neutrons for nuclide k $\left(\frac{1}{\text{s}}\right)$
${}_k\{\,\eta(\hat{r},t)\,\}$	concentration of nuclide k $\left(\frac{\text{nuclei}}{\text{barn}\cdot\text{cm}}\right)$
$\kappa\Sigma_f(\hat{r},E,t)$	macroscopic kappa-fission cross section $\left(\frac{\text{MeV}}{\text{cm}}\right)$
$p(\hat{r},t)$	local fission power density $\left(\frac{\text{MeV}}{\text{cm}^3\cdot\text{s}}\right)$

4.2 Nuclide Field Equation

The model the field of nuclei, we use the time-dependent nuclide transmutation equations (also called the Bateman equations, burnup equations, and depletion equations) to be solved for nuclide concentrations, $\vec{\eta}(\hat{r},t)$, at all positions $\hat{r}$ in the reactor from BOC at t_0 to EOC at t_N is given by

$$\frac{d}{dt}\vec{\eta} = \Big[\ \widetilde{\mathbf{R}}\phi\ \Big]_{\epsilon}\,\vec{\eta} + \widetilde{\mathbf{D}}\,\vec{\eta} \tag{4.3}$$

i. from $t_0 < t \leq t_N$ with initial condition $\vec{\eta}(\hat{r},t_0) = \vec{\eta}_0(\hat{r})$

where the reaction matrix $\widetilde{\mathbf{R}}$ is composed of cross sections describing the transmutation of nuclei to other nuclei from reactions with neutrons,

$$ {}_{k,k'}\{\,\mathbf{R}\,\} \;=\; \begin{cases} -\,{}_{k}\{\,\sigma_a(\hat{r},E,t)\,\} & k = k' \\ {}_{k,k'}\{\,\sigma(\hat{r},E,t)\,\} & \text{elsewhere,} \end{cases} \tag{4.4a} $$

while the decay matrix $\widetilde{\mathbf{D}}$ describes the transmutation of nuclei to other nuclei via decay,

$$ {}_{k,k'}\{\,\mathbf{D}\,\} \;=\; \begin{cases} -\,{}_{k}\{\,\lambda_{tot}\,\} & k = k' \\ {}_{k,k'}\{\,\lambda\,\} & \text{elsewhere.} \end{cases} \tag{4.4b} $$

The decay constant λ for a specific transmutation path is usually expressed as

$$ {}_{k,k'}\{\,\lambda\,\} \;=\; {}_{k,k'}\{\,\mathrm{f}_\lambda\,\}\;{}_{k'}\{\,\lambda_{tot}\,\}\,, \tag{4.4c} $$

in terms of path branch ratio ${}_{k,k'}\{\,\mathrm{f}_\lambda\,\}$ and total decay constant ${}_{k'}\{\,\lambda_{tot}\,\}$. Similarly, the cross section σ for the fissioning of nuclide k' creating nuclide k is usually expressed as

$$ {}_{k,k'}\{\,\sigma\,\} \;=\; {}_{k,k'}\{\,\mathrm{f}_f\,\}\;{}_{k'}\{\,\sigma_f\,\}\,, \tag{4.4d} $$

in terms of fission fraction f_f times microscopic fission cross section σ_f. The absorption cross section σ_a for nuclide k' may be expressed as the summation of all other transmutation cross sections for nuclide k',

$$ {}_{k'}\{\,\sigma_a\,\} \;=\; \Big[\;{}_{k,k'}\{\,\sigma\,\}\;\Big]_k\,. \tag{4.4e} $$

For reference, the terms appearing in Eq. (4.3) are outlined below.

$\phi(\hat{r},E,t)$	scalar flux $\left(\frac{\text{neutrons}}{\text{MeV}\cdot\text{cm}^2\cdot\text{s}}\right)$
${}_{k}\{\,\sigma_a(\hat{r},E,t)\,\}$	microscopic absorption cross section of nuclide k (barn)
${}_{k,k'}\{\,\sigma(\hat{r},E,t)\,\}$	microscopic cross section of nuclide k' which produces k (barn)
${}_{k}\{\,\eta(\hat{r},t)\,\}$	concentration of nuclide k $\left(\frac{\text{nuclei}}{\text{barn}\cdot\text{cm}}\right)$
${}_{k}\{\,\lambda_{tot}\,\}$	total decay rate for nuclide k $\left(\frac{1}{\text{s}}\right)$
${}_{k,k'}\{\,\lambda\,\}$	decay production of nuclide k from k' $\left(\frac{1}{\text{s}}\right)$
${}_{k,k'}\{\,\mathrm{f}_\lambda\,\}$	fraction of nuclide k' decays which produce k
${}_{k,k'}\{\,\mathrm{f}_f\,\}$	fraction of nuclide k' fissions which produce k

4.3 Microscopic and Macroscopic Cross Sections, σ and Σ

The coupling between the neutron field equation, Eq. (4.1), and neutron field equation, Eq. (4.3), is more than just the delayed neutron contribution, $P_d\,\vec{\eta}$. All macroscopic cross sections, Σ—which describe the interaction probabilities of neutrons with the surrounding media—are actually just a convenient grouping of nuclide concentrations, $\vec{\eta}$, and microscopic cross sections, σ, which describe the interaction probabilities per nuclide in the system.

$$\Sigma_x(\hat{r},E,t) = \Sigma\,[\,\vec{\sigma}_x(\hat{r},E,t)\;;\;\vec{\eta}(\hat{r},t)\,] \tag{4.5}$$

The functional, Σ, which maps microscopic cross sections of type x to macroscopic cross sections of type x is given by

$$\Sigma\,[\,\vec{\sigma}_x(\hat{r},E,t)\;;\;\vec{\eta}(\hat{r},t)\,] \stackrel{\text{def}}{=} \Big[\;\vec{\sigma}_x(\hat{r},E,t)\;\vec{\eta}(\hat{r},t)\;\Big]_k \tag{4.6}$$

where the microscopic cross sections, σ, are described below.

${}_k\{\,\sigma_x(\hat{r},E,t)\,\}$ microscopic cross section of type x for nuclide k (barn)

4.4 Reactor Cycle Equations

For a simulation of the reactor cycle, we would like to solve the neutron field equation, Eq. (4.1), coupled with the nuclide field equation, Eq. (4.3), for the reactor system from the BOC to the EOC. Such a calculation is called a *reactor cycle calculation* and employs a set of standard assumptions and modifications [6] to Eq. (4.1) to accurately calculate of the scalar flux, ϕ, and the nuclide concentrations, $\vec{\eta}$, of important nuclei over the reactor cycle. In order to arrive at the equations we use for reactor cycle calculations, we make the following assumptions:

1. the scalar flux, ϕ, varies slowly in time, and thus the time derivative in Eq. (4.1) may be neglected,

2. the scalar flux, ϕ, may be decomposed into a shape function, φ, and an amplitude function, Φ, such that $\phi(\hat{r},E,t) = \varphi(\hat{r},E,t)\Phi(t)$,

3. over the entire cycle, from t_0 to t_N, our reactor operates at some constant power p_{core}, and

4. the external source of neutrons, $Q_{ext}(\hat{r}, E, t)$, may be neglected.

Neutron Field Equations for reactor cycle calculations

With these four assumptions, Eq. (4.1) becomes an equation for the flux shape, φ and an equation for the flux amplitude, Φ.

$$L\varphi = \frac{1}{k_e} F\varphi \tag{4.7}$$

i. for separable scalar flux, $\phi = \varphi\Phi$, with amplitude function

$$\Phi = \frac{p_{core}}{\left[\, p\,(\,\hat{r}, t\,)\,\right]_V}$$

ii. from $t_0 < t \leq t_N$ with initial condition $\vec{\eta}(\hat{r}, t_0) = \vec{\eta}_0(\hat{r})$

iii. with boundary condition $\phi(\hat{r}_{bc}, E, t) = \phi_{bc}(\hat{r}, E, t)$ for $\hat{r} \in \hat{r}_{bc}$

iv. with eigenvalue

$$k_e = \frac{\left[\, F\varphi \,\right]_{V,\epsilon}}{\left[\, L\varphi \,\right]_{V,\epsilon}}$$

In Eq. (4.7), the equation for the flux shape is an eigenvalue problem with eigenvalue k_e and associated eigenfunction φ. The equation for the flux amplitude is basically a constraint based on the fact that the reactor operates at some constant power, p_{core}. To formulate Eq. (4.7), it is necessary to modify the fission source to include delayed neutron contributions. The (unchanged) loss/leakge operator L and new fission operator F are given by

$$L\circ \;\stackrel{\text{def}}{=}\; -\nabla d_c \cdot \nabla \circ + \Sigma_t \circ - \left[\, \Sigma_s(E' \to E)\circ \,\right]_{\epsilon'}, \tag{4.8a}$$

$$F\circ \;\stackrel{\text{def}}{=}\; \left(\chi_p(E)(1-\beta_{tot}) + \left[\, \vec{\beta}_d\, \vec{\chi}_d(E) \,\right]_k\right) \left[\, \nu\Sigma_f(E')\circ \,\right]_{\epsilon'}. \tag{4.8b}$$

The total delayed neutron fraction, β_{tot}, satisfies

$$\beta_{tot} = \left[\, \vec{\beta}_d \,\right]_k. \tag{4.8c}$$

For reference, the new terms appearing in Eq. (4.7) are outlined below.

$\varphi(\hat{r}, E, t)$	scalar flux shape function $\left(\frac{\text{neutrons}}{\text{MeV}\cdot\text{cm}^2\cdot\text{s}}\right)$
$\Phi(t)$	scalar flux amplitude function
${}_k\{\,\chi_d(E)\,\}$	delayed neutron energy spectrum for nuclide k $(-)$
${}_k\{\,\beta_d\,\}$	delayed neutron fraction for nuclide k
β_{tot}	total delayed neutron fraction
k_e	effective neutron multiplication factor

Nuclide Field Equation for reactor cycle calculations

For reactor cycle calculations, the nuclide field equation stated in Eq. (4.3) becomes

$$\frac{d}{dt}\vec{\eta} = \left[\,\widetilde{\mathbf{R}}\,\Phi\,\varphi\,\right]_{\epsilon}\vec{\eta} + \widetilde{\mathbf{D}}\,\vec{\eta} \tag{4.9}$$

i. from $t_0 < t \leq t_N$ with initial condition $\vec{\eta}(\hat{r}, t_0) = \vec{\eta}_0(\hat{r})$

where the only difference between Eq. (4.9) and Eq. (4.3) is that now the scalar flux is defined as an amplitude function times a shape function, $\phi = \Phi\varphi$.

Chapter 5

The Discretized Reactor Cycle Equations

Now let us develop the discretized versions of reactor cycle equations for the neutron field of Eq. (4.7) and the nuclide field of Eq. (4.9). Then we will discuss the solution methods employed in NESTLE for these calculations. Note that the description and methods discussed here apply only to cores with rectangular-prism fuel assemblies–those which may easily be described with Cartesian geometry. Although NESTLE can perform reactor physics calculations for cores with hexagonal-prism fuel assemblies—which are described using special Hexagonal geometry including conformal mapping and a special nodal burnup gradient treatment (see NESTLE documentation [2])—this research project was concerned only with US PWR and BWR cores which utilize rectangular-prism fuel assemblies.

5.1 Discretized Neutron Field Equations

The continuous neutron field equations for a reactor cycle calculation are given by Eq. (4.7). In NESTLE, the following discretizations are applied to yield the set of nodal equations NESTLE solves numerically.

1. The standard energy group approximation is used to discretize energy, E, into energy

groups, $g = 1, ..., N_g$.

2. The spatial domain is broken up into a finite number of subregions/nodes, $i = 1, ..., N_{dom}$.

3. N_{gst} extra "ghost nodes" are placed at the surface boundary ($i = N_{dom}+1, ..., N_{dom}+N_{gst}$) to help treat boundary conditions. Thus, the total number of space nodes is $N_i = N_{dom}+N_{gst}$. Boundary conditions are no longer needed as they are incorporated into the system through the extra "ghost nodes".

4. We choose some appropriate approximation for the streaming term (see NESTLE Discretization Options).

5. All material properties, cross sections, etc. are assumed piecewise-constant—that is constant in each node/subregion i.

6. Time is discretized into time nodes, t_j, $j = 0, ..., N_j$.

The results of the aforementioned discretizations are the system of equations NESTLE solves for the neutron field in a thermal reactor system over a cycle,

$$\{\,\widetilde{\mathbf{L}}\,\}^j\ \{\,\vec{\varphi}\,\}^j = \frac{1}{\{\,k_e\,\}^j}\ \{\,\widetilde{\mathbf{F}}\,\}^j\ \{\,\vec{\varphi}\,\}^j \tag{5.1}$$

i. for separable scalar flux, $\{\,\vec{\phi}\,\}^j = \{\,\vec{\varphi}\,\}^j\ \{\,\Phi\,\}^j$, with amplitude function

$$\{\,\Phi\,\}^j = \frac{p_{core}}{\left[\ \{\,\vec{p}\,\}^j\ \right]_V}$$

ii. for times t_j, $j = 0, ..., N_j$ with initial condition $\{\,\vec{\eta}(t_0)\,\}^0 = \vec{\eta}_0$

iii. with eigenvalue

$$\{\,k_e\,\}^j = \frac{\left[\ \{\,\widetilde{\mathbf{F}}\,\}^j\ \{\,\vec{\varphi}\,\}^j\ \right]_{i,\epsilon}}{\left[\ \{\,\widetilde{\mathbf{L}}\,\}^j\ \{\,\vec{\varphi}\,\}^j\ \right]_{i,\epsilon}}$$

where the loss/leakge matrix $\widetilde{\mathbf{L}}$ and fission matrix $\widetilde{\mathbf{F}}$ are defined by

$$^{gg'}\{\,\mathbf{L}\,\}^j_{ii'} \stackrel{\text{def}}{=} -\,^{g}\{\,d\,\}^j_{i,i'}\,\delta_{gg'} + \left(\,^{g}\{\,\Sigma_r\,\}^j_i\,\delta_{gg'}\delta_{ii'} - \,^{g,g'}\{\,\Sigma_s\,\}^j_i\,(1-\delta_{gg'})\delta_{ii'}\right)V_i, \tag{5.2a}$$

$$^{gg'}\{\,\mathbf{F}\,\}^j_{ii'} \stackrel{\text{def}}{=} \left(\left(\,^{g}\{\,\chi_p\,\}^j_i\,(1-\beta_{tot}) + \left[\ \vec{\beta}_d\ \,^{g}\{\,\vec{\chi}_d\,\}^j_i\ \right]_k\right)\,^{g'}\{\,\nu\Sigma_f\,\}^j_i\,\delta_{ii'}\right)V_i. \tag{5.2b}$$

We are also interested in the local fission power density shape, $\{\,\vec{p}\,\}^j$, described by

$$\{\,p\,\}_i^j \;=\; p[\,\{\,\kappa\vec{\Sigma}_f\,\}_i^j\,,\,\{\,\vec{\varphi}\,\}_i^j\,] \stackrel{\text{def}}{=} \Big[\,\{\,\kappa\vec{\Sigma}_f\,\}_i^j\;\;\{\,\vec{\varphi}\,\}_i^j\,\Big]_g . \tag{5.3}$$

For reference, the terms appearing in Eq. (5.1) are outlined below.

${}^g\{\,\varphi\,\}_i^j$	scalar flux shape for group g, node i, time t_j $\left(\frac{\text{neutrons}}{\text{cm}^2\cdot\text{s}}\right)$
$\{\,\Phi\,\}^j$	scalar flux amplitude for time t_j
${}^g\{\,d\,\}_{i,i'}^j$	nodal coupling coefficient $\left(\frac{1}{\text{cm}}\right)$
${}^g\{\,\Sigma_r\,\}_i^j$	macroscopic removal cross section $\left(\frac{1}{\text{cm}}\right)$
${}^{g',g}\{\,\Sigma_s\,\}_i^j$	macroscopic scattering cross section, group $g' \to g$ $\left(\frac{1}{\text{cm}}\right)$
${}^g\{\,\chi_p\,\}_i^j$	prompt neutrons energy spectrum $(-)$
${}^g\{\,\nu\Sigma_f\,\}_i^j$	macroscopic nu-fission cross section $\left(\frac{1}{\text{cm}}\right)$
${}^g\{\,\kappa\Sigma_f\,\}_i^j$	macroscopic kappa-fission cross section $\left(\frac{\text{MeV}}{\text{cm}}\right)$
${}^g_k\{\,\chi_d\,\}^j$	delayed neutron energy spectrum for nuclide k $(-)$
${}_k\{\,\beta_d\,\}^j$	delayed neutron fraction for nuclide k
$\{\,\beta_{tot}\,\}^j$	total delayed neutron fraction
$\{\,k_e\,\}^j$	effective neutron multiplication factor
$\{\,p\,\}_i^j$	local fission power density shape $\left(\frac{\text{MeV}}{\text{cm}^3\cdot\text{s}}\right)$
p_{core}	reactor core fission power $\left(\frac{\text{MeV}}{\text{s}}\right)$

5.2 Discretized Nuclide Field Equations

The continuous nuclide field equation of Eq. (4.9) is easily discretized in space by just considering the node-average nuclide concentrations in each subregion/node of the problem domain, $i = 1, ..., N_{dom}$. We do not solve for the nuclide field in ghost nodes—they are only used for the scalar flux boundary condition treatment. We do not discretize the nuclide field equation in time so we still have the ODE

$$\frac{d}{dt}\,\{\,\vec{\eta}(t)\,\}_i^j \;=\; \{\,\widetilde{\mathbf{M}}(t)\,\}_{ii}^j\;\{\,\vec{\eta}(t)\,\}_i^j \tag{5.4}$$

i. from $t_{j-1} < t \leq t_j$, for $j = 1, ..., N_j$, with initial/interval condition

$$\{\, \vec{\eta}(t_{j-1}) \,\}_i^j = \begin{cases} \{\, \vec{\eta}_0 \,\}_i & j = 1 \\ \{\, \vec{\eta}(t_{j-1}) \,\}_i^{j-1} & j = 2, ..., N_j \end{cases}$$

ii. for nodes $i = 1, ..., N_{dom}$

where we have introduced the transmutation coefficient matrix, $\widetilde{\mathbf{M}}(t)$, for the nuclide field defined by

$$\{\, \widetilde{\mathbf{M}}(t) \,\}_{ii}^j \overset{\text{def}}{=} \sum_g {}^{gg}\{\, \widetilde{\mathbf{R}}(t) \,\}_{ii}^j \; {}^g\{\, \phi(t) \,\}_i^j + \widetilde{\mathbf{D}}.$$

Just like the continuous case, the reaction coefficient matrix $\widetilde{\mathbf{R}}$ is contains cross sections which describe the transmutation of nuclei to other nuclei via neutron activation,

$${}^{gg}_{kk'}\{\, \mathbf{R}(t) \,\}_{ii}^j \overset{\text{def}}{=} -{}^g_k\{\, \sigma_a(t) \,\}_i^j \, \delta_{kk'} + {}^g_{k,k'}\{\, \sigma(t) \,\}_i^j \, (1 - \delta_{kk'}) \tag{5.5a}$$

while the decay coefficient matrix $\widetilde{\mathbf{D}}$ contains decay constants which describe the transmutation of nuclei to other nuclei via decay,

$${}_{kk'}\{\, \mathbf{D} \,\} \overset{\text{def}}{=} -{}_k\{\, \lambda_{tot} \,\} \, \delta_{kk'} + {}_{k,k'}\{\, \lambda \,\} \, (1 - \delta_{kk'}). \tag{5.5b}$$

For reference, the terms appearing in Eq. (5.4) are outlined below.

${}_k\{\, \eta(t) \,\}_i^j$	concentration of nuclide k in node i over interval τ_j $\left(\frac{\text{nuclei}}{\text{barn}\cdot\text{cm}}\right)$
${}^g\{\, \phi(t) \,\}_i^j$	interval group scalar flux $\left(\frac{\text{neutrons}}{\text{cm}^2\cdot\text{s}}\right)$
${}^g_k\{\, \sigma_a(t) \,\}_i^j$	interval microscopic absorption cross section of nuclide k (barn)
${}^g_{k,k'}\{\, \sigma(t) \,\}_i^j$	interval microscopic cross section for production of nuclide k by k' (barn)
${}_k\{\, \lambda_{tot} \,\}$	total decay rate for nuclide k $\left(\frac{1}{\text{s}}\right)$
${}_{k,k'}\{\, \lambda \,\}$	decay production of nuclide k from k' $\left(\frac{1}{\text{s}}\right)$

5.3 NESTLE Discretization Options

Now we will discuss various facets of the discretized neutron and nuclide field equations presented in Eq. (5.1) and Eq. (5.4), respectively. Note that these discretization schemes only apply to Cartesian geometry—Hexagonal geometry is not discussed in this work.

5.3.1 Streaming Term Discretization

Two methods exist in NESTLE for the discretization of the so-called "streaming term" in Eq. (4.1), $\nabla d_c \cdot \nabla \phi$. The discretization method determines the form of the nodal coupling term introduced in Eq. (5.1), ${}^{g}\{\, d \,\}^{j}_{i,i'}$, for all subregions/nodes i' coupled to node i (6 neighbors in 3D Cartesian geometry and 8 in 3D hexagonal geometry). Let us introduce the following subscripts for node i' in Cartesian geometry, describing it's location in relation to the node of interest, i.

1.	western node	(negative $x-$direction)	$i' = i_w$
2.	eastern node	(positive $x-$direction)	$i' = i_e$
3.	northern node	(negative $y-$direction)	$i' = i_n$
4.	southern node	(positive $y-$direction)	$i' = i_s$
5.	down node	(negative $z-$direction)	$i' = i_d$
6.	up node	(positive $z-$direction)	$i' = i_u$

Finite Difference Method (FDM)

The FDM uses a finite difference approximation for ∇ with the requirement that the current across an interface ($i' \rightarrow i$) be continuous, resulting in Eq. (5.6) for the neighbor node coupling terms, ${}^{g}\{\, d \,\}^{j}_{i,i'}$, in terms of corrected diffusion coefficients, ${}^{g}\{\, d_{cc} \,\}^{j}_{i,i'}$, and cell i thicknesses Δx_i, Δy_i, and Δz_i.

$$
\begin{aligned}
{}^{g}\{\, d \,\}^{j}_{i,i'} = \quad & {}^{g}\{\, d_{cc} \,\}^{j}_{i,i'} (1 - \delta_{ii'}) + \\
\Big(\quad & ({}^{g}\{\, d_{cc} \,\}^{j}_{i,i_w} + {}^{g}\{\, d_{cc} \,\}^{j}_{i,i_e}) \Delta y_i \Delta z_i + \\
& ({}^{g}\{\, d_{cc} \,\}^{j}_{i,i_n} + {}^{g}\{\, d_{cc} \,\}^{j}_{i,i_s}) \Delta x_i \Delta z_i + \\
& ({}^{g}\{\, d_{cc} \,\}^{j}_{i,i_u} + {}^{g}\{\, d_{cc} \,\}^{j}_{i,i_d}) \Delta x_i \Delta y_i \Big) \delta_{ii'}
\end{aligned}
\tag{5.6a}
$$

where ${}^{g}\{\, d_{cc} \,\}^{j}_{i,i'}$ for two cells joined at an y-z plane interface is given by

$$
{}^{g}\{\, d_{cc} \,\}^{j}_{i,i'} = \frac{{}^{g}\{\, d_c \,\}^{j}_{i} \; {}^{g}\{\, d_c \,\}^{j}_{i'} \, (\Delta x_i + \Delta x_{i'})}{{}^{g}\{\, d_c \,\}^{j}_{i} \, \Delta x_i + {}^{g}\{\, d_c \,\}^{j}_{i'} \, \Delta x_{i'}}. \tag{5.6b}
$$

Nodal Expansion Method (NEM)

The NEM introduces a correction term to the FDM, ${}^{g}\{\, d_l \,\}^{j}_{i,i'}$, in an attempt to more accurately approximate neutron currents at the interfaces of subregions/nodes, as

the currents produced by the finite difference method is inaccurate for coarse cells—as we usually have with reactor physics problems. The values of the NEM correction terms are calculated by expanding the current in a series of moments with unknown coefficients, then solving for the coefficients with a sequence of one-node and/or two-node current calculations [2]. The result for the neighbor node coupling terms, ${}^{g}\{\, d \,\}^{j}_{i,i'}$, in terms of corrected diffusion coefficients, ${}^{g}\{\, d_{cc} \,\}^{j}_{i,i'}$; cell thicknesses Δx_i, Δy_i, and Δz_i; and the NEM corrections, ${}^{g}\{\, d_l \,\}^{j}_{i,i'}$, is

$$
\begin{aligned}
{}^{g}\{\, d \,\}^{j}_{i,i'} = \quad & ({}^{g}\{\, d_{cc} \,\}^{j}_{i,i'} + {}^{g}\{\, d_l \,\}^{j}_{i,i'})(1-\delta_{ii'}) + \\
\Big(\quad & ({}^{g}\{\, d_{cc} \,\}^{j}_{i,i_w} + {}^{g}\{\, d_{cc} \,\}^{j}_{i,i_e} + {}^{g}\{\, d_l \,\}^{j}_{i,i_w} - {}^{g}\{\, d_l \,\}^{j}_{i,i_e})\Delta y_i \Delta z_i + \\
& ({}^{g}\{\, d_{cc} \,\}^{j}_{i,i_n} + {}^{g}\{\, d_{cc} \,\}^{j}_{i,i_s} + {}^{g}\{\, d_l \,\}^{j}_{i,i_n} - {}^{g}\{\, d_l \,\}^{j}_{i,i_s})\Delta x_i \Delta z_i + \\
& ({}^{g}\{\, d_{cc} \,\}^{j}_{i,i_u} + {}^{g}\{\, d_{cc} \,\}^{j}_{i,i_d} + {}^{g}\{\, d_l \,\}^{j}_{i,i_d} - {}^{g}\{\, d_l \,\}^{j}_{i,i_u})\Delta x_i \Delta y_i \quad \Big)\delta_{ii'}
\end{aligned}
\tag{5.7a}
$$

where ${}^{g}\{\, d_{cc} \,\}^{j}_{i,i'}$ for two cells joined at an y-z plane interface is given by

$$
{}^{g}\{\, d_{cc} \,\}^{j}_{i,i'} = \frac{{}^{g}\{\, d_c \,\}^{j}_{i}\ {}^{g}\{\, d_c \,\}^{j}_{i'}\,(\Delta x_i + \Delta x_{i'})}{{}^{g}\{\, d_c \,\}^{j}_{i}\,\Delta x_i + {}^{g}\{\, d_c \,\}^{j}_{i'}\,\Delta x_{i'}}. \tag{5.7b}
$$

5.3.2 Neutron/Nuclide Field Coupling Methods

The neutron and nuclide fields satisfying equations Eq. (5.1) and Eq. (5.4), respectively, are coupled through the influence of $\vec{\eta}$ on macroscopic cross sections, Σ, and the influence of φ and Φ on the rates of neutron-induced transmutation events. NESTLE has two methods to resolve this coupling.

Predictor Method

With the predictor (P) method of neutron/nuclide field coupling, the interval group scalar flux, $\{\, \vec{\phi}(t) \,\}^{j}$, is approximated at its beginning-of-interval value,

$$
\{\, \vec{\phi}(t) \,\}^{j} \approx \{\, \Phi \,\}^{j-1}\ \{\, \vec{\varphi} \,\}^{j-1} \Big(H(t-t_{j-1}) - H(t-t_j) \Big) \tag{5.8}
$$

where H is the Heaviside function. The result is an "explicit" system of equations, which may be solved sequentially from one time step to the next.

Predictor-Corrector Method

With the predictor-corrector (P-C) method of neutron/nuclide field coupling, the interval scalar flux, $\{\,\vec{\phi}(t)\,\}^j$, is approximated as linear from the beginning-of-interval to end-of-interval,

$$\{\,\vec{\phi}(t)\,\}^j \approx \{\,\Phi\,\}^{j-1}\,\{\,\vec{\varphi}\,\}^{j-1}\left(\frac{t_j - t}{\tau_j}\right) + \{\,\Phi\,\}^j\,\{\,\vec{\varphi}\,\}^j\left(\frac{t - t_{j-1}}{\tau_j}\right). \tag{5.9}$$

The result is a system in which the nuclide field calculation may depend on a neutron field calculation that has not yet been performed. This "implicit" system of equations is solved through the iteration process summarized below.

1. Use the P method to solve the nuclide field equations from t_{j-1} to t_j (time step τ_j) and determine "predicted" end-of-interval nuclide concentrations, $\{\,\vec{\eta}^{(0)}(t_j)\,\}^j$.

2. Use the "predicted" nuclide concentrations, $\{\,\vec{\eta}^{(0)}(t_j)\,\}^j$, to solve the neutron field equations at t_j and determine "predicted" scalar flux, $\{\,\vec{\phi}^{(0)}\,\}^j$.

3. Now use the P-C method to re-solve the nuclide field equations over time step τ_j and determine "once-corrected" end-of-interval nuclide concentrations, $\{\,\vec{\eta}^{(1)}\,\}^j_{(t_j)}$.

4. Use the "once-corrected" nuclide concentrations, $\{\,\vec{\eta}^{(1)}(t_j)\,\}^j$, to re-solve the neutron field equations at t_j and determine "once-corrected" scalar flux, $\{\,\vec{\phi}^{(1)}\,\}^j$.

5. Steps 3 and 4 above may be repeated indefinitely and although this process seems reasonable, we are not aware of proof that this process converges—this is certainly not the conventional Predictor-Corrector algorithm [8]. Nonetheless, it appears convergent and exhibits the second order behavior of the conventional algorithm. Currently in NESTLE, corrector updates of the nuclide field occur after a user-defined number of iterations on the neutron field solution. In the problems we tested, the nuclide field was "corrected" an average of 2-3 times before convergence of the neutron field solution.

5.4 NESTLE Neutron Field Solvers

To solve the discretized neutron field equation, Eq. (5.1), NESTLE uses the Gauss-Seidel (G-S) method of iteratively solving a linear algebraic system with Red-Black Line

Successive Over Relaxation (LSOR) in Cartesian geometry and Red-Black-Yellow LSOR in Hexagonal geometry. At each time node t_j, the matrix $\{\,\widetilde{\mathbf{L}}\,\}^j$ from Eq. (5.1) is iteratively inverted using G-S LSOR, with right side $\{\,\widetilde{\mathbf{F}}\,\}^j\ \{\,\vec{\varphi}\,\}^j$. The system is very sparse—the 3D Cartesian system has only $6 + N_g$ nonzero bands. From NESTLE v5.2.1 documentation on the strategy for solving the resulting system of equations [2]:

> ...much work has been done on formulating, understanding and implementing the iterative solution of this large, sparse matrix system. NESTLE takes advantage of this wealth of knowledge in its iterative solution implementation, utilizing an *outer-inner iterative strategy*. The outer iterations are used to update the fission source term and the inner iterations to approximately solve the resulting fixed source problem. The outer iterations correspond to a *power method*.

5.5 NESTLE Nuclide Field Solvers

We have created and implemented three generalized nuclide field solvers to replace the old explicit linear chain solvers:

1. `EQUI` — a simple equilibrium method to calculate concentrations of nuclei in equilibrium,

2. `MATEXPSS` — a matrix exponential method with scaling and squaring for solving systems of ODEs,

3. `ROSENBROCK2` — A 2^{nd} order Rosenbrock method for solving stiff systems of ODEs (SODEs).

The following sections will discuss the methodology behind each procedure in detail, but before we continue, let us introduce the following representation of Eq. (5.4),

$$\frac{d}{dt}\vec{\eta}(t) = \widetilde{\mathbf{M}}(t)\ \vec{\eta}(t) \tag{5.10}$$

i. for a single time step from $t_a < t \leq t_b$ with initial/interval condition $\vec{\eta}(t_a) = \vec{\eta}_a$

where we have suppressed some notation by using $\vec{\eta}(t)$ instead of $\{\,\vec{\eta}(t)\,\}_i^j$ and $\widetilde{\mathbf{M}}(t)$ instead of $\{\,\widetilde{\mathbf{M}}(t)\,\}_{ii}^j$. The nuclide field equation in Eq. (5.10) may be considered a SODE if

1. it describes simultaneous processes with significantly different rates of change for the components of the solution (highly varying eigenvalues) and

2. we must find the solution on the time scale of the slowest changing component [9].

From fission products such as Xe and I to heavy metals like U and minor actinides like Am, the system of Eq. (5.10) contains rates of change for different components which may differ by many orders of magnitude and we wish to solve the system on the time scale for which we can expect significant changes in fuel nuclei concentrations, which is very slow compared to initially fast changing nuclei such as fission products. Thus we may consider Eq. (5.10) as an SODE. The matrix exponential method of `MATEXPSS` is not inherently well-suited to solving SODEs, but when we split the nuclide field into two parts, as we discuss in the next section **Equilibrium Method**, `MATEXPSS` appears to be a fairly efficient solver. The Rosenbrock method implemented in `ROSENBROCK2` is well suited to solving SODEs (see 2^{nd} **Order Rosenbrock Method with Complex Coefficients**).

5.5.1 Equilibrium Method

In most reactor cycles, a number of nuclei (especially fission products) achieve an equilibrium state relatively fast because their transmutation rates are very fast compared to fuel nuclei—again this is the mathematical property of this system called *stiffness*. We attempt to reduce stiffness by removing nuclei from the system of equations when they achieve an equilibrium state. First we divide the nuclide field into two sets, nuclei which have reached equilibrium, $\vec{\eta}^e$, and nuclei that have not and still require the full ODE solution, $\vec{\eta}^h$, via either `MATEXPSS` or `ROSENBROCK2`.

$$\begin{pmatrix} \frac{d}{dt}\vec{\eta}^h \\ \frac{d}{dt}\vec{\eta}^e \end{pmatrix} = \begin{pmatrix} \widetilde{\mathbf{M}}^{h\to h} & \widetilde{\mathbf{M}}^{e\to h} \\ \widetilde{\mathbf{M}}^{h\to e} & \widetilde{\mathbf{M}}^{e\to e} \end{pmatrix} \begin{pmatrix} \vec{\eta}^h \\ \vec{\eta}^e \end{pmatrix}$$

The matrices $\widetilde{\mathbf{M}}^{h\to h}$, $\widetilde{\mathbf{M}}^{e\to h}$, $\widetilde{\mathbf{M}}^{h\to e}$, and $\widetilde{\mathbf{M}}^{e\to e}$ represent internal coupling of the full–calculation nuclei, coupling of the equilibrium nuclei to the full-calculation nuclei, coupling of the full-calculation nuclei to the equilibrium nuclei, and internal coupling of the equilibrium nuclei, respectively. Because the equilibrium nuclei's concentrations do not change with time, $\frac{d}{dt}\vec{\eta}^e = 0$. We also require that equilibrium nuclei do not transmute into full-

calculation nuclei ($\widetilde{\mathbf{M}}^{e\to h} = 0$) and we obtain the system

$$\begin{pmatrix} \frac{d}{dt}\vec{\eta}^{\,h} \\ 0 \end{pmatrix} = \begin{pmatrix} \widetilde{\mathbf{M}}^{h\to h} & 0 \\ \widetilde{\mathbf{M}}^{h\to e} & \widetilde{\mathbf{M}}^{e\to e} \end{pmatrix} \begin{pmatrix} \vec{\eta}^{\,h} \\ \vec{\eta}^{\,e} \end{pmatrix}$$

for the nuclide field. Now (in our full notation) we solve the system of ODEs

$$\frac{d}{dt}\{\,\vec{\eta}^{\,h}(t)\,\}_i^j \;=\; \{\,\widetilde{\mathbf{M}}^{h\to h}(t)\,\}_{ii}^j \;\; \{\,\vec{\eta}^{\,h}(t)\,\}_i^j \tag{5.11}$$

i. from $t_{j-1} < t \le t_j$, for $j = 1, ..., N_j$, with initial/interval condition

$$\{\,\vec{\eta}^{\,h}(t_{j-1})\,\}_i^j = \begin{cases} \vec{\eta}_0^{\,h} & j = 1 \\ \{\,\vec{\eta}^{\,h}(t_{j-1})\,\}_i^{j-1} & j = 2, ..., N_j \end{cases}$$

for the full-calculation nuclei concentrations, $\{\,\vec{\eta}^{\,h}(t)\,\}_i^j$—which do not depend on equilibrium nuclei, $\{\,\vec{\eta}^{\,e}(t)\,\}_i^j$. Then, because of the impact many equilibrium nuclei may have on the neutron field (e.g. fission products), we calculate equilibrium nuclei whenever we solve for the neutron field,

$$\{\,\vec{\eta}^{\,e}(t_j)\,\}_i^j \;= -\left(\{\,\widetilde{\mathbf{M}}^{e\to e}(t_j)\,\}_{ii}^j\right)^{-1} \;\{\,\widetilde{\mathbf{M}}^{h\to e}(t_j)\,\}_{ii}^j \;\; \{\,\vec{\eta}^{\,h}(t_j)\,\}_i^j \tag{5.12}$$

i. for times t_j, $j = 0, ..., N_j$

where $^{-1}$ denotes a matrix inverse.

5.5.2 Matrix Exponential Method

The matrix exponential method seeks a solution to a system of ODEs analogous to the solution of the simple system, $d\eta(t)/dt = \lambda\eta(t)$ for $t_a < t \le t_b$ with initial condition $\eta(t_a) = \eta_a$, has end-of-interval solution $\eta_b = e^{\lambda\tau}\eta_a$. Thus the linear system of ODEs—Eq. (5.10) or Eq. (5.4) in full notation)—repeated below for convenience,

$$\frac{d}{dt}\vec{\eta}(t) = \widetilde{\mathbf{M}}(t)\;\vec{\eta}(t)$$

i. for a single time step from $t_a < t \leq t_b$ with initial/interval condition $\vec{\eta}(t_a) = \vec{\eta}_a$.

The matrix exponential solution requires that we fix $\widetilde{\mathbf{M}}(t)$ at some time t' [5]. Integration of the above ODE yields

$$\vec{\eta}_b - \vec{\eta}_a = \int_{t_a}^{t_b} \widetilde{\mathbf{M}}(t')\, \vec{\eta}(t')\, dt'. \tag{5.13}$$

Without knowledge of the behavior of $\vec{\eta}(t')$ over the interval, the fixed value of $\widetilde{\mathbf{M}}(t')$ which best satisfies the above expression is $\widetilde{\mathbf{M}}(t_a + \frac{t_b - t_a}{2})$, the transmutation coefficient matrix is fixed at the midpoint of the interval. Thus the solution to Eq. (5.10) utilizing the matrix exponential [5] is,

$$\vec{\eta}_b = e^{\widetilde{\mathbf{M}}\tau} \vec{\eta}_a \tag{5.14a}$$

where $\tau \stackrel{\text{def}}{=} t_b - t_a$, $\widetilde{\mathbf{M}} \stackrel{\text{def}}{=} \widetilde{\mathbf{M}}(t_a + \frac{\tau}{2})$, and the exponential of a matrix is defined by

$$e^{\widetilde{\mathbf{M}}\tau} \stackrel{\text{def}}{=} \sum_{m=0}^{\infty} \widetilde{\mathbf{Y}}_m \tag{5.14b}$$

and

$$\widetilde{\mathbf{Y}}_m \stackrel{\text{def}}{=} \begin{cases} \mathbf{E} & m = 0, \\ \frac{(\widetilde{\mathbf{M}}\tau)^m}{m!} & \text{elsewhere.} \end{cases} \tag{5.14c}$$

Solution Verification

We will now show that our matrix exponential solution satisfies the nuclide field equation by substituting our proposed solution, Eq. (5.14), into the integrated nuclide field equation, Eq. (5.13), with our fixed $\widetilde{\mathbf{M}} = \widetilde{\mathbf{M}}(t_a + \frac{\tau}{2})$.

$$\begin{aligned}
\vec{\eta}_b - \vec{\eta}_a &= \widetilde{\mathbf{M}} \int_{t_a}^{t_b} \vec{\eta}(t')\, dt' \\
e^{\widetilde{\mathbf{M}}\tau}\vec{\eta}_a - \vec{\eta}_a &= \widetilde{\mathbf{M}} \int_{t_a}^{t_b} \vec{\eta}(t')\, dt' \\
\sum_{m=1}^{\infty} \widetilde{\mathbf{Y}}_m \vec{\eta}_a &= \widetilde{\mathbf{M}} \int_{t_a}^{t_b} e^{\widetilde{\mathbf{M}}\tau'} \vec{\eta}_a\, dt' \\
\sum_{m=1}^{\infty} \widetilde{\mathbf{Y}}_m \vec{\eta}_a &= \widetilde{\mathbf{M}}\tau\vec{\eta}_a + \sum_{m=1}^{\infty} \frac{\widetilde{\mathbf{M}}^{m+1}}{m!} \vec{\eta}_a \int_0^{\tau} (\tau')^m\, d\tau' \\
\sum_{m=1}^{\infty} \widetilde{\mathbf{Y}}_m &= \widetilde{\mathbf{M}}\tau + \sum_{m=1}^{\infty} \frac{\widetilde{\mathbf{M}}^{m+1}\tau^{m+1}}{m+1!}
\end{aligned}$$

$$\begin{aligned}
\sum_{m=1}^{\infty} \widetilde{\mathbf{Y}}_m &= \sum_{m=0}^{\infty} \frac{\widetilde{\mathbf{M}}^{m+1}\tau^{m+1}}{m+1!} \\
\sum_{m=1}^{\infty} \widetilde{\mathbf{Y}}_m &= \sum_{m=0}^{\infty} \widetilde{\mathbf{Y}}_{m+1} \\
\sum_{m=1}^{\infty} \widetilde{\mathbf{Y}}_m &= \sum_{m=1}^{\infty} \widetilde{\mathbf{Y}}_m
\end{aligned}$$

Thus the matrix exponential solution as stated in Eq. (5.14) satisfies the system of first order ODEs integrated in Eq. (5.13).

Matrix Exponential Series Properties 1: Convergence

So we know that the matrix exponential is a solution to Eq. (5.10). Now let us show the series we have defined converges by showing that the ratio of the matrix norms of successive terms goes to zero,

$$\lim_{m\to\infty} \frac{\left\|\widetilde{\mathbf{Y}}_m\right\|}{\left\|\widetilde{\mathbf{Y}}_{m-1}\right\|} = 0. \tag{5.15}$$

We begin with the left side of Eq. (5.15), substitute the definition of $\widetilde{\mathbf{Y}}_m$, and use the law of norms, $\|xy\| \leq \|x\|\,\|y\|$,

$$\begin{aligned}
\lim_{m\to\infty} \frac{\left\|\widetilde{\mathbf{Y}}_m\right\|}{\left\|\widetilde{\mathbf{Y}}_{m-1}\right\|} &= \lim_{m\to\infty} \frac{\left\|\frac{\left(\widetilde{\mathbf{M}}\tau\right)^m}{m!}\right\|}{\left\|\frac{\left(\widetilde{\mathbf{M}}\tau\right)^{m-1}}{(m-1)!}\right\|} \\
&= \lim_{m\to\infty} \frac{\frac{1}{m!}\left\|\left(\widetilde{\mathbf{M}}\tau\right)^m\right\|}{\frac{1}{(m-1)!}\left\|\left(\widetilde{\mathbf{M}}\tau\right)^{m-1}\right\|} \\
&= \lim_{m\to\infty} \frac{1}{m}\frac{\left\|\left(\widetilde{\mathbf{M}}\tau\right)^m\right\|}{\left\|\left(\widetilde{\mathbf{M}}\tau\right)^{m-1}\right\|} \\
&\leq \lim_{m\to\infty} \frac{1}{m}\frac{\left\|\left(\widetilde{\mathbf{M}}\tau\right)^{m-1}\right\|\left\|\widetilde{\mathbf{M}}\tau\right\|}{\left\|\left(\widetilde{\mathbf{M}}\tau\right)^{m-1}\right\|} \\
\lim_{m\to\infty} \frac{\left\|\widetilde{\mathbf{Y}}_m\right\|}{\left\|\widetilde{\mathbf{Y}}_{m-1}\right\|} &\leq \lim_{m\to\infty} \frac{\left\|\widetilde{\mathbf{M}}\tau\right\|}{m}
\end{aligned} \tag{5.16a}$$

$$\lim_{m\to\infty} \frac{\left\|\widetilde{\mathbf{Y}}_m\right\|}{\left\|\widetilde{\mathbf{Y}}_{m-1}\right\|} \quad \leq \quad 0. \tag{5.16b}$$

and because norms are always positive, the inequality in Eq. (5.16b) is actually an equality, which proves convergence of the matrix exponential series by Eq. (5.15).

Matrix Exponential Series Properties 2: The Hump

To calculate the matrix exponential, as with any series, one must truncate the series and know the effect of that truncation—i.e. what is neglected in the truncation. To investigate *how* the matrix exponential series converges, we shall consider the ratio of two successive terms as in Eq. (5.16a)—but *not* in the limit as m approaches infinity,

$$\frac{\left\|\widetilde{\mathbf{Y}}_m\right\|}{\left\|\widetilde{\mathbf{Y}}_{m-1}\right\|} \leq \frac{\left\|\widetilde{\mathbf{M}}\,\tau\right\|}{m}. \tag{5.17}$$

If $\frac{\|\widetilde{\mathbf{Y}}_m\|}{\|\widetilde{\mathbf{Y}}_{m-1}\|} > 1$, the series is *increasing*. If $\frac{\|\widetilde{\mathbf{Y}}_m\|}{\|\widetilde{\mathbf{Y}}_{m-1}\|} < 1$, the series is *decreasing*. Because $\left\|\widetilde{\mathbf{M}}\,\tau\right\|$ is simply a fixed number, we are guaranteed that eventually with some m, the series will be decreasing. Once we know the series is decreasing, we can think about truncation, making the argument that what we will truncate is small compared to what we have kept. However, by Eq. (5.17), it is quite possible that terms increase in magnitude before they decrease. This is called the *hump phenomenon*—when the numerator, $(\widetilde{\mathbf{M}}\,\tau)^m$, dominates the denominator, $m!$, for a number of terms. The practical concern is where the hump lies. If we cannot estimate its position a priori—or cannot guarantee we pass over it in a certain number of terms—we may be required to calculate billions of terms, each with one more matrix multiplication than the last, in order to crest the hump. Luckily, we avoid this possibility with the matrix exponential property of *scalability*.

Matrix Exponential Series Property 3: Scalability

We cannot overstate the usefulness of scalability with the matrix exponential. This is the property that makes the efficient computation of the matrix exponential possible for a wide range of $\widetilde{\mathbf{M}}\tau$. For some real scaling factor, q, we can write

$$e^{\widetilde{\mathbf{M}}\,\tau} = e^{\left(\widetilde{\mathbf{M}}\,\tau/q\right)^q},$$

which is true for all scaling factors q. If we choose a special scaling factor, $q = 2^r$, where r is some integer, then we can utilize a procedure called "scaling and squaring". In this procedure, we

1. modify the time step from τ to τ/q,
2. calculate $e^{\widetilde{\mathbf{M}}\tau/q}$, and then
3. repeatedly square the resultant matrix r times to obtain the exponential matrix for the full time step, $e^{\widetilde{\mathbf{M}}\tau} = e^{\left(\widetilde{\mathbf{M}}\tau/q\right)^{2^r}}$, with a substantial reduction in required matrix multiplications.

An especially wise choice of scaling factor q is such that term m_{hump} of the series is guaranteed to be over the hump,

$$\frac{\left\|\widetilde{\mathbf{Y}}_{m_{\text{hump}}}\right\|}{\left\|\widetilde{\mathbf{Y}}_{m_{\text{hump}}-1}\right\|} < 1.$$

From Eq. (5.17), let us use the maximum value of the ratio of successive terms (the most restrictive case),

$$\frac{\left\|\widetilde{\mathbf{M}}\tau/q\right\|}{m_{\text{hump}}} < 1,$$

to choose q in the following way,

$$q > \frac{\left\|\widetilde{\mathbf{M}}\tau\right\|}{m_{\text{hump}}}. \tag{5.18}$$

We should require that q is a power of 2 to take advantage of the repeated squaring algorithm and that we bypass the hump by term $m_{\text{hump}} = 1$ and we have

$$r = \log_2 \left\|\widetilde{\mathbf{M}}\tau\right\| + 1, \tag{5.19a}$$

$$q = 2^r\ . \tag{5.19b}$$

Truncation Error

Now we must truncate the infinite series after some finite number of terms. In [5], the truncation error ξ_{trc} associated with considering only N terms of the matrix exponential series satisfies

$$\left\|\widetilde{\mathbf{Y}}^{(N)} - e^{\widetilde{\mathbf{M}}\tau/q}\right\| \leq \left(\frac{\|\widetilde{\mathbf{M}}\|^{N+1}}{(N+1)!}\right)\left(\frac{1}{q/\tau - \|\widetilde{\mathbf{M}}\|/(N+2)}\right) \leq \xi_{\text{trc}}$$

where $\widetilde{\mathbf{Y}}^{(N)}$ is the sum of all terms up to term N, defined by

$$\widetilde{\mathbf{Y}}^{(N)} \stackrel{\text{def}}{=} \mathbf{E} + \sum_{m=1}^{N} \frac{\left(\widetilde{\mathbf{M}}\tau\right)^m}{q^m m!}.$$

Therefore, we should truncate the series when the expression below is true to achieve an absolute truncation error less than ξ_{trc} for the scaled matrix exponential.

$$\left(\frac{\|\widetilde{\mathbf{M}}\|^{N+1}}{(N+1)!}\right)\left(\frac{1}{q/\tau - \|\widetilde{\mathbf{M}}\|/(N+2)}\right) \leq \xi_{\text{trc}} \tag{5.20}$$

Roundoff Error

Now we shall consider the roundoff error associated with the repeated matrix multiplies necessary to scale our intermediate matrix exponential, $e^{\widetilde{\mathbf{M}}\tau/q}$, to the full time step matrix exponential, $e^{\widetilde{\mathbf{M}}\tau}$. According to scaling-and-squaring, accounting for finite precision arithmetic with machine precision ξ_{eps}, the following is true:

$$(1 \pm \xi_{\text{tol}})\vec{\eta}_b = \left((1 \pm \xi_{\text{eps}})(e^{\widetilde{\mathbf{M}}\tau/q} \pm \xi_{\text{trc}})\right)^{2^r} (1 \pm \xi_{\text{eps}})\vec{\eta}_a, \tag{5.21}$$

where ξ_{trc} is the truncation error discussed in the previous section and ξ_{tol} is some error tolerance on the solution specified as input to `MATEXPSS`. Let us neglect the terms of order greater than $O(\xi)$ to get

$$\vec{\eta}_b = \left((1 \pm \xi_{\text{eps}})e^{\widetilde{\mathbf{M}}\tau/q} \pm \xi_{\text{trc}}\right)^{2^r} (1 \pm \xi_{\text{eps}})\vec{\eta}_a. \tag{5.22}$$

Now let us perform the first squaring to get

$$(1 \pm \xi_{\text{tol}})\vec{\eta}_b = \left((1 \pm \xi_{\text{eps}})^2 e^{2\widetilde{\mathbf{M}}\tau/q} \pm 2\xi_{\text{trc}}(1 \pm \xi_{\text{eps}})e^{\widetilde{\mathbf{M}}\tau/q} + \xi_{\text{trc}}^2\right)^{2^{r-1}} (1 \pm \xi_{\text{eps}})\vec{\eta}_a$$

and neglect the terms of order greater than $O(\xi)$ to get

$$(1 \pm \xi_{\text{tol}})\vec{\eta}_b = \left((1 \pm 2\xi_{\text{eps}})e^{2\widetilde{\mathbf{M}}\tau/q} \pm 2\xi_{\text{trc}}e^{\widetilde{\mathbf{M}}\tau/q}\right)^{2^{r-1}} (1 \pm \xi_{\text{eps}})\vec{\eta}_a.$$

We repeat this process over and over to arrive at the expression

$$(1 \pm \xi_{\text{tol}})\vec{\eta}_b = \left((1 \pm q\xi_{\text{eps}})e^{\widetilde{\mathbf{M}}\tau} \pm q\xi_{\text{trc}}e^{\widetilde{\mathbf{M}}\tau(q-1)/q}\right)(1 \pm \xi_{\text{eps}})\vec{\eta}_a,$$

and then simplify to obtain

$$(1 \pm \xi_{\text{tol}})\vec{\eta}_b \quad = \quad \left(1 \pm q\xi_{\text{eps}} \pm q\xi_{\text{trc}}e^{-\widetilde{\mathbf{M}}\tau/q} \pm \xi_{\text{eps}}\right)e^{\widetilde{\mathbf{M}}\tau}\vec{\eta}_a$$

which means $\xi_{\text{tol}} = \left(q\xi_{\text{eps}} \pm q\xi_{\text{trc}} e^{-\widetilde{\mathbf{M}}\tau/q} \pm \xi_{\text{eps}}\right)$. But let us assume the worst so we get a simple expression:

$$\xi_{\text{tol}} = \left((1+q)\xi_{\text{eps}} + q\xi_{\text{trc}} \left\| e^{-\widetilde{\mathbf{M}}\tau/q} \right\|\right), \tag{5.23}$$

with ξ_{eps} specified by the machine and ξ_{trc} calculated by

$$\xi_{\text{trc}} = \left(\frac{\|\widetilde{\mathbf{M}}\|^{N+1}}{(N+1)!}\right)\left(\frac{1}{q/\tau - \|\widetilde{\mathbf{M}}\|/(N+2)}\right).$$

However, using Eq. (5.23) to determine N may demand a significant increase in computational burden to calculate $\left\| e^{-\widetilde{\mathbf{M}}\tau/q} \right\|$. Let us use more laws of norms to arrive at a more agreeable expression for $\left\| e^{-\widetilde{\mathbf{M}}\tau/q} \right\|$.

$$\left\| e^{-\widetilde{\mathbf{M}}\tau/q} \right\| = \left\| \sum_{m=0}^{\infty} \frac{\left(-\widetilde{\mathbf{M}}\tau\right)^m}{q^m m!} \right\| \leq \sum_{m=0}^{\infty} \frac{\left\| \left(-\widetilde{\mathbf{M}}\tau\right)^m \right\|}{q^m m!} \leq \sum_{m=0}^{\infty} \frac{\left\| \widetilde{\mathbf{M}}\tau \right\|^m}{q^m m!}$$

Because our scaling procedure requires $\left\| \widetilde{\mathbf{M}}\tau \right\| / q < 1$, we can assume the worst case, $\left\| \widetilde{\mathbf{M}}\tau \right\| / q = 1$, and thus the normed series becomes

$$\left\| e^{-\widetilde{\mathbf{M}}\tau/q} \right\| \leq \sum_{m=0}^{\infty} \frac{1}{m!},$$

which is the series representation of the number $e = 2.71828....$ So we now can write an expression (simplified using $\left\| \widetilde{\mathbf{M}}\tau \right\| / q = 1$ again) which we may evaluate *a priori* to choose q by Eq. (5.19) and choose N to achieve a solution within tolerance, ξ_{tol},

$$\left((1+q)\xi_{\text{eps}} + 2.71828\left(\frac{\|\widetilde{\mathbf{M}}\|^N}{(N+1)!}\right)\left(\frac{1}{1-1/(N+2)}\right)\right) \leq \xi_{\text{tol}}. \tag{5.24}$$

Summary of the Matrix Exponential Method

1. The matrix exponential is a solution to a system of first order ODEs like our nuclide field equation, Eq. (5.10), with transmutation coefficient matrix fixed at the interval midpoint over an interval, $\{\,\widetilde{\mathbf{M}}\,\}_{ii}^{j} = \{\,\widetilde{\mathbf{M}}(t_{j-1/2})\,\}_{ii}^{j}$.

2. The series may exhibit an increasing trend for a number of terms before the $m!$ in the denominator starts to dominate the numerator (hump phenomenon).

3. The matrix exponential may be scaled such that term m_{hump} of the series is guaranteed to be over the hump. For example, if we choose $m_{\text{hump}} = 1$, then we are guaranteed the first term of the series will be over the hump if

$$\begin{aligned} r &= \log_2 \left\| \{ \widetilde{\mathbf{M}} \}_{ii}^{j} \, \tau_j \right\| + 1, \\ q &= 2^r \, . \end{aligned}$$

4. Once we calculate the matrix exponential for a scaled time step, $e^{\{ \widetilde{\mathbf{M}} \}_{ii}^{j} \, \tau_j / q}$, we may square the scaled time step matrix r times to determine the full time step matrix exponential.

$$e^{\{ \widetilde{\mathbf{M}} \}_{ii}^{j} \, \tau_j} = \left(e^{\{ \widetilde{\mathbf{M}} \}_{ii}^{j} \, \tau_j / q} \right)^{2^r}$$

5. The series representation of the matrix exponential is a convergent series for all $\{ \widetilde{\mathbf{M}} \}_{ii}^{j}$ and τ_j.

6. We may choose when to truncate the series expansion to achieve a given tolerance, ξ_{tol}, by using Eq. (5.24).

7. For any time step, $\tau_j = t_j - t_{j-1}$,the matrix exponential solution of end-of-interval nuclide concentrations, ${}_k\{ \eta(t_j) \}_i^j$, is

$$\{ \vec{\eta}(t_j) \}_i^j = e^{\{ \widetilde{\mathbf{M}} \}_{ii}^{j} \tau_j} \, \{ \vec{\eta}(t_{j-1}) \}_i^j \, . \tag{5.25}$$

5.5.3 2^{nd} Order Rosenbrock Method with Complex Coefficients

This Rosenbrock method of solving systems of ODEs may be thought of as one of the initial-final-weighting scheme which approximates an integral as some weighted sum of the initial and final values of the integrand. Consider the following simple system, $d\eta(t)/dt = \lambda\eta(t)$ for $t_a < t \leq t_b$ with initial condition $\eta(t_a) = \eta_a$. This ODE has a solution given by

$$\eta_b = \eta_a + \left[\, \lambda\eta \, \right]_\tau$$

where time step, $\tau = t_b - t_a$. If we use an initial-final-weighting scheme we get a solution of the form

$$\eta_b = \eta_a + \left(\frac{1+\gamma}{2} \eta_a + \frac{1-\gamma}{2} \eta_b \right) \tau$$

where γ is some weight. If we use $\gamma = \imath$, where $\imath$ is the imaginary number $\sqrt{-1}$, then we get the 2^{nd} order Rosenbrock method.

A Derivation

We now present a derivation of this Rosenbrock Method for solving systems of first order ODEs. Note that this is not the way that this Rosenbrock Method was originally presented by H. H. Rosenbrock [3], where it was simply stated as a family of schemes with unknown coefficients. With our notation, choosing coefficients $\gamma = \imath$ and fixing the transmutation coefficient matrix $\widetilde{\mathbf{M}}(t)$ at its middle-of-interval value, $\widetilde{\mathbf{M}} = \widetilde{\mathbf{M}}(t_a + \frac{\tau}{2})$, leads to the *only* one-stage method in this family which is of second order and both L-monotonous and L-decremented [9]. For our "derivation", let us start with the integration of Eq. (5.10) over some time interval τ,

$$\vec{\eta}_b = \vec{\eta}_a + \widetilde{\mathbf{M}} \left[\, \vec{\eta}(t) \, \right]_\tau . \tag{5.26}$$

Now let's use our initial-final-weighting scheme with $\gamma = \imath$ to evaluate the integral of $\vec{\eta}$. Our choice of γ causes Eq. (5.26) to have complex values—$\vec{\eta}$ is the real-valued solution to Eq. (5.26) while $\vec{u}$ is the complex-valued solution of

$$\vec{u}_b = \vec{u}_a + \widetilde{\mathbf{M}} \left(\frac{1+\imath}{2} \, \vec{u}_a + \frac{1-\imath}{2} \, \vec{u}_b \right) \tau, \tag{5.27}$$

$$\vec{\eta}_b = \mathrm{Re} \left[\, \vec{u}_b \, \right].$$

The above system may be solved many ways—we choose to define $\Delta\vec{u} \stackrel{\text{def}}{=} \vec{u}_b - \vec{u}_a$ [4] and reorganize Eq. (5.27) to obtain

$$\left(\mathbf{E} - \frac{1+\imath}{2} \widetilde{\mathbf{M}} \tau \right) \Delta\vec{u} = \widetilde{\mathbf{M}} \tau \, \vec{\eta}_a,$$

where we have used the fact that our initial vector is always real, $\vec{u}_a = \vec{\eta}_a$. Thus the 2^{nd} order Rosenbrock method with complex coefficients is fully specified by

$$\Delta\vec{u} = \left(\mathbf{E} - \frac{1+\imath}{2} \widetilde{\mathbf{M}} \tau \right)^{-1} \left(\widetilde{\mathbf{M}} \tau \, \vec{\eta}_a \right), \tag{5.28}$$

$$\vec{\eta}_b = \mathrm{Re} \left[\, \Delta\vec{u} \, \right] + \vec{\eta}_a.$$

Summary of the 2^{nd} Order Rosenbrock Method with Complex Coefficients

1. The 2^{nd} order Rosenbrock method with complex coefficients is an efficient one stage method which is both L-monotonous and L-decremented—both properties well-suited to solving SODEs.

2. To preserve the second order accuracy of the method, the transmutation coefficient matrix must be fixed at the midpoint of the interval, $\{\,\widetilde{\mathbf{M}}\,\}_{ii}^{j} = \{\,\widetilde{\mathbf{M}}(t_{j-1/2})\,\}_{ii}^{j}$.

3. For any time step, $\tau_j = t_j - t_{j-1}$, the solution is given in terms of auxiliary complex solution $\Delta\vec{u}$, as in [4]

$$\{\,\Delta\vec{u}(t_j)\,\}_i^j = \left(\mathbf{E} - \frac{1+\imath}{2}\,\{\,\widetilde{\mathbf{M}}\,\}_{ii}^{j}\,\tau_j\right)^{-1}\left(\,\{\,\widetilde{\mathbf{M}}\,\}_{ii}^{j}\,\tau_j\;\{\,\vec{\eta}(t_{j-1})\,\}_i^j\right), \tag{5.29}$$

$$\{\,\vec{\eta}(t_j)\,\}_i^j = \mathrm{Re}\left[\,\{\,\Delta\vec{u}(t_j)\,\}_i^j\,\right] + \{\,\vec{\eta}(t_{j-1})\,\}_i^j\,.$$

Chapter 6

Sensitivity Analysis Methods

In the following sections we will discuss three sensitivity analysis methods applied to our set of reactor physics equations for reactor cycle calculations developed in the previous chapter. First we will reorganize the reactor cycle equations so that there is no division of terms and most terms reside on the left side. Then we will discuss the following sensitivity analysis methods:

1. direct perturbation of data and recalculation (DPAR) of perturbed solution $\vec{x}'$,
2. calculation of first variation in solutions, $\delta\vec{x}$, via a modified forward system (MFS), and
3. calculation of auxiliary solutions, $\delta\vec{x}^*$, via an adjoint system (AS) to the MFS—with the AS we can calculate the first variation in any response, δr_s.

Note that we do not consider the transverse-integrated NEM equations in our description of the system, nor do we consider thermal hydraulics (T/H) feedback parameters (coolant density, coolant temperature, fuel temperature, etc.) These T/H and NEM equations are solved by NESTLE for the forward system only. In other words, we assume that, compared to neutron and nuclide distributions, perturbations in data have a negligible impact on T/H parameters and NEM current corrections.

6.1 Forward System

The forward system (or main system) for which we will analyze sensitivities has a neutron field equation of the form

$$\{\,\widetilde{\mathbf{B}}\,\}^j\ \{\,\vec{\varphi}\,\}^j\ = 0 \tag{6.1}$$

i. with amplitude function

$$\Big[\ \{\,\vec{p}\,\}^j\ \Big]_V\ \ \{\,\Phi\,\}^j\ = p_{core}$$

ii. for times t_j, $j = 0, ..., N_j$ with initial condition $\{\,\vec{\eta}(t_0)\,\}^0\ = \vec{\eta}_0$

iii. with eigenvalue

$$\{\,k_e\,\}^j\ = \frac{\Big[\ \{\,\widetilde{\mathbf{F}}\,\}^j\ \{\,\vec{\varphi}\,\}^j\ \Big]_{i,\epsilon}}{\Big[\ \{\,\widetilde{\mathbf{L}}\,\}^j\ \{\,\vec{\varphi}\,\}^j\ \Big]_{i,\epsilon}}$$

where we have defined a new diffusion operator, $\{\,\widetilde{\mathbf{B}}\,\}^j$ which combines the loss and fission operators,

$$\{\,\widetilde{\mathbf{B}}\,\}^j\ \stackrel{\text{def}}{=}\ \{\,k_e\,\}^j\ \{\,\widetilde{\mathbf{L}}\,\}^j\ -\ \{\,\widetilde{\mathbf{F}}\,\}^j\,. \tag{6.2}$$

The form of the nuclide field equations for which we will analyze sensitivities is given by nuclide field equations below.

$$\frac{d}{dt}\,\{\,\vec{\eta}(t)\,\}_i^j\ -\ \{\,\widetilde{\mathbf{M}}\,\}_{ii}^j\ \{\,\vec{\eta}(t)\,\}_i^j\ = 0 \tag{6.3}$$

i. from $t_{j-1} < t \le t_j$, for $j = 1, ..., N_j$, with initial/interval condition

$$\{\,\vec{\eta}(t_{j-1})\,\}_i^j\ = \begin{cases} \{\,\vec{\eta}_0\,\}_i & j = 1 \\ \{\,\vec{\eta}(t_{j-1})\,\}_i^{j-1} & j = 2, ..., N_j \end{cases}$$

ii. for nodes $i = 1, ..., N_{dom}$

The forward system may be put in a compact form using master matrix $\widetilde{\mathbf{A}}$ and master solution vector $\vec{x}$,

$$\widetilde{\mathbf{A}}\ \vec{x} = \vec{q}. \tag{6.4}$$

The master matrix $\widetilde{\mathbf{A}}$ is a block diagonal matrix of the form

$$\widetilde{\mathbf{A}} \stackrel{\text{def}}{=} \begin{pmatrix} \{\,\widetilde{\mathbf{A}}\,\}^0 & 0 & 0 & 0 & 0 & 0 \\ 0 & \{\,\widetilde{\mathbf{A}}\,\}^1 & 0 & 0 & 0 & 0 \\ 0 & 0 & \ddots & 0 & 0 & 0 \\ 0 & 0 & 0 & \{\,\widetilde{\mathbf{A}}\,\}^j & 0 & 0 \\ 0 & 0 & 0 & 0 & \ddots & 0 \\ 0 & 0 & 0 & 0 & 0 & \{\,\widetilde{\mathbf{A}}\,\}^{N_j} \end{pmatrix}, \tag{6.5}$$

the master solution vector $\vec{x}$ is a column vector of the form

$$\vec{x} \stackrel{\text{def}}{=} \left(\,\{\,\vec{x}\,\}^0,\,\{\,\vec{x}\,\}^1,\ldots,\,\{\,\vec{x}\,\}^j,\ldots,\,\{\,\vec{x}\,\}^{N_j}\,\right)^T, \tag{6.6}$$

and the master source vector $\vec{q}$ is a column vector of the form

$$\vec{q} \stackrel{\text{def}}{=} \left(\,\{\,\vec{q}\,\}^0,\,\{\,\vec{q}\,\}^1,\ldots,\,\{\,\vec{q}\,\}^j,\ldots,\,\{\,\vec{q}\,\}^{N_j}\,\right)^T. \tag{6.7}$$

At time t_j, the solution vector $\{\,\vec{x}\,\}^j$ has the form

$$\{\,\vec{x}\,\}^j \stackrel{\text{def}}{=} \left(\,\{\,\vec{\eta}(t)\,\}^j,\,\{\,\vec{\varphi}\,\}^j,\,\{\,\Phi\,\}^j\,\right)^T, \tag{6.8}$$

the matrix $\{\,\widetilde{\mathbf{A}}\,\}^0$ has the form

$$\{\,\widetilde{\mathbf{A}}\,\}^0 \stackrel{\text{def}}{=} \begin{pmatrix} 2\delta(t-t_0)\mathbf{E} & 0 & 0 \\ 0 & \{\,\widetilde{\mathbf{B}}\,\}^0 & 0 \\ 0 & 0 & \{\,\vec{p}\,\}^0 \end{pmatrix}, \tag{6.9}$$

while the matrices $\{\,\widetilde{\mathbf{A}}\,\}^j$, $j = 1, ..., N_j$, has the form

$$\{\,\widetilde{\mathbf{A}}\,\}^j \stackrel{\text{def}}{=} \begin{pmatrix} \frac{d}{dt} - \{\,\widetilde{\mathbf{M}}\,\}^j & 0 & 0 \\ 0 & \{\,\widetilde{\mathbf{B}}\,\}^j & 0 \\ 0 & 0 & \{\,\vec{p}\,\}^j \end{pmatrix}, \tag{6.10}$$

and the source vector $\{\,\vec{q}\,\}^0$ has the form

$$\{\,\vec{q}\,\}^0 \stackrel{\text{def}}{=} \left(\,2\delta(t-t_0)\vec{\eta}_0\,,\,0\,,\,p_{core}\,\right)^T \tag{6.11}$$

while the source vector $\{\,\vec{q}\,\}^j$, $j = 1, ..., N_j$ has the form

$$\{\,\vec{q}\,\}^j \quad \stackrel{\text{def}}{=} \quad (\,0\,,\,0\,,\,p_{core}\,)^T\,. \tag{6.12}$$

Probably, the only surprising element of these equations is the $2\delta(t - t_0)\mathbf{E}$ in the equation for $j = 0$. We include this term because we wish the solution vectors at all times to have the same 3 components and there is no equation to solve for the nuclide field at t_0 so we fabricate this simple condition that when integrated over some bounds which include t_0, we obtain the initial condition for the nuclide field, $\{\,\vec{\eta}(t_0)\,\}^0 = \vec{\eta}_0$. We want solution vectors (and matrices) to have the same form for all t_j because this facilitates taking the transpose of the system which we will do when we develop the adjoint system equations.

6.2 The Response Functional

6.2.1 A General Response Functional r_s

Let us define the following master inner product for master vector $\vec{x}$,

$$\left\langle \vec{x}_1\,,\,\vec{x}_2 \right\rangle_x \stackrel{\text{def}}{=} \left\langle \vec{\eta}_1(t)\,,\,\vec{\eta}_2(t) \right\rangle_\eta + \left\langle \vec{\varphi}_1\,,\,\vec{\varphi}_2 \right\rangle_\varphi + \left\langle \vec{\Phi}_2\,,\,\vec{\Phi}_2 \right\rangle_\Phi \tag{6.13}$$

where we will define the component inner products for η, φ, and Φ shortly. Once we have solved the forward problem defined by Eq. (6.4), we can evaluate a response, r_s, given in terms of a "direct effect" $\left\langle\ ,\ \right\rangle_\alpha$ and an "indirect effect" $\left\langle\ ,\ \right\rangle_x$,

$$r_s = r_s\,[\,\vec{\alpha}\,,\vec{x}\,] = \left\langle \vec{h}_{s,\alpha}\,,\,\vec{\alpha} \right\rangle_\alpha + \left\langle \vec{h}_{s,x}\,,\,\vec{x} \right\rangle_x. \tag{6.14}$$

Let us use the definition in Eq. (6.13) to break the inner product in Eq. (6.14) into its η, φ, and Φ components,

$$\begin{aligned} r_s = r_s\,[\,\vec{\alpha}\,,\vec{x}\,] \quad = \quad & \left\langle \vec{h}_{s,\alpha}\,,\,\vec{\alpha} \right\rangle_\alpha + && \text{(6.15a)} \\ & \left\langle \vec{h}_{s,\eta}(t)\,,\,\vec{\eta}(t) \right\rangle_\eta + && \text{(6.15b)} \\ & \left\langle \vec{h}_{s,\varphi}\,,\,\vec{\varphi} \right\rangle_\varphi + && \text{(6.15c)} \\ & \left\langle \vec{h}_{s,\Phi}\,,\,\vec{\Phi} \right\rangle_\Phi. && \text{(6.15d)} \end{aligned}$$

If we perturb $\vec{\alpha} \rightarrow \vec{\alpha}\,'$, then we have a perturbed response,

$$\begin{aligned}
\{\, r_s{}' \,\}_p \;=\; r_s\,[\,\vec{\alpha}\,'\,,\vec{x}\,'\,] \quad &= \quad \Big\langle\, \vec{h}_{s,\alpha}\,,\, \vec{\alpha}\,' \,\Big\rangle_{\alpha} + && (6.16a)\\
&\quad\; \Big\langle\, \vec{h}_{s,\eta}(t)\,,\; \{\, \vec{\eta}\,'(t)\,\}_p \,\Big\rangle_{\eta} + && (6.16b)\\
&\quad\; \Big\langle\, \vec{h}_{s,\varphi}\,,\; \{\, \vec{\varphi}\,'\,\}_p \,\Big\rangle_{\varphi} + && (6.16c)\\
&\quad\; \Big\langle\, \vec{h}_{S,\Phi}\,,\; \{\, \vec{\Phi}\,'\,\}_p \,\Big\rangle_{\Phi}. && (6.16d)
\end{aligned}$$

The inner products for the 3 components are defined by

$$\begin{aligned}
\Big\langle\, \vec{\varphi}_1\,,\, \vec{\varphi}_2 \,\Big\rangle_{\varphi} \quad &= \quad \Big[\, \vec{\varphi}_1\; \vec{\varphi}_2 \,\Big]_{j,g,i} && (6.17a)\\
&= \quad \sum_{j=0}^{N_j} \sum_{g=1}^{N_g} \sum_{i=1}^{N_{dom}} V_i\; {}^{g}\{\, \varphi_1 \,\}_i^j\; {}^{g}\{\, \varphi_2 \,\}_i^j\,,\\
\Big\langle\, \vec{\Phi}_1\,,\, \vec{\Phi}_2 \,\Big\rangle_{\Phi} \quad &= \quad \Big[\, \vec{\Phi}_1\; \vec{\Phi}_2 \,\Big]_{j}\\
&= \quad \sum_{j=0}^{N_j} \{\, \Phi_1 \,\}^j \;\; \{\, \Phi_2 \,\}^j\,, && (6.17b)\\
\Big\langle\, \vec{\eta}_1(t)\,,\, \vec{\eta}_2(t) \,\Big\rangle_{\eta} \quad &= \quad \Big[\, \vec{\eta}_1(t)\, \vec{\eta}_2(t) \,\Big]_{j,k,i,\tau_j} && (6.17c)\\
&= \quad \sum_{j=1}^{N_j} \sum_{k=1}^{N_k} \sum_{i=1}^{N_{dom}} V_i \int_{t_{j-1}}^{t_j} {}_{k}\{\, \eta_1(t) \,\}_i^j\; {}_{k}\{\, \eta_2(t) \,\}_i^j\; dt.
\end{aligned}$$

6.2.2 Some Specific Responses

In this section we shall introduce the necessary realization vectors, $\vec{h}$, to evaluate some specific responses.

The End Of Cycle Nuclide Response $r_\ell\,[\,\vec{\eta}\,]$

Now let us introduce a specific response $s = \ell$, the number of nuclide ℓ in the core at EOC,

$$r_\ell\,[\,\vec{\eta}\,] \;=\; \Big\langle\, \vec{h}_{\eta,\ell}(t)\,,\, \vec{\eta}(t) \,\Big\rangle_{\eta}. \tag{6.18}$$

where $\{\, \vec{h}_{\eta}(t) \,\}_\ell$ is the realization vector given by

$$ {}_{k}\{\, h_{\eta,\ell}(t) \,\}_i^j \;\stackrel{\text{def}}{=}\; 2\delta(t - t_N)\; \delta_{\ell,k}\; \delta_{j,N_j}. \tag{6.19a}$$

Note that the EOC nuclide response does not have a "direct effect" part. Using the realization vector $\vec{h}_{\eta,\ell}(t)$ in the inner product $\left\langle \ , \ \right\rangle_\eta$ produces

$$\left\langle \vec{h}_{\eta,\ell}(t)\,,\,\vec{\eta}(t)\right\rangle_\eta = \left[\ \vec{h}_{\eta,\ell}(t)\,\vec{\eta}(t)\ \right]_{j,k,i,\tau_j} \tag{6.19b}$$

$$= \sum_{j=1}^{N_j}\delta_{j,N_j}\sum_{k=1}^{N_k}\delta_{\ell,k}\sum_{i=1}^{N_{dom}} V_i\int_{t_{j-1}}^{t_j} 2\delta(t-t_N)\ {}_k\{\,\eta(t)\,\}_i^j\ dt \tag{6.19c}$$

$$= \sum_{i=1}^{N_{dom}} V_i\ {}_\ell\{\,\eta(t_N)\,\}_i^{N_j} \tag{6.19d}$$

which verifies that the realization vector $\vec{h}_{\eta,\ell}(t)$ does indeed produce the number of nuclide ℓ in the core at EOC.

The Hazard Index Response $r_{\rm HI}\,[\,\vec{w}_{\rm HI}\,,\vec{\eta}(t)\,]$

The Hazard Index (HI) is meant to be a simple but effective measure of the hazard of SNF, given in the form of a response by

$$r_{\rm HI}\,[\,\vec{w}_{\rm HI}\,,\vec{\eta}(t)\,] = \left\langle \vec{h}_{\eta,{\rm HI}}(t)\,,\,\vec{\eta}(t)\right\rangle_\eta, \tag{6.20}$$

where the realization vector is given by

$${}_k\{\,h_{\eta,{\rm HI}}(t)\,\}_i \stackrel{\rm def}{=} 2\delta(t-t_N)\ \delta_{\ell,k}\ {}_k\{\,w_{\rm HI}\,\}\,, \tag{6.21}$$

where the HI weights are given by

$${}_k\{\,w_{\rm HI}\,\} = \frac{AWI}{{}_k\{\,ALI\,\}},$$

where AWI is the annual water intake of the reference human and ${}_k\{\,ALI\,\}$ is the annual limit on intake of nuclide k [10].

The Total Cancer Dose Response $r_{\rm TCD}\,[\,\vec{w}_{\rm TCD}\,,\vec{\eta}(t)\,]$

The Total Cancer Dose (TCD) is another simple measure for the hazard of SNF, given in the form of a response by

$$r_{\rm TCD}\,[\,\vec{w}_{\rm TCD}\,,\vec{\eta}(t)\,] = \left\langle \vec{h}_{\eta,{\rm TCD}}(t)\,,\,\vec{\eta}(t)\right\rangle_\eta, \tag{6.22}$$

where the realization vector is given by

$$ {}_k\{\, h_{\eta,\mathrm{TCD}}(t)\,\}_i \stackrel{\mathrm{def}}{=} 2\delta(t-t_N)\;\delta_{\ell,k}\;\;{}_k\{\, w_{\mathrm{TCD}}\,\}\,, \tag{6.23} $$

where the TCD weights are given by

$$ {}_k\{\, w_{\mathrm{TCD}}\,\} \;=\; {}_k\{\, TF\,\}\;{}_k\{\, \lambda_{tot}\,\}\,, $$

in terms of toxicity factor, ${}_k\{\, TF\,\}$, for nuclide k [11] and the total decay constants $\vec{\lambda}_{tot}$.

6.2.3 Response Sensitivity

In order to analyze sensitivities of responses, let us write the change in response to first order for response r_s and perturbation p,

$$ \{\, \Delta r_s\,\}_p \;=\; \{\, \delta r_s\,\}_p \;+ O(\delta^2 r_s) \tag{6.24} $$

where δr_s is the 1^{st} variation of r_s about the nominal state. Now let us write the change in response as a Taylor series of our perturbed response about our nominal response and nominal data,

$$ \{\, r_s{}'\,\}_p = r_s + \sum_m \frac{dr_s}{d\,\{\,\alpha\,\}_m}\bigg|_{\vec{\alpha}} \{\, \Delta\alpha\,\}_{m,p} + O(\Delta\alpha^2). \tag{6.25} $$

In this work, only the linear term above is considered with our forward system of reactor cycle equations in order to develop a linearized system of equations [12]. We calculate the first order term of Eq. (6.25) by assuming that $\Delta\alpha$ is small enough to discard higher order terms, then we have a relationship for the first variation δr_s in terms of derivatives of response r_s with respect to data parameter α.

$$ \sum_m \frac{dr_s}{d\,\{\,\alpha\,\}_m}\bigg|_{\vec{\alpha}} \{\, \Delta\alpha\,\}_{m,p} \;=\; \{\, \delta r_s\,\}_p $$

Assuming that we can separate the m-components of δr_s, we can arrive at

$$ \sum_m \frac{dr_s}{d\,\{\,\alpha\,\}_m}\bigg|_{\vec{\alpha}} \{\, \Delta\alpha\,\}_{m,p} = \sum_m \{\, \delta r_s\,\}_{m,p} $$

and then equating each component for data parameter m, we obtain an expression for the response sensitivity, ϱ_s, independently of the perturbation p,

$$ \{\, \varrho_s\,\}_m \stackrel{\mathrm{def}}{=} \frac{dr_s}{d\,\{\,\alpha\,\}_m}\bigg|_{\vec{\alpha}} = \frac{\{\, \delta r_s\,\}_{m,p}}{\{\, \Delta\alpha\,\}_{m,p}}. \tag{6.26} $$

The sensitivity coefficient $\{\, c_s \,\}_m$ may also be useful in analyzing sensitivities,

$$\{\, c_s \,\}_m \stackrel{\text{def}}{=} \frac{\{\, \alpha \,\}_m}{r_s} \left. \frac{dr_s}{d\,\{\, \alpha \,\}_m} \right|_{\vec{\alpha}} = \frac{\{\, \alpha \,\}_m}{r_s} \{\, \varrho_s \,\}_m \,. \tag{6.27}$$

The sensitivity coefficient is basically a relative change in response s per relative change in parameter m often used to rank the importance of system parameters to aid in identifying *key players*—parameters which have a great impact on a certain response of interest. For example, maybe key players satisfy $|\, \{\, c_s \,\}_m \,| > 1$, that is a 1% change in the data parameter produces a greater-than 1% change in the response of interest.

6.2.4 Response Variance

Assuming that the dominant terms of Eq. (6.24) and Eq. (6.25) are the linear ones (the condition for which we can consider first order perturbation theory) we may estimate the variance of responses as per [12] by

$$v_s^2 = \left(\vec{\varrho}_s\right)\left(\widetilde{\mathbf{V}}\right)\left(\vec{\varrho}_s\right)^T \tag{6.28}$$

where $\widetilde{\mathbf{V}}$ is the *covariance matrix* given by

$$\{\, \mathbf{V} \,\}_{mn} = \begin{cases} \{\, \rho_\alpha \,\}_{m,n} \{\, v \,\}_m \{\, v \,\}_n & \text{for } m \neq n \\ \{\, v^2 \,\}_m & \text{for } m = n \end{cases} \tag{6.29}$$

where ρ_α is a correlation coefficient and $\{\, v^2 \,\}_m$ is the variance in input data parameter m. Eq. (6.28) is known colloquially as the *sandwich rule* [12].

6.3 Direct Perturbation and Recalculation (DPAR)

The DPAR methodology is the simplest way to investigate sensitivities and/or propagate uncertainties. Assuming the nominal calculation of the Eq. (6.4) system is already complete, the change in all responses s are given simply by subtracting Eq. (6.15) from Eq. (6.16) to obtain

$$\begin{aligned} \{\, \Delta r_s \,\}_p = & \quad \left\langle \vec{h}_{s,\alpha}\,,\ \{\, \Delta\vec{\alpha} \,\}_p \right\rangle_\alpha \\ & + \left\langle \vec{h}_{s,\eta}\,,\ \{\, \Delta\vec{\eta} \,\}_p \right\rangle_\eta \\ & + \left\langle \vec{h}_{s,\varphi}\,,\ \{\, \Delta\vec{\varphi} \,\}_p \right\rangle_\varphi \\ & + \left\langle \vec{h}_{s,\Phi}\,,\ \{\, \Delta\vec{\Phi} \,\}_p \right\rangle_\Phi \end{aligned} \tag{6.30}$$

where $\{\,\Delta\vec{\alpha}\,\}_p$, $\{\,\Delta\vec{\eta}\,\}_p$, $\{\,\Delta\vec{\varphi}\,\}_p$, and $\{\,\Delta\vec{\Phi}\,\}_p$ are the exact change in quantities which we calculate by perturbing parameters and re-solving Eq. (6.4) for $\{\,\vec{x}\,'\,\}_p$ for each perturbation set p and then using the definition

$$\{\,\Delta\vec{x}\,\}_p \stackrel{\text{def}}{=} \{\,\vec{x}'\,\}_p - \vec{x}. \tag{6.31}$$

6.3.1 Response Surfaces with DPAR

One of the strengths of DPAR is the ability to generate response surfaces. With each perturbation set p we can calculate the perturbed response, $\{\,r_s\,'\,\}_p$, of all N_s responses for the perturbation of input data vector $\vec{\alpha}$ by $\{\,\Delta\vec{\alpha}\,\}_p$. Particularly for searches on values of a few parameters, DPAR may be used effectively to hone in on parameter combinations that do not violate a number of constraints. But for calculating response sensitivities or variances, DPAR may be inefficient because

1. each perturbation set p may contain only one perturbed parameter m' and
2. multiple runs of the same perturbed parameter m' with different perturbations p (1%, 5%, 10%, etc.) should be performed to ensure the *total variation* $\{\,\Delta\vec{x}\,\}_p$ calculated is approximately equal to the *first variation*, $\{\,\delta\vec{x}\,\}_p$.

These two inefficiencies will be discussed in the next section.

6.3.2 Sensitivity Analysis with DPAR

For sensitivity analysis, we must split the first variation for an entire perturbation set $\{\,\delta r_s\,\}_p$ into the sum of components $\sum_{m'}\{\,\delta r_s\,\}_{m',p}$ in order to arrive at the expression for $\{\,\varrho_s\,\}_{m'}$ of Eq. (6.26). In order to do this with DPAR, each perturbation set p may contain only one nonzero component, $\{\,\Delta\alpha\,\}_{m',p}$ so that when the total variation $\{\,\Delta r_s\,\}_p$ is calculated, it is the total variation of the response with respect to only one data parameter m' at a time, $\{\,\Delta r_s\,\}_{m',p}$.

$$\begin{aligned}\{\,\Delta r_s\,\}_{m',p} \;&=\; r_s\,[\,\{\,\Delta\vec{\alpha}\,\}_{m',p}\,,\,\{\,\Delta\vec{x}\,\}_p\,] \\ &\qquad \text{where } \{\,\Delta\alpha\,\}_{m,m',p} = 0 \text{ for } m' \neq m\end{aligned} \tag{6.32}$$

To apply Eq. (6.26), we must also verify that our total variation used a small enough perturbation $\{\,\Delta\alpha\,\}_{m,m',p}$ such that it is approximately equal to the first variation, $\{\,\Delta r_s\,\}_{m',p} \approx$

$\{\,\delta r_s\,\}_{m',p}$—but, the perturbation $\{\,\Delta\alpha\,\}_{m,m',p}$ must not be too small or noise will dominate the calculation.

6.3.3 Uncertainty Propagation with DPAR

Using DPAR to propagate uncertainties has similar problems to using DPAR for sensitivity analysis, because we still need to calculate response sensitivity $\{\,\varrho_s\,\}_{m'}$ with Eq. (6.26). However, for uncertainty propagation, we need the vector of response sensitivities $\vec{\varrho}_s$ for all parameters m' which are present in the covariance matrix $\widetilde{\mathbf{V}}$ in order to calculate response variance, v_s, with the sandwich rule, Eq. (6.28).

6.3.4 DPAR Efficiency Remarks

Again, the upside of DPAR is that all N_s response sensitivities may be calculated with one perturbation run—the downside is that the response sensitivities, $\{\,\varrho_s\,\}_{m'}$, needed for sensitivity analysis or uncertainty propagation require that perturbations in data parameters are performed one at a time.

Sensitivity Analysis

To calculate sensitivities for N_s responses with respect to $N_{m'}$ input data parameters for N_p different perturbation sets, one would need a number of runs given by

$$N_{\text{DPAR-sa}} = N_{m'} \times N_p \text{ efs}$$

where we have introduced the unit (efs) which stands for Equivalent Forward Solutions. In this way we can compare (approximately) the computational advantages of DPAR, MFS, and AS sensitivity analysis methodologies. For example:

- with a case of 100 parameters ($N_m = 100$),
- considering one quarter of them for sensitivity analysis ($N_{m'} = 25$),
- with interest in 20 different responses ($N_s = 20$), and
- requiring 2 different perturbations of each parameter ($N_p = 2$) to make sure we are in the "range of linearity",

we would need $N_{\text{DPAR-sa}} = 25 \times 2 = 50$efs to analyze sensitivities of responses to variations in input data.

Uncertainty Propagation

If we have covariance data for all parameters, then we should propagate all uncertainties (variances), and thus one would need a number of runs given by

$$N_{\text{DPAR-up}} = N_m \times N_p \text{ efs.}$$

For example:

- with a case of 100 parameters ($N_m = 100$),
- considering all of them for uncertainty propagation ($N_{m'} = N_m$), and
- with interest in 20 different responses ($N_s = 20$),

we would need $N_{\text{DPAR-up}} = 100 \times 2 = 200$efs to propagate variances in input data to variances in system responses.

6.4 Modified Forward System (MFS)

The MFS is another way to investigate sensitivities, using a modified form of the forward system of equations in Eq. (6.4) to calculate the derivative term of Eq. (6.26), $\frac{dr_s}{d\{\alpha\}_m}\Big|_{\vec{\alpha}}$, exactly. To determine the MFS equations, we take the unperturbed reactor cycle equations in Eq. (6.4) and subtract this set of equations from the perturbed reactor cycle equations

$$\begin{aligned} \widetilde{\mathbf{B}}'\vec{\varphi}' &= 0 \\ \Phi' p' &= {p_{core}}' \\ \frac{d}{dt}\vec{\eta}'(t) - \widetilde{\mathbf{M}}'\vec{\eta}'(t) &= 0 \end{aligned}$$

where for clarity we have suppressed some notation. Now we carry out the subtraction of perturbed system minus forward system, and linearize by assuming that the perturbation is small, neglecting all terms of order of smallness greater than first. Then we get the following linear system of equations for the first variation.

6.4.1 Equations for the First Variations

The first variation in the neutron field, resulting from linearization of the difference between perturbed and unperturbed forward equations, is given by

$$\left[\{ \vec{b}_\eta(t) \}^j \{ \delta\vec{\eta}(t) \}^j \right]_{k,\tau_j} + \{ \widetilde{\mathbf{B}} \}^j \{ \delta\vec{\varphi} \}^j = - \{ \Delta\vec{b}_\alpha \}^j - \{ \delta k_e \}^j \{ \widetilde{\mathbf{L}} \}^j \{ \vec{\varphi} \}^j \tag{6.33a}$$

i. with amplitude function

$$\left[\{ \vec{p}_\eta(t) \}^j \{ \delta\vec{\eta}(t) \}^j \right]_{i,k,\tau_j} + \left[\{ \vec{p}_\varphi \}^j \{ \delta\vec{\varphi} \}^j \right]_{i,g} + \left[\{ \vec{p} \}^j \right]_i \{ \delta\Phi \}^j = \delta p_{core} - \{ \Delta p_\alpha \}^j$$

ii. for times t_j, $j = 0, ..., N_j$ with initial condition $\{ \delta\vec{\eta}(t_0) \}^0 = \Delta\vec{\eta}_0$

iii. with change in eigenvalue

$$\{ \delta k_e \}^{j'} = \frac{\left\langle \delta_{jj'} \{ \Delta\vec{b}_\alpha \}^j , \{ \vec{\varphi}^* \}^j \right\rangle_\varphi}{\left\langle \delta_{jj'} \{ \widetilde{\mathbf{L}} \}^j \{ \vec{\varphi} \}^j , \{ \vec{\varphi}^* \}^j \right\rangle_\varphi}$$

where the new operators are defined below in the section titled **New Operator Definitions**. The nuclide field equations which result from linearizing Eq. (6.4) are given below.

$$\left(\frac{d}{dt} - \{ \widetilde{\mathbf{M}} \}^j \right) \{ \delta\vec{\eta}(t) \}^j - \{ \widetilde{\mathbf{M}}_{\varphi-}(t) \}^j \{ \delta\vec{\varphi} \}^{j-1} - \{ \widetilde{\mathbf{M}}_{\varphi+}(t) \}^j \{ \delta\vec{\varphi} \}^j - \{ \vec{m}_{\Phi-}(t) \}^j \{ \delta\Phi \}^{j-1} - \{ \vec{m}_{\Phi+}(t) \}^j \{ \delta\Phi \}^j = \{ \Delta\vec{m}_\alpha(t) \}^j \tag{6.33b}$$

i. from $t_{j-1} < t \leq t_j$, for $j = 1, ..., N_j$, with initial/interval condition

$$\{ \delta\vec{\eta}(t_{j-1}) \}_i^j = \begin{cases} \{ \Delta\vec{\eta}_0 \}_i & j = 1 \\ \{ \delta\vec{\eta}(t_{j-1}) \}_i^{j-1} & j = 2, ..., N_j \end{cases}$$

ii. for nodes $i = 1, ..., N_{dom}$

New Operator Definitions

As a result of the linearization process we have created the following new operators: $\vec{b}_\eta$, $\widetilde{\mathbf{M}}_{\varphi-}$, $\vec{m}_{\Phi-}$, $\vec{M}_{\varphi+}$, $\vec{m}_{\Phi+}$, $\vec{p}_\eta$, $\vec{p}_\varphi$, $\Delta\vec{b}_\alpha$, $\Delta\vec{m}_\alpha$, and $\Delta\vec{p}_\alpha$, defined below. Note that some operators have different definitions based on whether predictor (P) or predictor-corrector (P-C) coupling is used.

$$
\begin{aligned}
{}^{g}_{k}\{\, b_\eta(t)\,\}^{j}_{i} &\stackrel{\text{def}}{=} 2\delta(t-t_j)\,\{\, k_e\,\}^{j}\;{}^{gg}_{k}\{\, \mathbf{L}_\eta\,\}^{j}_{ii'}\;{}^{g}\{\,\varphi\,\}^{j}_{i'} - \qquad (6.34a)\\
&\quad 2\delta(t-t_j)\sum_{g'}{}^{gg'}_{k}\{\, \mathbf{F}_\eta\,\}^{j}_{ii}\;{}^{g'}\{\,\varphi\,\}^{j}_{i'}\\
{}^{gg}_{k}\{\, \mathbf{L}_\eta\,\}^{j}_{ii'} &\stackrel{\text{def}}{=} {}^{g}_{k}\{\,\sigma_a\,\}^{j}_{i}\,\delta_{ii'}\,V_i \qquad (6.34b)\\
{}^{gg'}_{k}\{\, \mathbf{F}_\eta\,\}^{j}_{ii} &\stackrel{\text{def}}{=} \left({}^{g}\{\,\chi_p\,\}^{j}_{i}\,(1-\beta_{tot}) + \left[\,\vec{\beta}_d\;{}^{g}\{\,\vec{\chi}_d\,\}^{j}_{i}\,\right]_k\right)\left({}^{g'}_{k}\{\,\nu\sigma_f\,\}^{j}_{i}\right)V_i\\
{}^{g}\{\,\Delta b_\alpha\,\}^{j}_{i} &\stackrel{\text{def}}{=} \sum_{g'}\sum_{i'}\{\, k_e\,\}^{j}\;{}^{gg'}\{\, \mathbf{L}_\alpha\,\}^{j}_{ii'}\;{}^{g'}\{\,\varphi\,\}^{j}_{i'} - {}^{gg'}\{\, \mathbf{F}_\alpha\,\}^{j}_{i'i'}\;{}^{g'}\{\,\varphi\,\}^{j}_{i'} \qquad (6.34c)\\
{}^{gg'}\{\, \mathbf{L}_\alpha\,\}^{j}_{ii'} &\stackrel{\text{def}}{=} -{}^{g}\{\,\Delta d\,\}^{j}_{i,i'}\,\delta_{gg'} - {}^{g,g'}\{\,\Delta\Sigma_s\,\}^{j}_{i}\,\delta_{ii'}\,V_i \qquad (6.34d)\\
&\quad +{}^{g}\{\,\Delta\Sigma_a\,\}^{j}_{i}\,\delta_{gg'}\delta_{ii'}\,V_i + \sum_{k}{}^{g}_{k}\{\,\Delta\sigma_a\,\}^{j}_{i}\;{}_{k}\{\,\eta(t_j)\,\}^{j}_{i}\,\delta_{gg'}\delta_{ii'}\,V_i\\
{}^{gg'}\{\, \mathbf{F}_\alpha\,\}^{j}_{ii} &\stackrel{\text{def}}{=} \left({}^{g}\{\,\chi_p\,\}^{j}_{i}\,(1-\beta_{tot}) + \left[\,\vec{\beta}_d\;{}^{g}\{\,\vec{\chi}_d\,\}^{j}_{i}\,\right]_k\right)\times \qquad (6.34e)\\
&\quad \Big(\sum_{k}{}^{g'}_{k}\{\,\Delta\nu\sigma_f\,\}^{j}_{i}\;{}_{k}\{\,\eta(t_j)\,\}^{j}_{i} + {}^{g'}\{\,\Delta\nu\Sigma_f\,\}^{j}_{i}\Big)V_i\\
&\quad +\Big({}^{g}\{\,\Delta\chi_p\,\}^{j}_{i}\,(1-\beta_{tot}) + \left[\,\Delta\vec{\beta}_d\;{}^{g}\{\,\vec{\chi}_d\,\}^{j}_{i}\,\right]_k\Big)\Big({}^{g'}\{\,\nu\Sigma_f\,\}^{j}_{i}\Big)V_i\\
&\quad +\Big({}^{g}\{\,\chi_p\,\}^{j}_{i}\,(1-\Delta\beta_{tot}) + \left[\,\vec{\beta}_d\;{}^{g}\{\,\Delta\vec{\chi}_d\,\}^{j}_{i}\,\right]_k\Big)\Big({}^{g'}\{\,\nu\Sigma_f\,\}^{j}_{i}\Big)V_i\\
\{\,\Delta p_\alpha\,\}^{j} &\stackrel{\text{def}}{=} \sum_{i}V_i\sum_{g}{}^{g}\{\,\Delta\kappa\Sigma_f\,\}^{j}_{i}\;{}^{g}\{\,\varphi\,\}^{j}_{i}\;\{\,\Phi\,\}^{j} + \qquad (6.34f)\\
&\quad \sum_{i}V_i\sum_{g}\sum_{k}{}^{g}_{k}\{\,\Delta\kappa\sigma_f\,\}^{j}_{i}\;{}_{k}\{\,\eta(t_j)\,\}^{j}_{i}\;{}^{g}\{\,\varphi\,\}^{j}_{i}\;\{\,\Phi\,\}^{j}\\
{}_{k}\{\, p_\eta(t)\,\}^{j}_{i} &\stackrel{\text{def}}{=} \sum_{g}2\delta(t-t_j)\,{}^{g}_{k}\{\,\kappa\sigma_f\,\}^{j}_{i}\;{}^{g}\{\,\varphi\,\}^{j}_{i}\;\{\,\Phi\,\}^{j} \qquad (6.34g)\\
{}^{g}\{\, p_\varphi\,\}^{j}_{i} &\stackrel{\text{def}}{=} {}^{g}\{\,\kappa\Sigma_f\,\}^{j}_{i}\;\{\,\Phi\,\}^{j} \qquad (6.34h)\\
{}_{k}\{\,\Delta m_\alpha(t)\,\}^{j}_{i} &\stackrel{\text{def}}{=} \sum_{k'}\sum_{g}{}^{gg}_{kk'}\{\,\mathbf{\Delta R}(t_{j-1/2})\,\}_{i}\;{}^{g}\{\,\phi(t_{j-1/2})\,\}^{j}_{i}\;{}_{k'}\{\,\eta(t)\,\}^{j}_{i} + \qquad (6.34i)\\
&\quad \sum_{k'}{}_{kk'}\{\,\mathbf{\Delta D}\,\}\;{}_{k'}\{\,\eta(t)\,\}^{j}_{i}
\end{aligned}
$$

$$ {}_k\{\, m_{\Phi-}(t)\,\}_i^j \quad \stackrel{\text{def}}{=} \quad \begin{cases} \sum_{k'} \sum_g {}^{gg}_{kk'}\{\, \mathbf{R}(t_{j-1/2})\,\}_i \; {}^g\{\, \varphi\,\}_i^{j-1} \; {}_{k'}\{\, \eta(t)\,\}_i^j & \text{P} \\ 0.5 \sum_{k'} \sum_g {}^{gg}_{kk'}\{\, \mathbf{R}(t_{j-1/2})\,\}_i \; {}^g\{\, \varphi\,\}_i^{j-1} \; {}_{k'}\{\, \eta(t)\,\}_i^j & \text{P-C} \end{cases} \tag{6.34j} $$

$$ {}_k\{\, m_{\Phi+}(t)\,\}_i^j \quad \stackrel{\text{def}}{=} \quad \begin{cases} 0 & \text{P} \\ 0.5 \sum_{k'} \sum_g {}^{gg}_{kk'}\{\, \mathbf{R}(t_{j-1/2})\,\}_i \; {}^g\{\, \varphi\,\}_i^{j} \; {}_{k'}\{\, \eta(t)\,\}_i^j & \text{P-C} \end{cases} \tag{6.34k} $$

$$ {}^{1g}_{k}\{\, \mathbf{M}_{\varphi-}(t)\,\}_i^j \quad \stackrel{\text{def}}{=} \quad \begin{cases} \sum_{k'} {}^{gg}_{kk'}\{\, \mathbf{R}(t_{j-1/2})\,\}_i \; \{\, \Phi\,\}^{j-1} \; {}_{k'}\{\, \eta(t)\,\}_i^j & \text{P} \\ 0.5 \sum_{k'} {}^{gg}_{kk'}\{\, \mathbf{R}(t_{j-1/2})\,\}_i \; \{\, \Phi\,\}^{j-1} \; {}_{k'}\{\, \eta(t)\,\}_i^j & \text{P-C} \end{cases} \tag{6.34l} $$

$$ {}^{1g}_{k}\{\, \mathbf{M}_{\varphi+}(t)\,\}_i^j \quad \stackrel{\text{def}}{=} \quad \begin{cases} 0 & \text{P} \\ 0.5 \sum_{k'} {}^{gg}_{kk'}\{\, \mathbf{R}(t_{j-1/2})\,\}_i \; \{\, \Phi\,\}^{j} \; {}_{k'}\{\, \eta(t)\,\}_i^j & \text{P-C} \end{cases} \tag{6.34m} $$

Note that the first variation equations in Eq. (6.33) have some of the same operators as the forward system's operators in Eq. (6.4), so it is reasonable to thing that the same solution methods we used for the forward system could apply, but because of the presence of some additional terms, we cannot solve these equations *exactly* like we would solve the forward system. The subject of the next section is how we solve the first variation equations presented in Eq. (6.33).

6.4.2 Solving the MFS

The first problem one may notice with Eq. (6.33), is that we have introduced another unknown, the first variation in eigenvalue, $\{\, \delta k_e \,\}^j$, at all times t_j we will solve the scalar flux equations. To determine this extra unknown, we must introduce another equation. Let us first introduce some shorthand for the sources in Eq. (6.33).

$$ \{\, \delta \vec{q}_\eta(t)\,\}^j \quad \stackrel{\text{def}}{=} \quad -\{\, \Delta \vec{m}_\alpha(t)\,\}^j \;\; \text{for } j = 1, ..., N_j \tag{6.35a} $$

$$ \{\, \delta \vec{q}_\varphi\,\}^j \quad \stackrel{\text{def}}{=} \quad -\{\, \Delta \vec{b}_\alpha\,\}^j \; - \; \{\, \delta k_e\,\}^j \; \{\, \widetilde{\mathbf{L}}\,\}^j \; \{\, \vec{\varphi}\,\}^j \;\; \text{for } j = 0, ..., N_j \tag{6.35b} $$

$$ \{\, \delta q_\Phi\,\}^j \quad \stackrel{\text{def}}{=} \quad -\{\, \Delta p_\alpha\,\}^j \; + \delta p_{core} \text{ for } j = 0, ..., N_j \tag{6.35c} $$

We propose to introduce an equation for the fundamental mode adjoint flux, $\{\, \vec{\varphi}^*\,\}^j$, which allows us to calculate $\{\, \delta k_e\,\}^j$ when we take the inner product of the neutron field equation of Eq. (6.33) with fundamental mode adjoint flux $\{\, \vec{\varphi}^*\,\}^j$,

$$ \left\langle\, \delta_{jj'}\, \widetilde{\mathbf{B}} \delta\vec{\varphi}\,,\, \vec{\varphi}^*\,\right\rangle_\varphi \;\; = \;\; \left\langle\, \delta_{jj'}\, \vec{q}_\varphi\,,\, \vec{\varphi}^*\,\right\rangle_\varphi . \tag{6.36} $$

Because our inner product for φ was defined as a sum over all times, we have introduced Kronecker delta $\delta_{jj'}$ so that we only consider only time t_j when we determine $\{\, \delta k_e\,\}^j$. Now

on the left side, we use the properties of inner products to transfer the operation of matrix $\widetilde{\mathbf{B}}$ from $\delta\vec{\varphi}$ to $\vec{\varphi}^*$:

$$\left\langle \delta_{jj'}\, \delta\vec{\varphi}\,,\, \widetilde{\mathbf{B}}^*\vec{\varphi}^* \right\rangle_\varphi \;=\; \left\langle \delta_{jj'}\, \vec{q}_\varphi\,,\, \vec{\varphi}^* \right\rangle_\varphi \tag{6.37}$$

where $\widetilde{\mathbf{B}}^* \stackrel{\text{def}}{=} \widetilde{\mathbf{B}}^T$. Now let us expand the source on the right side, $\vec{q}_\varphi$,

$$\begin{aligned}\left\langle \delta_{jj'}\, \delta\vec{\varphi}\,,\, \widetilde{\mathbf{B}}^*\vec{\varphi}^* \right\rangle_\varphi \;=\; & -\left\langle \delta_{jj'}\; \{\, \delta\vec{b}_\alpha \,\}^{(j')}\,,\, \vec{\varphi}^* \right\rangle_\varphi \\ & -\left\langle \delta_{jj'}\; \{\, \delta\vec{k}_e \,\}^{(j')}\; \{\, \widetilde{\mathbf{L}} \,\}^{(j')}\; \{\, \vec{\varphi} \,\}^{(j')}\,,\, \vec{\varphi}^* \right\rangle_\varphi\end{aligned} \tag{6.38}$$

and we see that if we solve

$$\{\, \widetilde{\mathbf{B}}^* \,\}^j\; \{\, \vec{\varphi}^* \,\}^j = 0 \tag{6.39a}$$

$$\Big[\; \{\, \vec{\varphi}^* \,\}^j \;\Big]_{g,i} = 1 \tag{6.39b}$$

$$\text{for } t_j,\; j = 0, ..., N_j$$

$$\text{using } \{\, \widetilde{\mathbf{B}}^* \,\}^j \stackrel{\text{def}}{=} \{\, k_e \,\}^j\; \{\, \widetilde{\mathbf{L}}^T \,\}^j \;+\; \{\, \widetilde{\mathbf{F}}^T \,\}^j$$

then we can determine $\{\, \delta k_e \,\}^j$ by

$$\{\, \delta k_e \,\}^j = \frac{\left\langle \delta_{jj'}\, \Delta\vec{b}_\alpha\,,\, \vec{\varphi}^* \right\rangle_\varphi}{\left\langle \delta_{jj'}\, \widetilde{\mathbf{L}}\vec{\varphi}\,,\, \vec{\varphi}^* \right\rangle_\varphi}. \tag{6.40}$$

The above equation, Eq. (6.40), for the first variation in eigenvalue is the same as the result presented in [13], among others.

Realizing Source Orthogonality

Calculating the first variation in eigenvalue as in Eq. (6.40) and using it in the expression for the source, $\vec{q}_\varphi$, results in the following orthogonality condition,

$$\left\langle \vec{q}_\varphi\,,\, \vec{\varphi}^* \right\rangle_\varphi = 0. \tag{6.41}$$

Eq. (6.41) must be satisfied whatever the formulation of the source term, $\vec{q}_\varphi$. It happens that here Eq. (6.41) is automatically satisfied because of the formulation of our eigenvalue problem and the choice of using Eq. (6.40), but this may not be the case. Especially when a "k-reset" procedure [14] is performed to search for the value of some control parameter that makes the system critical ($k_e = 1$), the form of $\vec{q}_\varphi$ is different than presented above (it will not include the δk_e term) but Eq. (6.41) must still be satisfied.

Realizing Fundamental Mode Orthogonality

The next problem we face is commonly called fundamental mode contamination [14]. It arises from the fact that Eq. (6.33) for the first variation of the scalar flux is valid for *any* solution of the form

$$\{\,\delta\vec{\varphi}_{\dagger}\,\}^{j} \;=\; \{\,\delta\vec{\varphi}\,\}^{j} + \mathrm{f}_{\dagger}\,\{\,\vec{\varphi}\,\}^{j} \tag{6.42}$$

where $\mathrm{f}_{\dagger}$ is *any* constant multiplying the fundamental mode, $\{\,\vec{\varphi}\,\}^{j}$, and $\{\,\delta\vec{\varphi}\,\}^{j}$ is the particular solution of such that the expansion of $\{\,\delta\vec{\varphi}\,\}^{j}$ does not contain any fundamental mode. We can remove contamination by demanding orthogonality of the fundamental mode and our "contaminated" solution,

$$\left\langle\, \delta\vec{\varphi}_{\dagger}\,,\, \vec{\varphi}\,\right\rangle_{\varphi} = 0. \tag{6.43}$$

Eq. (6.42) and Eq. (6.43) may be combined into the Gram-Schmidt orthogonalization expression

$$\{\,\delta\vec{\varphi}\,\}^{j} \;=\; \{\,\delta\vec{\varphi}_{\dagger}\,\}^{j} - \mathrm{f}_{\dagger}\,\{\,\vec{\varphi}\,\}^{j}\,, \tag{6.44}$$

where

$$\mathrm{f}_{\dagger} = \frac{\left\langle\, \delta_{jj'}\delta\vec{\varphi}_{\dagger}\,,\, \delta\vec{\varphi}\,\right\rangle_{\varphi}}{\left\langle\, \delta_{jj'}\vec{\varphi}\,,\, \vec{\varphi}\,\right\rangle_{\varphi}}.$$

Note that fundamental mode contamination is a numerical problem due to finite precision arithmetic, and periodically during our numerical solution of Eq. (6.39) we will make use of Eq. (6.44) to decontaminate our solution.

Summary of the First Variation in Neutron Field Solution

1. Calculate first variation in eigenvalue $\{\,\delta k_e\,\}^{j}$ with Eq. (6.40).

2. Solve for the first variation in flux shape $\{\,\delta\vec{\varphi}\,\}^{j}$ using Eq. (6.4.2) provided we know $\{\,\delta\vec{\eta}\,\}^{j}$ and $\{\,\delta k_e\,\}^{j}$. Periodically during the iterative solution of Eq. (6.4.2) it will be necessary to decontaminate $\{\,\delta\vec{\varphi}\,\}^{j}$ with Eq. (6.44).

3. The first variation in the amplitude function $\{\,\delta\Phi\,\}^{j}$ may be determined using constraint i) of Eq. (6.4.2) provided we have already determined $\{\,\delta\vec{\eta}\,\}^{j}$ and $\{\,\delta\vec{\varphi}\,\}^{j}$.

Matrix Form of the MFS

At this point, we would like to present the MFS in matrix form.

$$\widetilde{\mathbf{A}}_x \delta\vec{x} = \vec{q} \tag{6.45}$$

The master solution vector $\delta\vec{x}$ has the following form.

$$\delta\vec{x} \stackrel{\text{def}}{=} \left(\{\,\delta\vec{x}\,\}^0, \{\,\delta\vec{x}\,\}^1, \ldots, \{\,\delta\vec{x}\,\}^j, \ldots, \{\,\delta\vec{x}\,\}^{N_j} \right)^T \tag{6.46a}$$

The solution vector $\{\,\delta\vec{x}\,\}^j$ for $j = 0, ..., N_j$ has the following form.

$$\{\,\delta\vec{x}\,\}^j \stackrel{\text{def}}{=} \left(\{\,\delta\vec{\eta}(t)\,\}^j, \{\,\delta\vec{\varphi}\,\}^j, \{\,\delta\Phi\,\}^j \right)^T \tag{6.46b}$$

The master matrix $\widetilde{\mathbf{A}}_x$ has the following form.

$$\widetilde{\mathbf{A}}_x \stackrel{\text{def}}{=} \begin{pmatrix} \{\,\widetilde{\mathbf{A}}_{x+}\,\}^0 & 0 & 0 & 0 & 0 & 0 \\ \{\,\widetilde{\mathbf{A}}_{x-}\,\}^1 & \{\,\widetilde{\mathbf{A}}_{x+}\,\}^1 & 0 & 0 & 0 & 0 \\ 0 & \ddots & \ddots & 0 & 0 & 0 \\ 0 & 0 & \{\,\widetilde{\mathbf{A}}_{x-}\,\}^j & \{\,\widetilde{\mathbf{A}}_{x+}\,\}^j & 0 & 0 \\ 0 & 0 & 0 & \ddots & \ddots & 0 \\ 0 & 0 & 0 & 0 & \{\,\widetilde{\mathbf{A}}_{x-}\,\}^{N_j} & \{\,\widetilde{\mathbf{A}}_{x+}\,\}^{N_j} \end{pmatrix} \tag{6.47a}$$

The matrices $\{\,\widetilde{\mathbf{A}}_{x-}\,\}^j$ for $j = 1, ..., N_j$ and $\{\,\widetilde{\mathbf{A}}_{x+}\,\}^j$ for $j = 0, ..., N_j$ have the following form.

$$\{\,\widetilde{\mathbf{A}}_{x+}\,\}^0 \stackrel{\text{def}}{=} \begin{pmatrix} 2\delta(t-t_0)\mathbf{E} & 0 & 0 \\ \left[\, \{\,\widetilde{\mathbf{B}}_\eta(t)\,\}^0 \circ \,\right]_{k,\tau_0} & \{\,\widetilde{\mathbf{B}}\,\}^0 & 0 \\ \left[\, \{\,\vec{p}_\eta(t)\,\}^0 \circ \,\right]_{i,k,\tau_0} & \left[\, \{\,\vec{p}_\varphi\,\}^0 \circ \,\right]_{i,g} & \{\,p\,\}^0 \end{pmatrix} \tag{6.47b}$$

$$\{\,\widetilde{\mathbf{A}}_{x-}\,\}^j \stackrel{\text{def}}{=} \begin{pmatrix} 0 & -\{\,\widetilde{\mathbf{M}}_{\varphi-}(t)\,\}^j & -\{\,\vec{m}_{\Phi-}(t)\,\}^j \\ 0 & 0 & 0 \\ 0 & 0 & 0 \end{pmatrix} \tag{6.47c}$$

$$\{\,\widetilde{\mathbf{A}}_{x+}\,\}^j \stackrel{\text{def}}{=} \begin{pmatrix} \frac{d}{dt} - \{\,\widetilde{\mathbf{M}}\,\}^j & -\{\,\widetilde{\mathbf{M}}_{\varphi+}(t)\,\}^j & -\{\,\vec{m}_{\Phi+}(t)\,\}^j \\ \left[\, \{\,\widetilde{\mathbf{B}}_\eta(t)\,\}^j \circ \,\right]_{k,\tau_j} & \{\,\widetilde{\mathbf{B}}\,\}^j & 0 \\ \left[\, \{\,\vec{p}_\eta(t)\,\}^j \circ \,\right]_{k,i,\tau_j} & \left[\, \{\,\vec{p}_\varphi\,\}^j \circ \,\right]_{i,g} & \{\,p\,\}^j \end{pmatrix} \tag{6.47d}$$

The master source vector $\vec{q}$ has the following form.

$$\vec{q} \stackrel{\text{def}}{=} \left(\{\,\vec{q}\,\}^0\,,\, \{\,\vec{q}\,\}^1\,,\ldots,\, \{\,\vec{q}\,\}^j\,,\ldots,\, \{\,\vec{q}\,\}^{N_j} \right)^T \tag{6.48a}$$

The source vector $\{\,\vec{q}\,\}^j$ for $j = 0, ..., N_j$ has the following form.

$$\{\,\vec{q}\,\}^0 \stackrel{\text{def}}{=} \left(2\delta(t-t_0)\Delta\vec{\eta}_0,\, \{\,\vec{q}_\varphi\,\}^0\,,\, \{\,\vec{q}_\Phi\,\}^0\right)^T \tag{6.48b}$$

$$\{\,\vec{q}\,\}^j \stackrel{\text{def}}{=} \left(\{\,\vec{q}_\eta(t)\,\}^j\,,\, \{\,\vec{q}_\varphi\,\}^j\,,\, \{\,\vec{q}_\Phi\,\}^j \right)^T \tag{6.48c}$$

6.4.3 First Variation in Responses

The response we may evaluate with MFS methodology is shown below. Note that we still must solve the forward system of Eq. (6.33) as the forward solutions are needed to construct the MFS equations.

$$\begin{aligned} \{\,\delta r\,\}_{s,p} &= r_s[\,\{\,\Delta\vec{\alpha}\,\}_p\,,\, \{\,\delta\vec{x}\,\}_p\,] \\ &= \left\langle\, \{\,\vec{h}_\alpha\,\}_s\,,\, \{\,\Delta\vec{\alpha}\,\}_p \,\right\rangle_\alpha + \left\langle\, \{\,\vec{h}_x\,\}_s\,,\, \{\,\delta\vec{x}\,\}_p \,\right\rangle_x \end{aligned} \tag{6.49}$$

where $\{\,\Delta\vec{\alpha}\,\}_p$ is the exact change in input parameters, and $\{\,\delta\vec{x}\,\}_p$, is the MFS solution obtained by taking the first variation of the forward system with perturbation of input parameters $\{\,\Delta\vec{\alpha}\,\}_p$. Note that the first variation *is* dependent on the perturbation set p, *but* it is *linearly* dependent such that our sensitivity coefficients, Eq. (6.27), will always be independent of the perturbation.

6.4.4 Response Surfaces with MFS

Generating response surfaces with the MFS is not very productive because the first variation is linearly dependent on the perturbation, so the response "surface" is flat and only valid in the some region of linearity about the location of the nominal calculation.

6.4.5 Sensitivity Analysis with MFS

The strengths of the MFS lie in the fact that it may generate *exact* first derivatives, as opposed to DPAR in which we must approximate derivatives with finite differences and perform multiple runs with various perturbation levels (1%, 5%, 10%, etc.) to check the validity of our finite difference approximation. However, just like for DPAR, each

perturbation set p may contain only one perturbed parameter m because we need to split $\{\,\delta r\,\}_{s,p}$ into the sum of components $\sum_m \{\,\delta r\,\}_{m,s,p}$ in order to arrive at the expression for $\{\,r_\alpha\,\}_{s,m}$ of Eq. (6.26). So if each perturbation set p contains only 1 nonzero m-component of $\{\,\Delta\vec{\alpha}\,\}_p$ then the first variation calculated by Eq. (6.30), $\{\,\delta r\,\}_{s,p}$, is the first variation of the response with respect to only one data parameter m, $\{\,\delta r\,\}_{s,m,p}$.

$$\begin{aligned} \{\,\delta r\,\}_{s,m,p} &= r_s[\,\{\,\Delta\vec{\alpha}\,\}_{m,p}\,,\,\{\,\Delta\vec{x}\,\}_{m,p}\,] \\ &\quad \text{where } \{\,\Delta\alpha\,\}_{m',m,p} = 0 \text{ for } m' \neq m \end{aligned} \tag{6.50}$$

The upside of MFS (as with DPAR) is that all N_s response sensitivities may be calculated with one run. However, in order to determine the sensitivity of responses (and sensitivity coefficients) we can only consider 1 perturbed parameter per run. However, whereas with DPAR, we estimated three different perturbation sets ($N_p = 3$) were needed to conclusively determine the finite difference first derivative, with MFS, only one perturbation set is needed. However, we have introduced another system of equations to solve at each time t_j, the fundamental mode adjoint system of Eq. (6.39). Solving Eq. (6.39) does not double the amount of work we must do, but with the extra work of fundamental mode decontamination and updating nuclide variations at time nodes, it is not too far off to assume that solving the MFS is double the work of a single forward system solution. So to calculate sensitivities for N_s responses with respect to $N_{m'}$ input data parameters, one would need approximately

$$N_{MFS} = 2 \times N_{m'} \text{ efs}$$

where the units (efs) have been previously introduced as Equivalent Forward Solutions. For example, with a case of 100 parameters ($N_m = 100$), considering one quarter of them for sensitivity analysis ($N_{m'} = 25$), with interest in 20 different responses ($N_s = 20$), we would need $N_{MFS,sa} = 2 \times 25 = 50$efs to analyze sensitivities. For this example, the DPAR method required $N_{DPAR,sa} = 75$efs to analyze sensitivities.

6.4.6 Uncertainty Propagation with MFS

Using MFS to propagate uncertainties is very similar to using MFS for sensitivity analysis, because we still need to calculate sensitivities of responses $\{\,r_\alpha\,\}_{s,m}$ with Eq. (6.26). However with uncertainty propagation, we use $\{\,r_\alpha\,\}_{s,m}$ to calculate the variance of responses $\{\,v\,\}_s$ with Eq. (6.28), and if we propagate all variances, we must consider

all parameters, not the one quarter of parameters we assumed for sensitivity analysis. For our previous example of 100 parameters ($N_m = 100$), considering all of them for uncertainty propagation ($N_{m'} = 100$), with interest in 20 different responses ($N_s = 20$), we would need approximately $N_{MFS,up} = 2 \times 100 = 200$efs to propagate uncertainties. For this example, the DPAR method required $N_{DPAR,up} = 300$efs to propagate uncertainties.

6.5 The Adjoint System (AS)

The concept of an adjoint equation has already been introduced in one of the auxiliary requirements of our modified forward system (MFS)—the fundamental mode adjoint scalar flux was introduced in Eq. (6.39) to calculate the change in eigenvalue, $\{ \delta k_e \}^j$. But first, before we go into the derivation of the AS, let us use a simplified version to illustrate some sensitivity analysis concepts and review.

$$\frac{d}{dt}\eta(t) = \lambda\eta(t)$$

$$\text{for } t_0 \leq t \leq t_N$$

$$\text{initial condition } \eta(t_0) = \eta_0$$

6.5.1 Inner Product

First we need an inner product for our system which maps functions to numbers to form our response.

$$\left\langle \eta_1 \, , \, \eta_2 \right\rangle = \int_{t_0}^{t_N} \eta_1(t) \, \eta_2(t) \, dt$$

The response we are interested in a final time nuclide concentration response, so the realization function is $h_\eta = 2\delta(t - t_N)$.

$$r = \left\langle h_\eta \, , \, \eta(t) \right\rangle = \int_{t_0}^{t_N} 2\delta(t - t_N) \, \eta(t) \, dt = \eta(t_N)$$

By perturbing parameter $\lambda \to \lambda' = \lambda + \Delta\lambda$ and/or initial condition $\eta_0 \to \eta_0' = \eta_0 + \Delta\eta_0$, we change the solution of the ODE, $\eta \to \eta' = \eta + \Delta\eta$.

$$\frac{d}{dt}\eta'(t) = \lambda'\eta'(t)$$

$$\eta'(0) = \eta_0'$$

The DPAR method

The DPAR method seeks to determine $\Delta r = r' - r = \left\langle h_\eta \, , \, \eta' - \eta \right\rangle = \left\langle h_\eta \, , \, \Delta\eta \right\rangle$ by solving for η'. The resulting sensitivity of the response to λ or initial conditions is given below, assuming only parameter λ *or* initial condition η_0 is perturbed.

$$s_\lambda \approx \frac{\Delta r}{\Delta\lambda} = \frac{\left\langle h_\eta \, , \, \Delta\eta \right\rangle}{\Delta\lambda} \tag{6.51a}$$

$$s_{ic} \approx \frac{\Delta r}{\Delta\eta_0} = \frac{\left\langle h_\eta \, , \, \Delta\eta \right\rangle}{\Delta\eta_0} \tag{6.51b}$$

The MFS method

The MFS system is the linearized forward system we may solve for the first variation in the solution, $\delta\eta$, in order to determine the first variation in response, $\delta r = \left\langle h_\eta \, , \, \delta\eta \right\rangle$.

$$\frac{d}{dt}\delta\eta(t) = \lambda\,\delta\eta(t) + \Delta\lambda\,\eta(t)$$

$$\delta\eta(t_0) = \Delta\eta_0$$

The resulting sensitivity of the response to λ or initial conditions is given below, assuming only parameter λ *or* initial condition η_0 is perturbed.

$$s_\lambda = \frac{\delta r}{\Delta\lambda} = \frac{\left\langle h_\eta \, , \, \delta\eta \right\rangle}{\Delta\lambda} \tag{6.52a}$$

$$s_{ic} = \frac{\delta r}{\Delta\eta_0} = \frac{\left\langle h_\eta \, , \, \delta\eta \right\rangle}{\Delta\eta_0} \tag{6.52b}$$

6.5.2 The AS method

To derive the AS equations we must make use of the following property for continuous and matrix operators, respectively.

$$\left\langle D\eta \, , \, \eta^* \right\rangle = \left\langle \eta \, , \, D^*\eta^* \right\rangle + \left\langle\left\langle \eta \, , \, \eta^* \right\rangle\right\rangle \tag{6.53a}$$

$$\left\langle \widetilde{\mathbf{D}}\vec{\eta} \, , \, \vec{\eta}^* \right\rangle = \left\langle \vec{\eta} \, , \, \widetilde{\mathbf{D}}^T\vec{\eta}^* \right\rangle \tag{6.53b}$$

Note that there are no formal boundary terms when dealing with a completely discretized system containing only matrix operators. With differential operators (as with our ODE for

nuclide concentrations), it is preferable to make some boundary terms vanish by choosing some appropriate initial conditions for our adjoint function η^*. Our goal is to compute the first variations in response, $\{\,\delta r\,\}_s = r_s[\Delta\vec{\alpha}, \delta\vec{x}\,]$, but avoid solving the MFS for *every* possible parameter perturbation—this is exactly what the AS allows.

Two different approaches are generally used to formulate the AS equations: the variational approach and the differential approach [15, 16]. Although the concept of the Frechêt derivative mathematically unifies the two approaches and proves that they will produce the same AS [15, 16], the actual operations each approach applies to a non-linear forward system of equations to arrive at an AS to solve is different. In the next two sections we shall briefly explain the two approaches and cite some of the advantages and disadvantages of each. For more information on variational and differential approaches applied to reactor physics problems, please see [6, 14, 15, 11, 17].

The Differential Approach

The differential approach basically defines a response, r_s and then its Gâteaux variation is taken, resulting in variation of the response given by $\{\,\delta r\,\}_s$. The first variations in solutions are obtained by taking the Frechêt differentials of the governing system of equations, resulting in a system we may solve for $\delta\vec{x}$. However, this system depends on the variation in input $\Delta\vec{\alpha}$. But we can create a linear system which does not depend on $\Delta\vec{\alpha}$—the adjoint system. We believe the differential approach to perturbation theory (and sensitivity analysis) has the following advantages over the variational approach.

1. With the differential approach, the equations to solve to obtain the adjoint functions easily "fall out". This is very different from the variational approach, where with complex problems especially, one must *almost* know the adjoint equations (or have developed good intuition in this regard) to guess the right variational principle. In some papers on perturbation theory, it appears as if the author derived the adjoint system using the differential approach in order to realize the variational principle he/she needs, then presents the derivation of the adjoint system using the variational approach with "given" variational principle.

2. With the differential approach, the AS is realized as a "transposed-and-time-reversed" MFS. The method of solving the AS is usually not much different than the method

to solve the MFS, but if it is, you will be able to see it in the equations. In the variational approach, the entire system is combined into one giant functional, the variational principle, and details such as the order in which to solve equations or the correct way to evaluate coupling between equations may be subtle.

With the differential approach, we begin with undefined operator D^*, undefined source $h_\eta(t)$, and undefined initial condition,

$$D^*\delta\eta^*(t) = h_\eta(t).$$

Let us now take the inner product of the AS with $\delta\eta$ and the inner product of the MFS with $\delta\eta^*$ and subtract the two equations,

$$\left\langle \frac{d}{dt}\delta\eta\,,\,\delta\eta^*\right\rangle - \left\langle D^*\delta\eta^*\,,\,\delta\eta\right\rangle = \left\langle \lambda\,\delta\eta\,,\,\delta\eta^*\right\rangle + \left\langle \Delta\lambda\,\eta\,,\,\delta\eta^*\right\rangle - \left\langle h_\eta\,,\,\delta\eta\right\rangle$$

$$\delta\eta(t_0) = \Delta\eta_0.$$

We would like to transfer operations on $\delta\eta$ to operations on $\delta\eta^*$ in order to group some terms in order to define D^*. This is trivial except for the left side of the MFS equation,

$$\left\langle \frac{d}{dt}\delta\eta\,,\,\delta\eta^*\right\rangle = \int_{t_0}^{t_N} \frac{d}{dt}\delta\eta\delta\eta^*\,dt,$$

which we shall use integration by parts to obtain

$$\int_{t_0}^{t_N} \frac{d}{dt}\delta\eta\,\delta\eta^*\,dt = \delta\eta\,\delta\eta^*|_{t_0}^{t_N} - \int_{t_0}^{t_N} \delta\eta\,\frac{d}{dt}\delta\eta^*\,dt.$$

Now we have realized the so-called "boundary terms", $\delta\eta\,\delta\eta^*|_{t_0}^{t_N}$. To avoid solving the MFS for $\delta\eta(t_N)$, we set $\delta\eta^*(t_N) = 0$, which becomes the initial condition for the AS equation. Let us revert to the inner product representation of the left side using the boundary inner product notation,

$$-\Delta\eta_0\delta\eta^*(t_0) - \int_{t_0}^{t_N} \delta\eta\,\frac{d}{dt}\delta\eta^*\,dt = -\left\langle\left\langle \Delta\eta_0\,,\,\delta\eta^*(t_0)\right\rangle\right\rangle - \left\langle \delta\eta\,,\,\frac{d}{dt}\delta\eta^*\right\rangle.$$

Notice that the initial condition for the adjoint system is at time t_N, the final time of our forward system. Therefore, we must solve the adjoint equations *backwards* through time. So completely transferring all operators to $\delta\eta^*$ and grouping terms, we have

$$\left\langle \delta\eta\,,\,\left(-\frac{d}{dt} - \lambda - D^*\right)\delta\eta^*\right\rangle = \left\langle\left\langle \Delta\eta_0\,,\,\delta\eta^*(t_0)\right\rangle\right\rangle + \left\langle \Delta\lambda\,\eta\,,\,\delta\eta^*\right\rangle - \left\langle h_\eta\,,\,\delta\eta\right\rangle$$

If we define $D^* \stackrel{\text{def}}{=} -\frac{d}{dt} - \lambda$ then we can remove dependence on the MFS solution $\delta\eta$, except at the initial time t_0 and evaluate the change in our response δr.

$$\delta r = \Big\langle\, h_\eta\,,\, \delta\eta \,\Big\rangle = \Big\langle\Big\langle\, \Delta\eta_0\,,\, \delta\eta^*(t_0) \,\Big\rangle\Big\rangle + \Big\langle\, \Delta\lambda\,\eta\,,\, \delta\eta^* \,\Big\rangle$$

Notice that our response now depends on $\delta\eta^*$ which is obtained by solving the following equation. So if we solve the following adjoint system,

$$-\frac{d}{dt}\delta\eta^*(t) = \lambda\,\delta\eta^*(t) + h_\eta$$

$$\delta\eta^*(t_N) = 0$$

we may estimate sensitivities of the response with

$$s_\lambda = \frac{\delta r}{\Delta\lambda} \;=\; \frac{\Big\langle\, h_\eta\,,\, \delta\eta \,\Big\rangle}{\Delta\lambda} = \frac{\Big\langle\, \Delta\lambda\,\eta\,,\, \delta\eta^* \,\Big\rangle}{\Delta\lambda} = \Big\langle\, \eta\,,\, \delta\eta^* \,\Big\rangle, \tag{6.54a}$$

$$s_{ic} = \frac{\delta r}{\Delta\eta_0} \;=\; \frac{\Big\langle\, h_\eta\,,\, \delta\eta \,\Big\rangle}{\Delta\eta_0} = \frac{\Big\langle\Big\langle\, \Delta\eta_0\,,\, \delta\eta^*(t_0) \,\Big\rangle\Big\rangle}{\Delta\eta_0} = \delta\eta^*(t_0). \tag{6.54b}$$

One of the beauties of the differential approach is how apparent it is that the MFS and AS methods are complimentary. With the MFS, the form of the equations is dependent on the data perturbation m' but solving the system of equations determines all N_s responses. With the AS, the form of the equations is dependent on the response s, but solving the system of equations determines the response for all data perturbations $N_{m'}$. In cases where $N_s > N_{m'}$, the MFS method is more efficient. In cases where $N_{m'} > N_s$, the AS method is more efficient.

The Variational Approach

The variational approach formulates a functional r_{var} as a combination of our desired response functional r_s and the inner product of each equation in our forward system with some unknown functions called Lagrange multipliers [18].

$$r_{var}[\vec{\alpha},\vec{x}] = r_s[\vec{\alpha},\vec{x}] \;-\; \Big\langle\, \frac{d}{dt}\vec{\eta} - \widetilde{\mathbf{M}}\vec{\eta}\,,\, \vec{\eta}^* \,\Big\rangle_\eta \tag{6.55}$$

$$-\; \Big\langle\, \widetilde{\mathbf{B}}\vec{\varphi}\,,\, \vec{\varphi}^* \,\Big\rangle_\varphi \tag{6.56}$$

$$-\; \Big\langle\, p\,\Phi - p_{core}\,,\, \Phi^* \,\Big\rangle_\Phi \tag{6.57}$$

Next, we attempt to find the stationary points of the functional r_{var} (just like with functions, we can have maxima, minima, or saddle points) by taking the functional derivative of r_{var} with respect to α and setting it equal to zero, $\frac{dr_{var}}{d\alpha} = 0$. The unknowns η, φ, and Φ also must be considered implicit functions of α [6]. The resulting equations imply the equations which Lagrange multipliers η^*, φ^*, and Φ^* must satisfy—the AS. The resulting expression for $\frac{dr_s}{d\alpha}$ involves only the forward equation solutions η, φ, and Φ and the adjoint equation solutions η^*, φ^*, and Φ^* and functional derivatives of operators $\widetilde{\mathbf{B}}$, $\widetilde{\mathbf{M}}$, and p with respect to α. We believe the variational approach to perturbation theory (and sensitivity analysis) has the following advantages over the differential approach.

1. Many equations which live in different spaces (have different independent variables in continuous space or have different sets of indices in discrete space) can be easily incorporated into one giant variational principle.

2. Additional constraints may be added to the variational principle with ease.

Let us illustrate the use of the variational method to derive the AS for the simple one nuclide problem we have already considered with the differential approach.

$$r_{var}[\lambda, \eta] = r_s[\lambda, \eta] - \left\langle \frac{d}{dt}\eta - \lambda\eta \,,\, \eta^* \right\rangle \tag{6.58a}$$

Apply the functional derivative (Frechêt differential) to the above equation to get

$$0 = \left\langle \frac{dr_s}{d\lambda} \,,\, \Delta\lambda \right\rangle + \left\langle \frac{dr_s}{d\eta_0} \,,\, \Delta\eta_0 \right\rangle + \left\langle \frac{dr_s}{d\eta} \,,\, \delta\eta \right\rangle - \left\langle \frac{d}{dt}\delta\eta - \lambda\delta\eta - \Delta\lambda\eta \,,\, \eta^* \right\rangle. \tag{6.58b}$$

Reorganize,

$$\begin{aligned} -\left\langle \frac{dr_s}{d\lambda} \,,\, \Delta\lambda \right\rangle - \left\langle \frac{dr_s}{d\eta_0} \,,\, \Delta\eta_0 \right\rangle + \left\langle \Delta\lambda\eta \,,\, \eta^* \right\rangle = \\ \left\langle \frac{dr_s}{d\eta} \,,\, \delta\eta \right\rangle - \left\langle \frac{d}{dt}\delta\eta - \lambda\delta\eta \,,\, \eta^* \right\rangle \end{aligned} \tag{6.58c}$$

and transfer operations on $\delta\eta$ to operations on η^* as we did before for the differential approach, to get

$$\begin{aligned} -\left\langle \frac{dr_s}{d\lambda} \,,\, \Delta\lambda \right\rangle - \left\langle \frac{dr_s}{d\eta_0} \,,\, \Delta\eta_0 \right\rangle + \left\langle \Delta\lambda\eta \,,\, \eta^* \right\rangle + \left\langle \left\langle \Delta\eta_0 \,,\, \eta_0^* \right\rangle \right\rangle = \\ -\left\langle \left(-\frac{d}{dt} - \lambda \right) \eta^* - \frac{dr_s}{d\eta} \,,\, \delta\eta \right\rangle. \end{aligned} \tag{6.58d}$$

Using integration by parts, the boundary terms $\left\langle\left\langle\, \Delta\eta_0\,,\, \eta_0^*\,\right\rangle\right\rangle$ have appeared again and the initial condition for η^* has been determined to be $\eta^*(t_N) = 0$. Now we can see that if we solve

$$-\frac{d}{dt}\eta^* = \lambda\eta^* + \frac{dr_s}{d\eta}, \qquad \eta^*(t_N) = 0 \tag{6.58e}$$

, then we can evaluate our responses

$$\left\langle\, \frac{dr_s}{d\lambda}\,,\, \Delta\lambda\,\right\rangle + \left\langle\, \frac{dr_s}{d\eta_0}\,,\, \Delta\eta_0\,\right\rangle - \left\langle\, \Delta\lambda\eta\,,\, \eta^*\,\right\rangle - \left\langle\left\langle\, \Delta\eta_0\,,\, \eta_0^*\,\right\rangle\right\rangle = 0, \tag{6.58f}$$

and response sensitivities using

$$s_\lambda = \frac{dr_s}{d\lambda} = \frac{\left\langle\, \frac{dr_s}{d\lambda}\,,\, \Delta\lambda\,\right\rangle}{\Delta\lambda} = \frac{\left\langle\, \Delta\lambda\,\eta\,,\, \eta^*\,\right\rangle}{\Delta\lambda} = \left\langle\, \eta\,,\, \eta^*\,\right\rangle, \tag{6.58g}$$

$$s_{ic} = \frac{dr_s}{d\eta_0} = \frac{\left\langle\, \frac{dr_s}{d\eta_0}\,,\, \Delta\eta_0\,\right\rangle}{\Delta\eta_0} = \frac{\left\langle\left\langle\, \Delta\eta_0\,,\, \eta_0^*\,\right\rangle\right\rangle}{\Delta\eta_0} = \eta^*(t_0). \tag{6.58h}$$

Notice that these two response sensitivities are the exact same as those derived using the differential approach.

6.5.3 More "Approaches"

In *Sensitivity Theory for General Systems of Nonlinear Equations* [15] D.G. Cacuci, et. al. notes that Generalized Perturbation Theory (GPT) is a widely used "approach" for sensitivity analysis in reactor physics, but should not really be considered another approach as the core of the core of GPT is the variational methodology. *Development of Depletion Perturbation Theory for Coupled Neutron/Nuclide Fields* by M.L. Williams [6] developed a GPT for reactor cycle calculations, calling the result Depletion Perturbation Theory (DPT), also viewed by many nuclear engineers as another approach to sensitivity analysis. But again it is merely an application of variational methods to reactor physics problems. D.G. Cacuci, et. al. introduced a another new "approach" called the "matrix approach" in [15] and later refined and revisited in [12]. The matrix approach deals with the completely discretized systems of equations that are actually solved in most real-life situations and has an advantage over other "approaches" in that it can analyze sensitivities of parameters of entirely numerical origin (e.g. time step size, relaxation factors, etc.) It is worth noting that the matrix AS is *not* the same as the AS obtained when the AS is found for the continuous

system of equations and *then* discretized. The first method of developing adjoint equations based on the discretized system, presented thoroughly in [15] as the "matrix approach", is known in the reactor physics community as the *mathematical adjoint*. The second method of developing adjoint equations based on the continuous system of equations, and then discretizing is known in the reactor physics community as the *physical adjoint*. The physical adjoint is widely used because it appears to be fairly accurate and all solvers used for the forward problem can be used (with small modification) to solve the physical AS. However, unfortunately, in many cases the AS equations found using the mathematical adjoint "approach" is not solvable by any of the forward system solvers and requires a solution via a sparse linear system solver. For the reactor cycle equations, we represent the flux part of our system (φ and Φ) as a completely discretized matrix system but represent the nuclide part of our system (η) as a first order ODE in time. In our case, the AS equations are actually a combination of "mathematical" adjoint and "physical" adjoint. One nice side effect of using the physical adjoint for the nuclide field is that we will develop an AS which is independent of the nuclide ODE solution method.

6.5.4 The AS Matrix System

Consider an auxiliary system for response-dependent auxiliary solution, $\{\,\delta\vec{x}^{\,*}\,\}_s$,

$$\widetilde{\mathbf{A}}_x^* \{\,\delta\vec{x}^{\,*}\,\}_s \;=\; \{\,\vec{q}^{\,*}\,\}_s \tag{6.59}$$

and some undefined source, $\{\,\vec{q}^{\,*}\,\}_s$, which also depends on response s. Let us take the complete inner product of the MFS with the auxiliary system solution, $\{\,\delta\vec{x}^{\,*}\,\}_s$, and the complete inner product of the auxiliary system with the MFS solution, $\{\,\delta\vec{x}\,\}_p$, and subtract the two.

$$\begin{aligned}\left\langle\, \widetilde{\mathbf{A}}_x \{\,\delta\vec{x}\,\}_p \;,\; \{\,\delta\vec{x}^{\,*}\,\}_s \,\right\rangle - \left\langle\, \widetilde{\mathbf{A}}_x^* \{\,\delta\vec{x}^{\,*}\,\}_s \;,\; \{\,\delta\vec{x}\,\}_p \,\right\rangle = \\ \left\langle\, \{\,\vec{q}^{\,*}\,\}_s \;,\; \{\,\delta\vec{x}\,\}_p \,\right\rangle - \left\langle\, \{\,\vec{q}\,\}_p \;,\; \{\,\delta\vec{x}^{\,*}\,\}_s \,\right\rangle\end{aligned} \tag{6.60}$$

If we can determine the master matrix $\widetilde{\mathbf{A}}_x^*$ which makes the left side of the above equation 0 (less boundary terms), then we have

$$\left\langle\, \{\,\vec{q}^{\,*}\,\}_s \;,\; \{\,\delta\vec{x}\,\}_p \,\right\rangle = \left\langle\, \{\,\vec{q}\,\}_p \;,\; \{\,\delta\vec{x}^{\,*}\,\}_s \,\right\rangle - \left\langle\!\left\langle\, \{\,\delta\vec{x}\,\}_p \;,\; \{\,\delta\vec{x}^{\,*}\,\}_s \,\right\rangle\!\right\rangle. \tag{6.61}$$

Now we can use the auxiliary source $\{\,\vec{q}^{\,*}\,\}_s$ to realize our response. To do this, let us define the auxiliary source as the realization vector for response s plus some extra term we will discuss shortly, $\{\,\vec{q}^{\,*}\,\}_s \stackrel{\text{def}}{=} \{\,\vec{h}_x\,\}_s + \{\,\vec{a}\,\}_s$. Substituting this in Eq. (6.61), we obtain

$$\begin{aligned} r_s &= \left\langle\, \{\,\vec{h}_x\,\}_s \,,\, \{\,\delta\vec{x}\,\}_p \,\right\rangle \\ &= \left\langle\, \{\,\vec{q}\,\}_p \,,\, \{\,\delta\vec{x}^{\,*}\,\}_s \,\right\rangle - \left\langle\, \{\,\vec{a}\,\}_s \,,\, \{\,\delta\vec{x}\,\}_p \,\right\rangle - \left\langle\!\left\langle\, \{\,\delta\vec{x}\,\}_p \,,\, \{\,\delta\vec{x}^{\,*}\,\}_s \,\right\rangle\!\right\rangle, \end{aligned} \tag{6.62}$$

our response as the inner product of our MFS source, $\vec{q}$, and AS solution, $\delta\vec{x}^{\,*}$, and two terms which we must make known or identically zero. First, let us discuss this extra term, $\vec{a}$, which is required when solvability conditions demand modification of the auxiliary source. The extra term has the form,

$$\{\,\vec{a}\,\}_s^j = \left(\,\{\,a_\eta(t)\,\}_s^j,\, \{\,a_\varphi\,\}_s^j,\, \{\,a_\Phi\,\}_s^j\,\right)^T \text{ for } j = 0, ..., N_j. \tag{6.63}$$

Note that $\vec{a}$ is a single scalar value for each equation. So upon further inspection the inner product $\left\langle\, \{\,\vec{a}\,\}_s \,,\, \{\,\delta\vec{x}\,\}_p \,\right\rangle$ must be 0 or the AS requires solution of the MFS, which we must avoid if the AS is to be useful. Therefore we have the following expression for change in response s for perturbation p.

$$\{\,\delta\vec{r}\,\}_{s,p} = \left\langle\, \{\,\vec{q}\,\}_p \,,\, \{\,\delta\vec{x}^{\,*}\,\}_s \,\right\rangle - \left\langle\!\left\langle\, \{\,\delta\vec{x}\,\}_p \,,\, \{\,\delta\vec{x}^{\,*}\,\}_s \,\right\rangle\!\right\rangle \tag{6.64}$$

All data perturbations are contained in $\{\,\vec{q}\,\}_p$ so we can solve the entire auxiliary (adjoint) system for $\{\,\delta\vec{x}^{\,*}\,\}_s$ and *then* perform data perturbations to calculation response changes—all provided we can determine the master matrix $\widetilde{\mathbf{A}}_x^*$ which makes the left side of Eq. (6.60) vanish and an expression for the boundary terms which does not depend on unknown values of $\delta\vec{x}$. But since boundary terms appear as a result of applying integration by parts to differential equations, the only boundary terms we have will come from the nuclide transmutation equation.

6.5.5 Determining the Form of the Adjoint Matrix

At this point, we would like to present the AS in matrix form.

$$\widetilde{\mathbf{A}}_x^* \delta\vec{x}^{\,*} = \vec{q}^{\,*} \tag{6.65}$$

The master solution vector $\delta\vec{x}^{\,*}$ has the following form.

$$\delta\vec{x}^{\,*} \stackrel{\text{def}}{=} \left(\,\{\,\delta\vec{x}^{\,*}\,\}^0,\, \{\,\delta\vec{x}^{\,*}\,\}^1, \ldots,\, \{\,\delta\vec{x}^{\,*}\,\}^j, \ldots,\, \{\,\delta\vec{x}^{\,*}\,\}^{N_j}\,\right)^T \tag{6.66a}$$

The solution vector $\{\,\delta\vec{x}\,\}^j$ for $j = 0, ..., N_j$ has the following form.

$$\{\,\delta\vec{x}^{\,*}\,\}^j \stackrel{\text{def}}{=} \left(\,\{\,\delta\vec{\eta}^{\,*}(t)\,\}^j\,,\,\{\,\delta\vec{\varphi}^{\,*}\,\}^j\,,\,\{\,\delta\Phi^*\,\}^j\,\right)^T \tag{6.66b}$$

The master matrix $\widetilde{\mathbf{A}}_x^*$ has the following form.

$$\widetilde{\mathbf{A}}_x \stackrel{\text{def}}{=} \begin{pmatrix} \{\,\widetilde{\mathbf{A}}_{x+}^*\,\}^0 & \{\,\widetilde{\mathbf{A}}_{x-}^*\,\}^0 & 0 & 0 & 0 & 0 \\ 0 & \{\,\widetilde{\mathbf{A}}_{x+}^*\,\}^1 & \{\,\widetilde{\mathbf{A}}_{x-}^*\,\}^1 & 0 & 0 & 0 \\ 0 & 0 & \ddots & \ddots & 0 & 0 \\ 0 & 0 & 0 & \{\,\widetilde{\mathbf{A}}_{x+}^*\,\}^j & \{\,\widetilde{\mathbf{A}}_{x-}^*\,\}^j & 0 \\ 0 & 0 & 0 & 0 & \ddots & \ddots \\ 0 & 0 & 0 & 0 & 0 & \{\,\widetilde{\mathbf{A}}_{x+}^*\,\}^{N_j} \end{pmatrix} \tag{6.67a}$$

The matrices $\{\,\widetilde{\mathbf{A}}_{x-}^*\,\}^j$ for $j = 1, ..., N_j - 1$ and $\{\,\widetilde{\mathbf{A}}_{x+}^*\,\}^j$ for $j = 0, ..., N_j$ have the following form.

$$\{\,\widetilde{\mathbf{A}}_{x+}^*\,\}^0 \stackrel{\text{def}}{=} \begin{pmatrix} 2\delta(t-t_0)\mathbf{E} & \{\,\widetilde{\mathbf{B}}_\eta^T(t)\,\}^0 & \{\,\vec{p}_\eta(t)\,\}^0 \\ 0 & \{\,\widetilde{\mathbf{B}}^T\,\}^0 & \{\,\vec{p}_\varphi\,\}^0 \\ 0 & 0 & \{\,p\,\}^0 \end{pmatrix} \tag{6.67b}$$

$$\{\,\widetilde{\mathbf{A}}_{x-}^*\,\}^j \stackrel{\text{def}}{=} \begin{pmatrix} 0 & 0 & 0 \\ -\left[\,\{\,\widetilde{\mathbf{M}}_{\varphi-}^T(t)\,\}^{j+1}\circ\,\right]_{k,\tau_{j+1}} & 0 & 0 \\ -\left[\,\{\,\vec{m}_{\Phi-}(t)\,\}^{j+1}\circ\,\right]_{k,i,\tau_{j+1}} & 0 & 0 \end{pmatrix} \tag{6.67c}$$

$$\{\,\widetilde{\mathbf{A}}_{x+}^*\,\}^j \stackrel{\text{def}}{=} \begin{pmatrix} -\frac{d}{dt} - \{\,\widetilde{\mathbf{M}}^T\,\}^j & \{\,\widetilde{\mathbf{B}}_\eta^T(t)\,\}^j & \{\,\vec{p}_\eta(t)\,\}^j \\ -\left[\,\{\,\widetilde{\mathbf{M}}_{\varphi+}^T(t)\,\}^j\circ\,\right]_{k,\tau_j} & \{\,\widetilde{\mathbf{B}}^T\,\}^j & \{\,\vec{p}_\varphi\,\}^j \\ -\left[\,\{\,\vec{m}_{\Phi+}(t)\,\}^j\circ\,\right]_{k,i,\tau_j} & 0 & \{\,p\,\}^j \end{pmatrix} \tag{6.67d}$$

We have also changed operator $\frac{d}{dt} \to -\frac{d}{dt}$ which introduces the boundary term $\left[\,\{\,\delta\vec{\eta}^{\,*}(t_0)\,\}^0\,\Delta\vec{\eta}_0\,\right]_{k,i}$, assuming we demand the adjoint nuclide function at EOC is zero, $\{\,\delta\vec{\eta}^{\,*}(t_N)\,\}^{N_j} = 0$. The master source vector $\vec{q}^{\,*}$ has the following form.

$$\vec{q}^{\,*} \stackrel{\text{def}}{=} \left(\,\{\,\vec{q}^{\,*}\,\}^0\,,\,\{\,\vec{q}^{\,*}\,\}^1\,,\ldots,\,\{\,\vec{q}^{\,*}\,\}^j\,,\ldots,\,\{\,\vec{q}^{\,*}\,\}^{N_j}\,\right)^T \tag{6.68a}$$

The source vector $\{\,\vec{q}^{\,*}\,\}^j$ for $j = 0, ..., N_j$ has the following form.

$$\{\,\vec{q}^{\,*}\,\}^j \stackrel{\text{def}}{=} \left(\,\{\,\vec{q}_\eta^{\,*}(t)\,\}^j\,,\,\{\,\vec{q}_\varphi^{\,*}\,\}^j\,,\,\{\,\vec{q}_\Phi^{\,*}\,\}^j\,\right)^T \tag{6.68b}$$

Now let us reconstruct our system of adjoint equations.

Adjoint Flux Shape Equation

For the adjoint flux shape equation at $j = N_j$ we have

$$\begin{aligned} \{\,\widetilde{\mathbf{B}}^T\,\}^{N_j}\ \{\,\delta\vec{\varphi}^*\,\}_s^{N_j} &= \Big[\ \{\,\widetilde{\mathbf{M}}^T_{\varphi+}(t)\,\}^{N_j}\ \{\,\delta\vec{\eta}^*(t)\,\}_s^{N_j}\ \Big]_{k,\tau_N} - \\ &\quad \{\,\vec{p}_\varphi\,\}^{N_j}\ \{\,\delta\Phi^*\,\}_s^{N_j} + \{\,\vec{h}_\varphi\,\}_s^{N_j} + \{\,a_\varphi\,\}_s^{N_j}, \end{aligned} \tag{6.69}$$

at $j = 1, ..., N_j - 1$, we have

$$\begin{aligned} \{\,\widetilde{\mathbf{B}}^T\,\}^{j}\ \{\,\delta\vec{\varphi}^*\,\}_s^{j} &= \Big[\ \{\,\widetilde{\mathbf{M}}^T_{\varphi+}(t)\,\}^{j}\ \{\,\delta\vec{\eta}^*(t)\,\}_s^{j}\ \Big]_{k,\tau_j} + \\ &\quad \Big[\ \{\,\widetilde{\mathbf{M}}^T_{\varphi-}(t)\,\}^{j+1}\ \{\,\delta\vec{\eta}^*(t)\,\}_s^{j+1}\ \Big]_{k,\tau_{j+1}} - \\ &\quad \{\,\vec{p}_\varphi\,\}^{j}\ \{\,\delta\Phi^*\,\}_s^{j} + \{\,\vec{h}_\varphi\,\}_s^{j} + \{\,a_\varphi\,\}_s^{j}, \end{aligned} \tag{6.70}$$

and at $j = 0$ we have

$$\begin{aligned} \{\,\widetilde{\mathbf{B}}^T\,\}^{0}\ \{\,\delta\vec{\varphi}^*\,\}_s^{0} &= \Big[\ \{\,\widetilde{\mathbf{M}}^T_{\varphi-}(t)\,\}^{1}\ \{\,\delta\vec{\eta}^*(t)\,\}_s^{1}\ \Big]_{k,\tau_1} - \\ &\quad \{\,\vec{p}_\varphi\,\}^{0}\ \{\,\delta\Phi^*\,\}_s^{0} + \{\,\vec{h}_\varphi\,\}_s^{0} + \{\,a_\varphi\,\}_s^{0}, \end{aligned} \tag{6.71}$$

Adjoint Flux Amplitude Equation

For the adjoint flux amplitude function at $j = N_j$ we have

$$\begin{aligned} \{\,\delta\Phi^*\,\}_s^{N_j} = \quad & \frac{\Big[\ \{\,\vec{m}_{\Phi+}(t)\,\}^{N_j}\ \{\,\delta\vec{\eta}^*(t)\,\}_s^{N_j}\ \Big]_{k,i,\tau_N}}{\{\,p\,\}^{N_j}} + \\ & \frac{\{\,h_\Phi\,\}_s^{N_j} + \{\,a_\Phi\,\}_s^{N_j}}{\{\,p\,\}^{N_j}}, \end{aligned} \tag{6.72}$$

at $j = 1, ..., N_j - 1$, we have

$$\begin{aligned} \{\,\delta\Phi^*\,\}_s^{j} = \quad & \frac{\Big[\ \{\,\vec{m}_{\Phi+}(t)\,\}^{j}\ \{\,\delta\vec{\eta}^*(t)\,\}_s^{j}\ \Big]_{k,i,\tau_j}}{\{\,p\,\}^{j}} + \\ & \frac{\Big[\ \{\,\vec{m}_{\Phi-}(t)\,\}^{j+1}\ \{\,\delta\vec{\eta}^*(t)\,\}_s^{j+1}\ \Big]_{k,i,\tau_{j+1}}}{\{\,p\,\}^{j}} + \\ & \frac{\{\,h_\Phi\,\}_s^{j} + \{\,a_\Phi\,\}_s^{j}}{\{\,p\,\}^{j}}, \end{aligned} \tag{6.73}$$

and at $j = 0$ we have

$$\{\,\delta\Phi^*\,\}_s^0 = \frac{\left[\,\{\,\vec{m}_{\Phi-}(t)\,\}^1\,\{\,\delta\vec{\eta}^*(t)\,\}_s^1\,\right]_{k,i,\tau_1}}{\{\,p\,\}^0} + \frac{\{\,h_\Phi\,\}_s^0 + \{\,a_\Phi\,\}_s^0}{\{\,p\,\}^0},$$

Adjoint Nuclide Field Equation

For the adjoint nuclide field equation for time steps τ_j, $j = 1, ..., N_j$ we have

$$-\frac{d}{dt}\{\,\delta\vec{\eta}^*(t)\,\}_s^j = \{\,\widetilde{\mathbf{M}}^T\,\}^j\,\{\,\delta\vec{\eta}^*(t)\,\}_s^j - \{\,\widetilde{\mathbf{B}}_\eta^T(t)\,\}^j\,\{\,\delta\vec{\varphi}^*\,\}_s^j - \{\,\vec{p}_\eta(t)\,\}^j\,\{\,\delta\Phi^*\,\}_s^j + \{\,\vec{h}_\eta\,\}_s^j + \{\,a_\eta\,\}_s^j, \tag{6.74}$$

and for $j = 0$, we have

$$\{\,\delta\vec{\eta}^*(t)\,\}_s^0 = -\left[\,\{\,\widetilde{\mathbf{B}}_\eta^T(t)\,\}^0\,\right]_{\tau_0}\{\,\delta\vec{\varphi}^*\,\}_s^0 - \{\,\vec{p}_\eta(t)\,\}^0\,\{\,\delta\Phi^*\,\}_s^0 + \{\,\vec{h}_\eta\,\}_s^0 + \{\,a_\eta\,\}_s^0. \tag{6.75}$$

Now, as we have said before, solvability concerns dictate the values of $\vec{a}$. For our first orthogonality condition, realized from our MFS equations, we realize we may need to take into account the fact that if we take the inner product of the adjoint flux shape equation with the nominal solution,

$$\begin{aligned}\left\langle\,\{\,\widetilde{\mathbf{B}}^T\,\}^j\,\{\,\delta\vec{\varphi}^*\,\}_s^j\,,\,\{\,\vec{\varphi}\,\}^j\,\right\rangle &= \left\langle\,\left[\,\{\,\widetilde{\mathbf{M}}_{\varphi+}^T(t)\,\}^j\,\{\,\delta\vec{\eta}^*(t)\,\}_s^j\,\right]_{k,\tau_j}\,,\,\{\,\vec{\varphi}\,\}^j\,\right\rangle + \\ &\left\langle\,\left[\,\{\,\widetilde{\mathbf{M}}_{\varphi-}^T(t)\,\}^{j+1}\,\{\,\delta\vec{\eta}^*(t)\,\}_s^{j+1}\,\right]_{k,\tau_{j+1}}\,,\,\{\,\vec{\varphi}\,\}^j\,\right\rangle - \\ &\left\langle\,\{\,\vec{p}_\varphi\,\}^j\,\{\,\delta\Phi^*\,\}_s^j\,,\,\{\,\vec{\varphi}\,\}^j\,\right\rangle + \\ &\left\langle\,\{\,\vec{h}_\varphi\,\}_s^j + \{\,a_\varphi\,\}_s^j\,,\,\{\,\vec{\varphi}\,\}^j\,\right\rangle \\ &= \left\langle\,\{\,\delta\vec{\varphi}^*\,\}_s^j\,,\,\{\,\widetilde{\mathbf{B}}\,\}^j\,\{\,\vec{\varphi}\,\}^j\,\right\rangle = 0\end{aligned} \tag{6.76}$$

then the following must be true,

$$\begin{aligned}\{\,a_\varphi\,\}_s^j = \frac{1}{\left\langle\,1\,,\,\{\,\vec{\varphi}\,\}^j\,\right\rangle} &\left(\left\langle\,\{\,\vec{p}_\varphi\,\}^j\,\{\,\delta\Phi^*\,\}_s^j\,,\,\{\,\vec{\varphi}\,\}^j\,\right\rangle - \right. \\ &\left\langle\,\{\,\vec{h}_\varphi\,\}_s^j\,,\,\{\,\vec{\varphi}\,\}^j\,\right\rangle - \\ &\left\langle\,\left[\,\{\,\widetilde{\mathbf{M}}_{\varphi+}^T(t)\,\}^j\,\{\,\delta\vec{\eta}^*(t)\,\}_s^j\,\right]_{k,\tau_j}\,,\,\{\,\vec{\varphi}\,\}^j\,\right\rangle - \\ &\left.\left\langle\,\left[\,\{\,\widetilde{\mathbf{M}}_{\varphi-}^T(t)\,\}^{j+1}\,\{\,\delta\vec{\eta}^*(t)\,\}_s^{j+1}\,\right]_{k,\tau_{j+1}}\,,\,\{\,\vec{\varphi}\,\}^j\,\right\rangle\right)\end{aligned} \tag{6.77}$$

which is small but not zero in most cases. For the adjoint flux amplitude equation to be solvable, we must require

$$\begin{aligned}
\left\langle \{\, p \,\}^j \{\, \delta\Phi^* \,\}_s^j \,,\, \{\, \Phi \,\}_s^j \right\rangle &= \left\langle \left[\{\, \vec{m}_{\Phi+}(t) \,\}^j \{\, \delta\vec{\eta}^*(t) \,\}_s^j \right]_{k,i,\tau_j} \,,\, \{\, \Phi \,\}_s^j \right\rangle + \\
&\left\langle \left[\{\, \vec{m}_{\Phi-}(t) \,\}^{j+1} \{\, \delta\vec{\eta}^*(t) \,\}_s^{j+1} \right]_{k,i,\tau_{j+1}} \,,\, \{\, \Phi \,\}_s^j \right\rangle + \\
&\left\langle \{\, h_\Phi \,\}_s^j + \{\, a_\Phi \,\}_s^j \,,\, \{\, \Phi \,\}_s^j \right\rangle \\
&= \left\langle \{\, \delta\Phi^* \,\}_s^j \,,\, \{\, p \,\}^j \{\, \Phi \,\}_s^j \right\rangle = \left\langle \{\, \delta\Phi^* \,\}_s^j \,,\, p_{core} \right\rangle
\end{aligned} \tag{6.78}$$

which actually is just the same as our original equation so we can set $\{\, a_\Phi \,\}_s^j = 0$. The adjoint nuclide field equation also does not require a solvability condition, $\{\, a_\eta \,\}_s^j = 0$

Chapter 7

Implementation

A The `INPUT_READER` section of NESTLE reads input from the directory set at compile time by parameter `dir_input`. The root input file is the first command-line argument of NESTLE *or* the `NESTLE.CNTL` by default. Memory for an input data variable is allocated upon first entry to that subroutine to the subroutine that reads the variable's data blocks.

B The `PREPROCESSOR` section of NESTLE has four main jobs.

- Convert units from input units to internal working units with `convert_units`.
- Set up the geometry with `geometry_setup`.
- Allocate the appropriate space for runtime variables based on input data variables and *runtype parameters* found in the input file.
- Produce an "input edit" output file—basically just a file easier on the human eyes than the input files to check for input data errors.

C The `CONTROLLER` section is the brains of NESTLE. It has complete control over the runtime behavior of NESTLE. It executes sequences of calculations based on the *runtype parameters* found in the input files. The main subroutines the `CONTROLLER` accesses for calculations are explained below, however, the `CONTROLLER` has the ability to direct the calculation back to re-reading input with `INPUT_READER` (and subsequent preprocessing) or preprocessing with `PREPROCESSOR`.

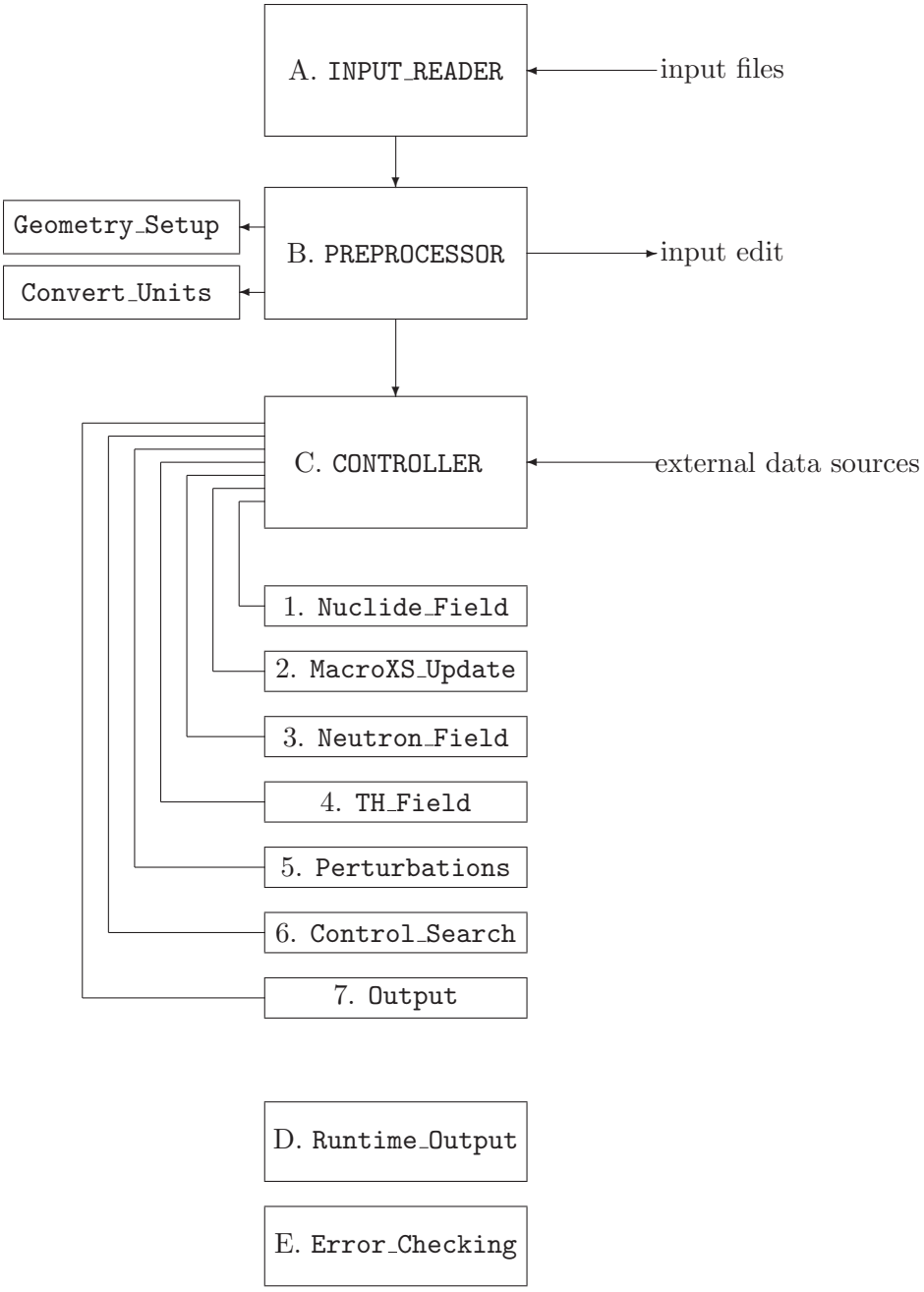

Figure 7.1: NESTLE Flow Diagram

1. The subroutine `Nuclide_Field` drives the calculation of the nuclide field (number density of various nuclei in the core). Usually the input is the beginning-of-interval nuclide concentrations and the neutron scalar flux over an interval and the output is the end-of-interval nuclide concentrations.
2. The subroutine `MacroXS_Update`, calculates macroscopic cross sections (parameters of the neutron transport equation) by interpolating them for burnup and feedback from thermal-hydraulic parameters. Macroscopic cross sections are also updated with new microscopic data and nuclide concentrations, if they have changed since the last update. Usually the input is burnup, macroscopic input data, and optionally microscopic input data and nuclide concentrations. The output is the burnup-interpolated and/or feedback-interpolated parameters of the diffusion equation.
3. The subroutine `Neutron_Field` calculates of the neutron field (neutron space and energy distribution in the core) by our chosen neutron transport equation using the macroscopic cross sections calculated in `MacroXS_Update`. Subroutine `Neutron_Field` also calculates the core power distribution.
4. The subroutine `TH_Field` calculates the thermal-hydraulic field resulting from the core power distribution calculated in `Neutron_Field`.
5. The subroutine `Perturbations` performs perturbations of data to facilitate sensitivity analysis and uncertainty analysis.
6. The subroutine `Control_Search` performs searches on various core control parameters to achieve some constraints (e.g. $k_e = 1$ for the eigenvalue problem, etc.)
7. The subroutine `Output` produces three types of output:
   - calculation results
   - data `CONTROLLER` will need later and does not wish to keep in RAM—the data becomes an external data source
   - input for another NESTLE run to be read by `INPUT_READER`

D Many procedures use `Runtime_Output`, which prints information about the stage of the calculation, residuals, stop messages, etc. assuming the parameter

`Requesting_RuntimeOutput=TRUE`. The output device is the second command-line argument of NESTLE *or* the screen if the second argument was not present.

E Many procedures use `Error_Checking`, which writes error and warning information to a file, assuming `Requesting_Errors=TRUE`' and `Requesting_Warnings=TRUE`, respectively. Traceback information may also be written using `Error_Checking` if `Requesting_Traceback=TRUE`, however traceback should only be used for debugging purposes as it writes information for every NESTLE procedure executed and will slow down the code tremendously. The output of errors, warnings, and traceback information before the input edit file is written (during the `INPUT_READER` and `PREPROCESSOR` sections) is set according to `Requesting_InputErrors`, `Requesting_InputWarnings`, and `Requesting_InputTraceback`.

Chapter 8

Results

8.1 Generalized Nuclide Field Solver Benchmark

In order to test our methods for solving the nuclide field equations, we have used a test problem found in an Argonne National Lab (ANL) Computational Benchmark Source Book [1]. The given data is a set of 2-group cross sections and decay constants for a variety of nuclei and a constant 2-group scalar flux. The initial material enriched uranium (5% ^{235}U and the rest ^{238}U) and the desired result is the nuclei concentrations after 50 days of irradiation. Other code systems have submitted results to this source book—most contributors to the ANL source book submitted two calculations of the nuclide field:

1. "standard-refinement" results obtained by using error tolerances and/or time step sizes representing that of a standard calculation and

2. "high-refinement" results obtained by using very small error tolerances and/or a very small time step size to achieve so-called "benchmark-quality" results.

The other code systems are Savanna River Lab's (SRL) 4^{th} order Runge-Kutta-Gill scheme, General Atomic's analytic and difference method, and MEDIUM-2—another analytic and difference method. With the `MATEXPSS` solver, error tolerances of *1E-6* and *1E-10* were used for the standard-refinement case and the high-refinement case, respectively. With the `ROSENBROCK2` solver, time steps of *1 day* and *1 second* were used for the standard-refinement

case and the high-refinement case, respectively. Both NESTLE's depletion methods show good agreement with the results of the codes of this benchmark, as shown in Fig. 8.1(a) and Fig. 8.1(b) for the standard-refinement and high refinement cases, respectively. The difference between `MATEXPSS` and the other nuclide ODE solution methods is shown in Fig. 8.2(a) (with zoomed view in Fig. 8.2(b)) and Fig. 8.3(a) (with zoomed view in Fig. 8.3(b)), for the standard-refinement and high-refinement cases, respectively. Note that the differences between solvers for the high-refinement case is much smaller than the difference for the standard-refinement case. The reason is different methods are being used with different orders of accuracy and this definitely matters for the standard-refinement case. But for the high-refinement case, as all numerical solutions tend to the real solution as the error tolerance or time step goes to zero, we see less method-dependent effects. The error tolerance for the matrix exponential with scaling and squaring as implemented in `MATEXPSS` dictates when to truncate the matrix exponential series expansion— the series is truncated when the maximum relative change in the nuclide concentrations at end-of-interval from adding a term is less than the error tolerance. We used *1E-6* as the tolerance for the standard-refinement case because this is the default value of the tolerance in NESTLE. Typically, with a tolerance of *1E-6*, 8 to 12 terms of the matrix exponential series are needed. With a tolerance of *1E-10*, up to 14 terms are needed. Overall, our matrix exponential method implemented in `MATEXPSS` and our second order Rosenbrock method implemented in `ROSENBROCK2` agree well with the data from other similar codes. Additionally, we tested `MATEXPSS` against MATLAB's `expm` as well as the matrix exponential solver in EXPOKIT, a Fortran matrix exponential toolkit [19] which utilizes the Pade approximation of the matrix exponential [5]. We have found a maximum relative difference between `MATEXPSS`-calculated and `expm`-calculated nuclide concentrations of about *1E-7%*. The maximum relative difference always occurred in nuclei of small concentrations—usually ^{234}U or ^{245}Cm.

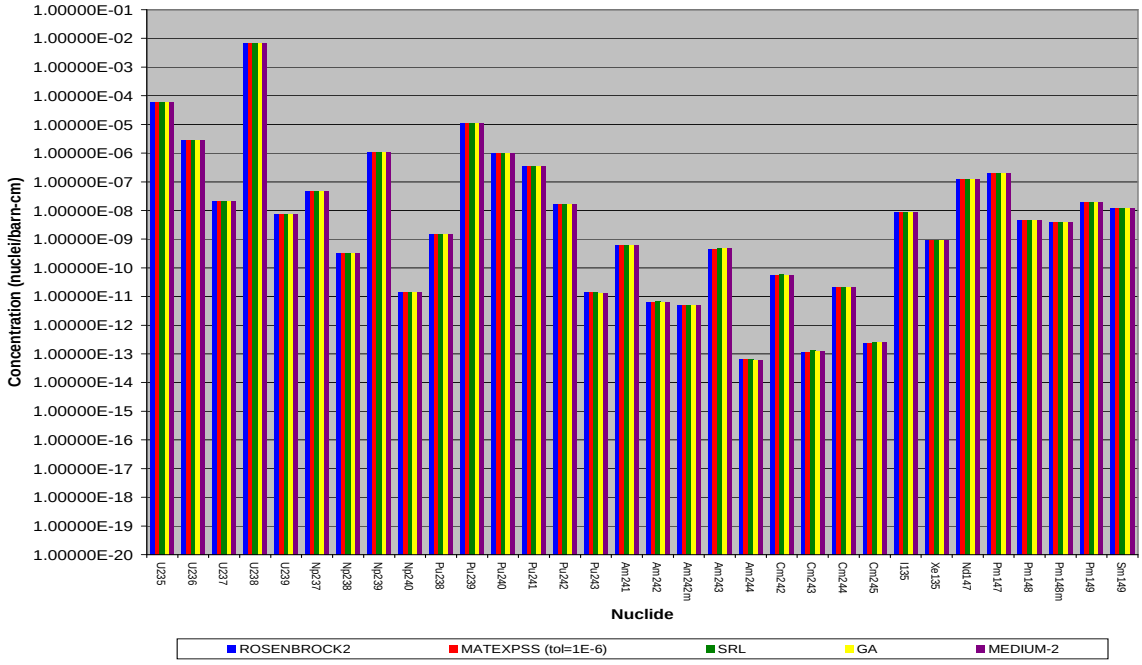

(a) Standard-Refinement Case

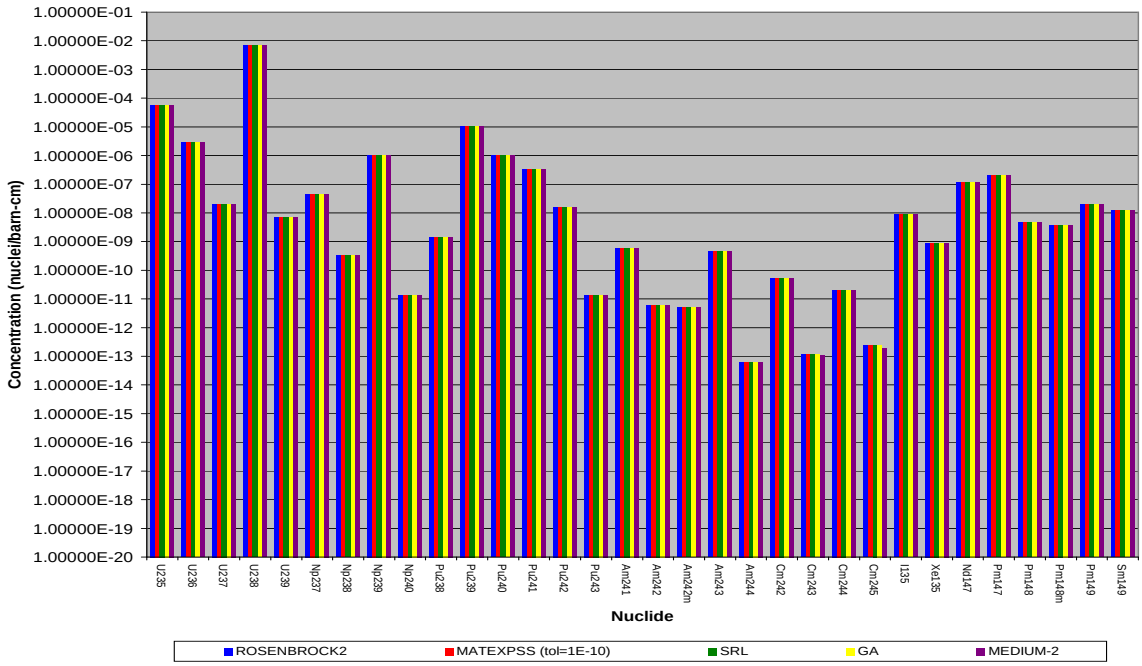

(b) High-Refinement Case

Figure 8.1: Generalized Nuclide Field Solver Benchmark Comparisons

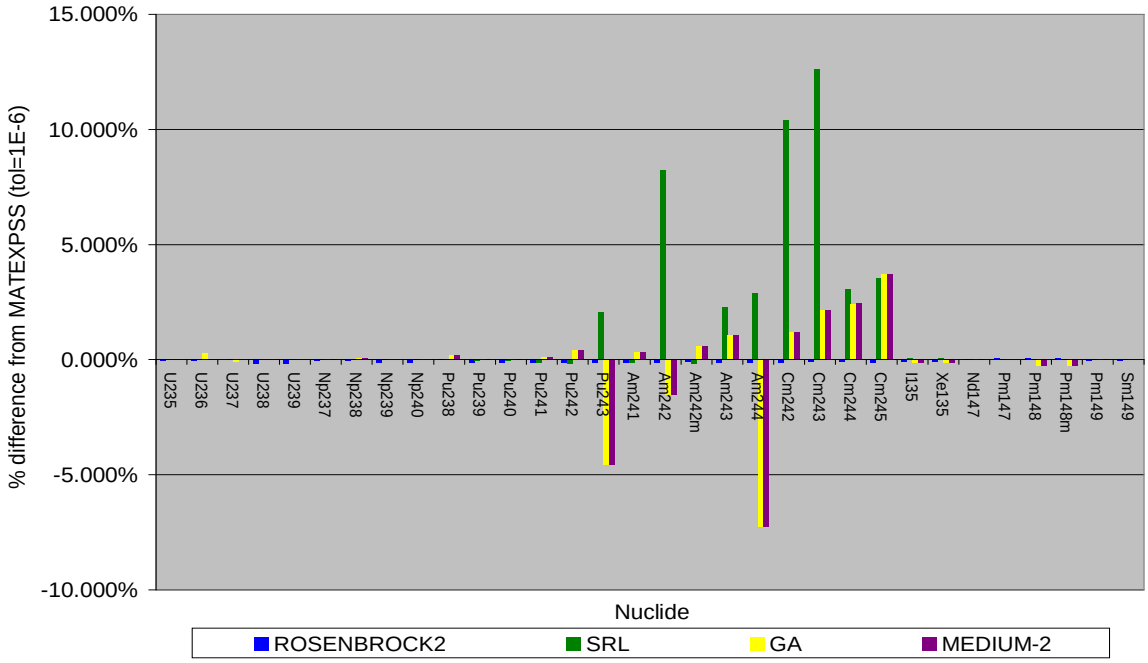

(a) Zoomed-Out

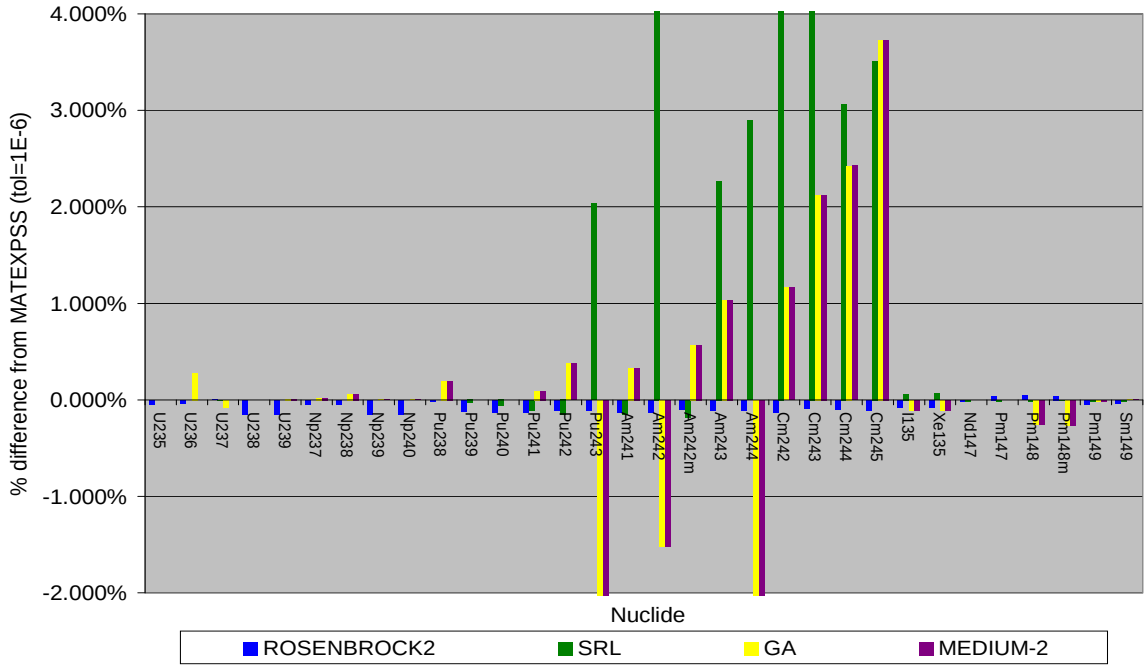

(b) Zoomed-In

Figure 8.2: Benchmark Differences in Concentrations for Standard-Refinement Case

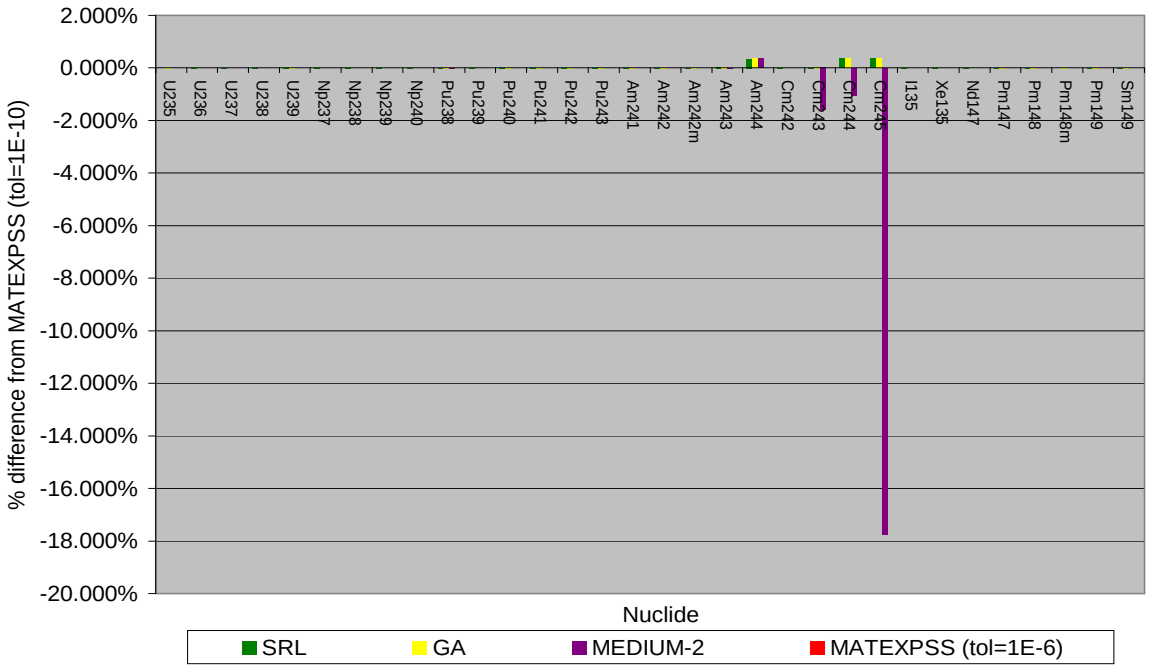

(a) Zoomed-Out

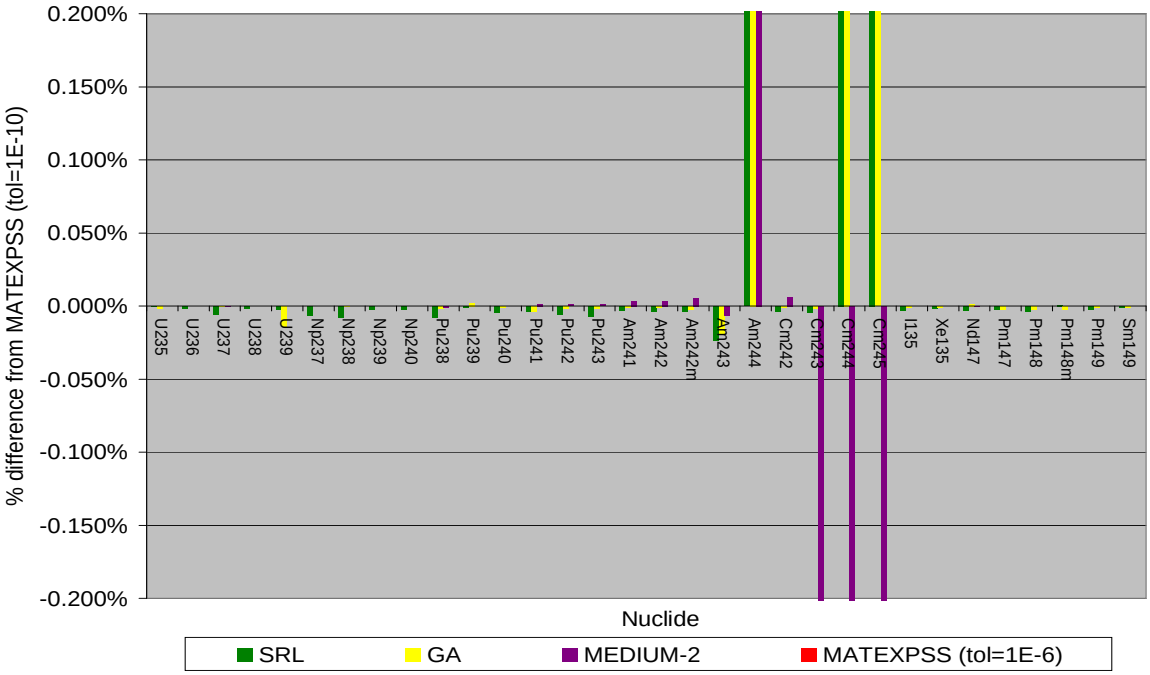

(b) Zoomed-In

Figure 8.3: Benchmark Differences in Concentrations for High-Refinement Case

8.2 Sensitivity Analysis Results

To demonstrate the use of the sensitivity analysis tool in NESTLE we consider a two-dimensional slice of a Westinghouse-style Pressurized Water Reactor (PWR). The fuel loading pattern contains 6 different materials, 5 of them fuel materials with UO_2 (see Fig. 8.4). Fig. 8.4 is a cycle 1 core, utilizing fresh UO_2 (contains only ^{235}U and ^{238}U at BOC),

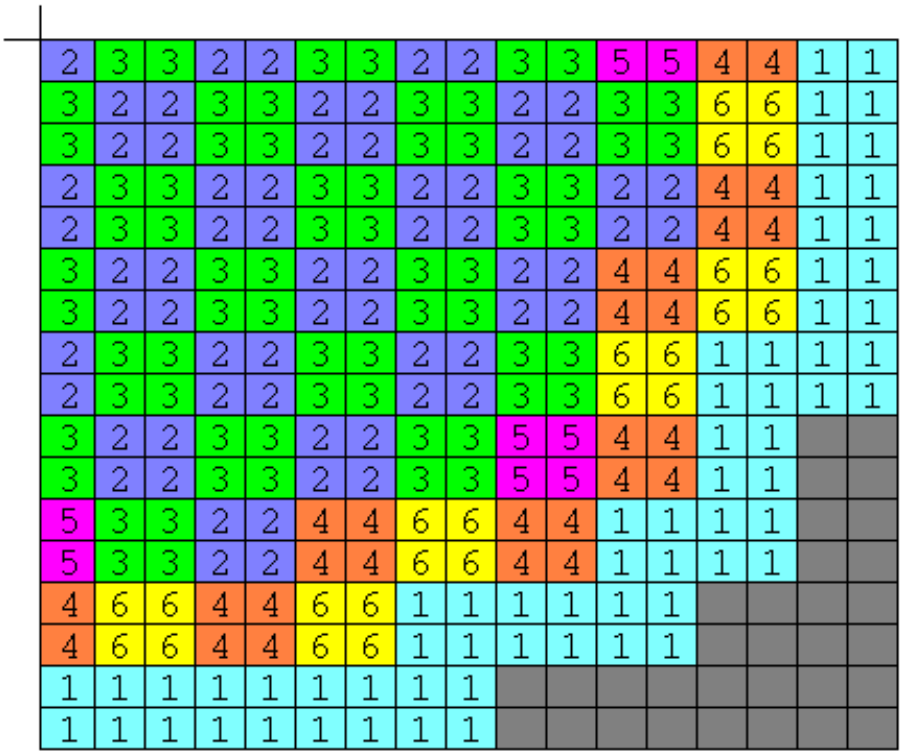

material id	$_{235_U}\{\vec{\eta}_0\}$	$_{238_U}\{\vec{\eta}_0\}$	$_{^1BP}\{\vec{\eta}_0\}$
1	-	-	-
2	1.40E-02	6.31E-01	0.00E+00
3	1.60E-02	6.29E-01	8.00E-04
4	2.20E-02	6.23E-01	8.00E-04
5	1.60E-02	6.29E-01	0.00E+00
6	2.20E-02	6.23E-01	0.00E+00

Figure 8.4: Core geometry (southeast quarter) and initial fuel composition.

taken from another ANL benchmark source book we will call CASE 10 [20]. The UO_2 fuel for CASE 10 is enriched in the fissile nuclide ^{235}U to varying degrees and materials 3 and 4 contain a simple burnable poison, ^1BP. Material 1 is a non-fuel material. For this problem,

we use the heavy metal nuclide field of Fig. 8.5. The fission products ^{135}I, ^{135}Xe, ^{147}Nd, ^{147}Pm, ^{148}Pm, ^{148m}Pm, ^{149}Pm, ^{149}Sm, and ^{135}Cs have also been included in the chain, but sensitivities of their concentrations to data perturbations will not be analyzed. In CASE 10, cross sections were only present for common fuel nuclei (U, Pu) so additional 2-group cross sections needed for all other nuclei were taken from the depletion methodology benchmark. Before we proceed into actual sensitivity analysis results, let us become familiar with the behavior of the core for the forward problem.

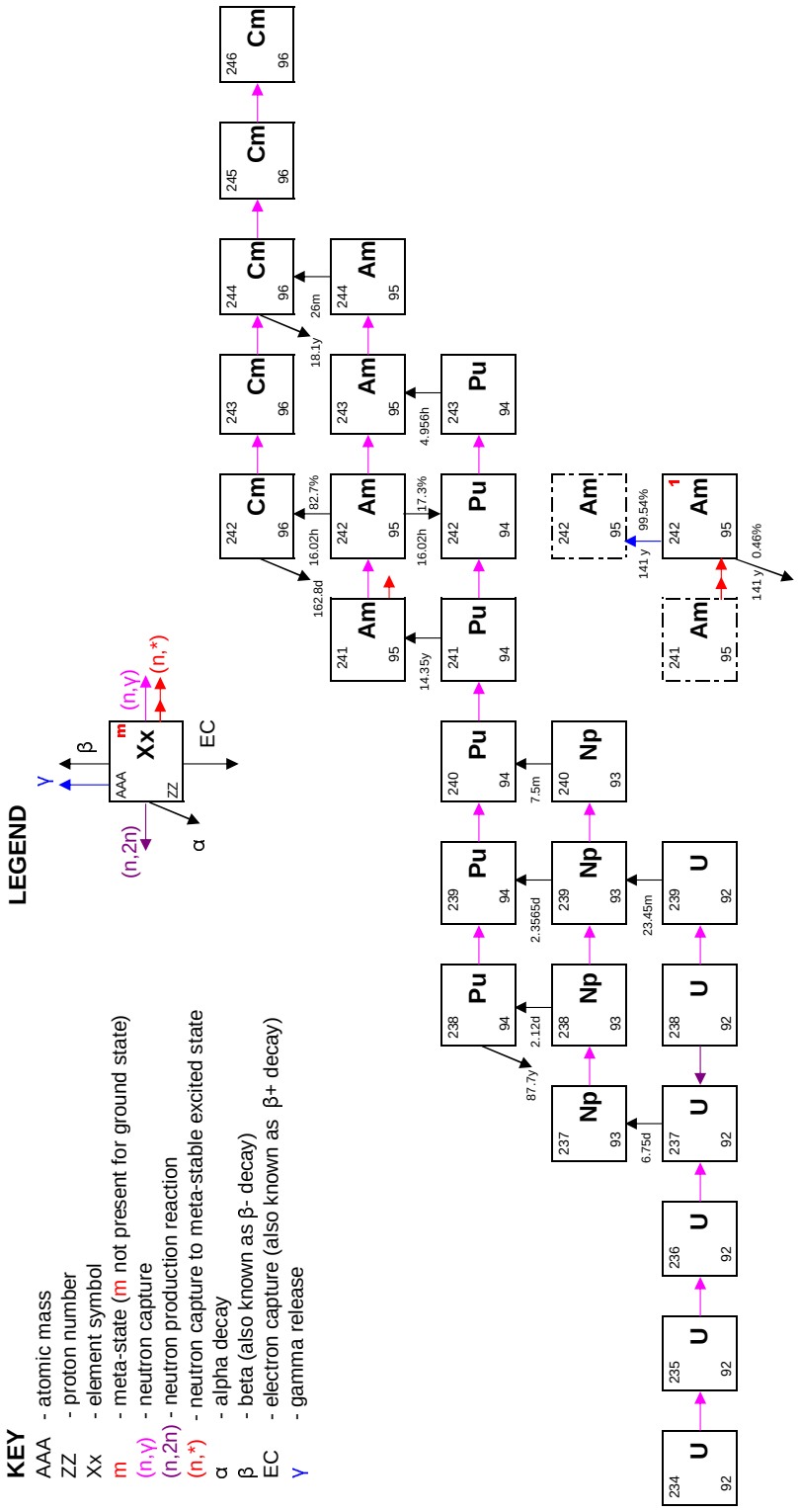

Figure 8.5: NESTLE nuclide field for heavy metal sensitivity analysis problems.

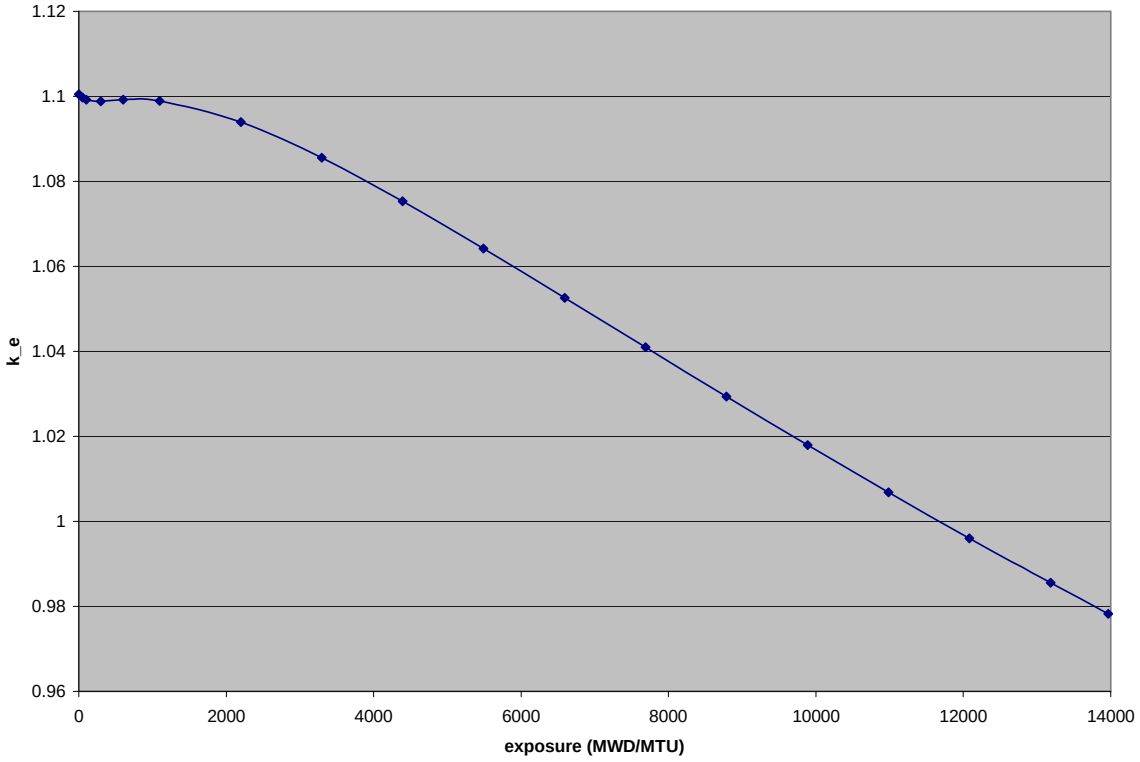

Figure 8.6: Eigenvalue, k_e, versus Exposure (MWD/MTU) over the reactor cycle.

8.2.1 Core Behavior

We now simulate our Fig. 8.4 core over a cycle using the reactor cycle equations presented in this paper. Let us look at various aspects of the core's behavior.

Eigenvalue

First let us look at the eigenvalue, k_e, as a function of core-average exposure (proportional to time) over the cycle. As you can see in Fig. 8.6, the fuel loading pattern is somewhat appropriate with the EOC k_e not too much less than 1. The reader should know that with the original CASE 10 nuclide field, with only the U-Pu chain and ^{135}Xe, k_e at EOC was much closer to unity. The extra nuclei we considered introduced some neutron sinks into the system, which were taken into account approximately by inclusion of these nuclei in "background" macroscopic absorption cross sections for materials in the benchmark. So

despite the slightly non-physical nature of this core (lacking sufficient reactivity for the whole cycle), because our goal here is to examine the behavior of a UO_2-fuelled core in terms of sensitivities of EOC nuclide concentrations to nuclear data, the CASE 10 core should be sufficient.

Scalar Flux Shape, $\vec{\varphi}$

The scalar flux shape function, $\{\vec{\varphi}\}^j$, is shown at initial time t_0 in Fig. 8.7(a)-8.7(b), middle times t_9 and t_{14} in Fig. 8.7(c)-8.8(b), and final time t_{18} in Fig. 8.8(c)-8.8(d). Notice that over the cycle, neutrons "move" from the center of the core to the outer edge of the core. Also, over the cycle, the flux distribution becomes much more uniform as neutrons "move" from the high thermal neutron-absorbing center of the core (due to the presence of fission products and minor actinides which absorb neutrons far more often than they release them) to the low(er) thermal neutron-absorbing periphery of the core.

Scalar Flux Amplitude, $\vec{\Phi}$

The neutron field amplitude function, $\vec{\Phi}$, changes over the cycle in a manner given by Fig. 8.9.

Scalar Flux Fast-To-Thermal Ratio

As the core becomes saturated with thermal neutron absorbing nuclei, the flux spectrum "hardens"—i.e. the ratio of fast neutrons to thermal neutrons in the core increases, which one can see in Fig. 8.10(a)-8.10(d).

EOC Nuclide Concentrations, $\vec{\eta}(t_N)$.

The EOC nuclide field versus position in the core for all heavy metal nuclei is shown in Fig. 8.11(a)-8.17(b). We will use the sensitivity analysis methods we have developed and implemented in NESTLE to analyze how sensitive this nuclide distribution is to perturbations in various data parameters. We present these graphs to familiarize the reader with the nominal distribution of nuclei as we believe this is helpful in understanding

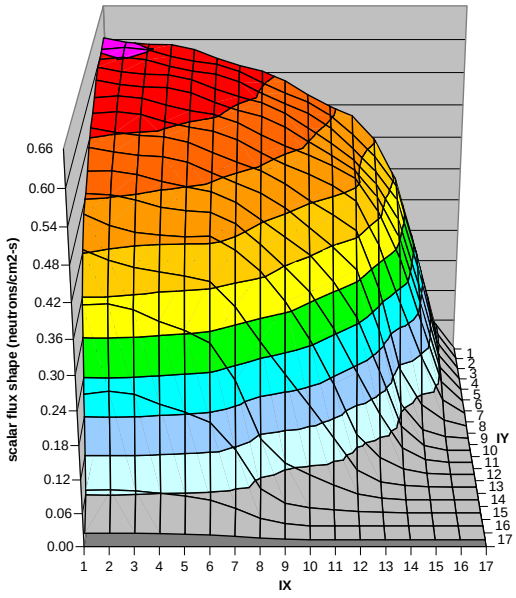

(a) Fast Flux at 0 MWD/MTU

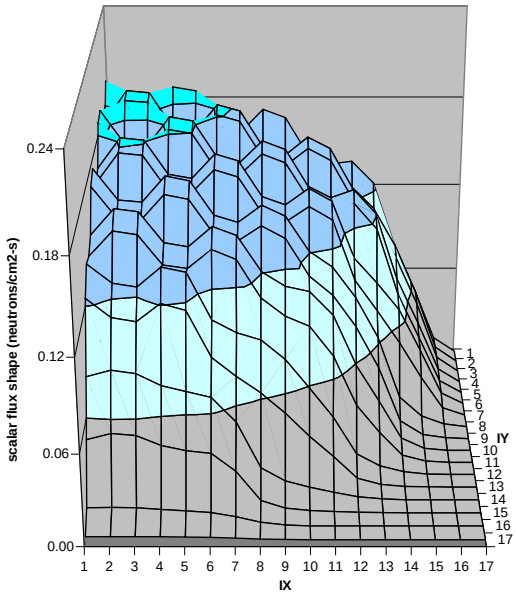

(b) Thermal Flux at 0 MWD/MTU

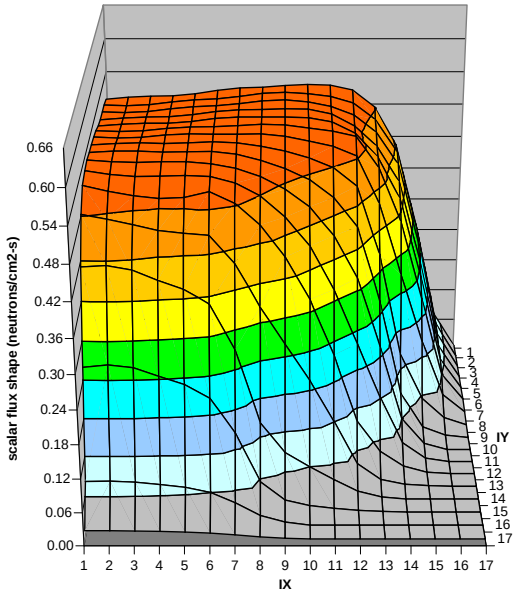

(c) Fast Flux at 5492 MWD/MTU

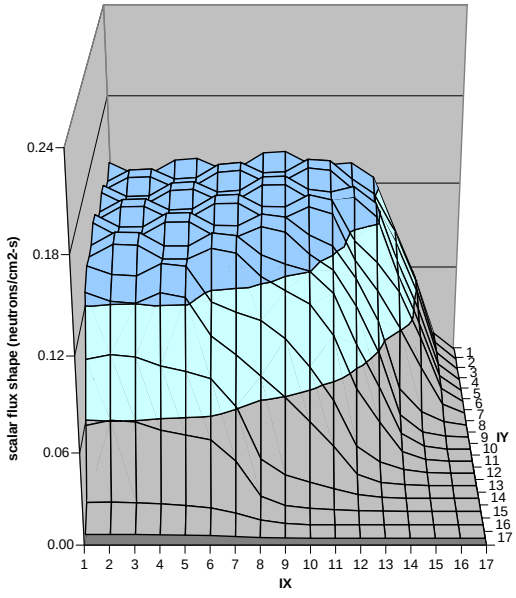

(d) Thermal Flux at 5492 MWD/MTU

Figure 8.7: Fast and Thermal Scalar Flux Shape versus Position in the reactor core at various Exposures (approximately BOC, 1/3 cycle)

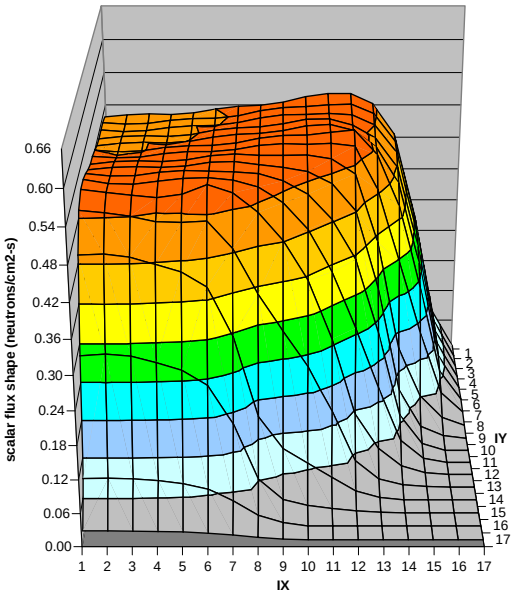

(a) Fast Flux at 9886 MWD/MTU

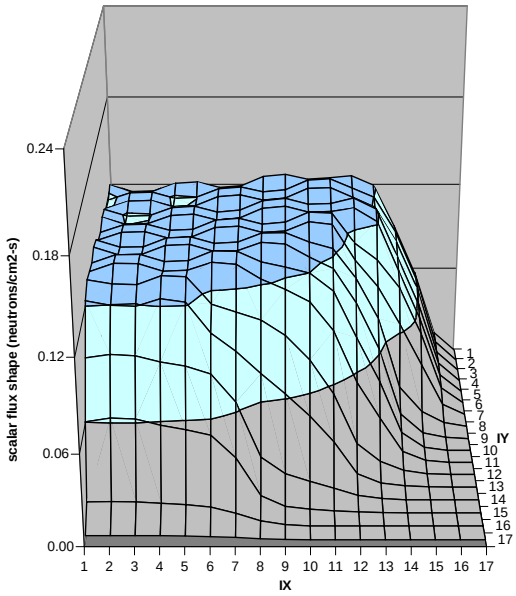

(b) Thermal Flux at 9886 MWD/MTU

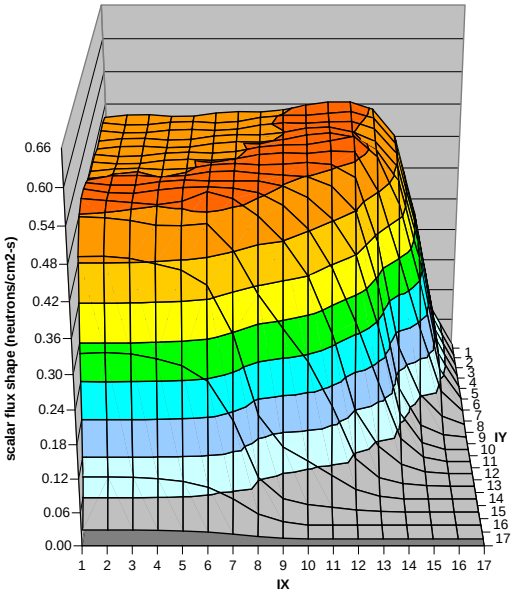

(c) Fast Flux at 13969 MWD/MTU

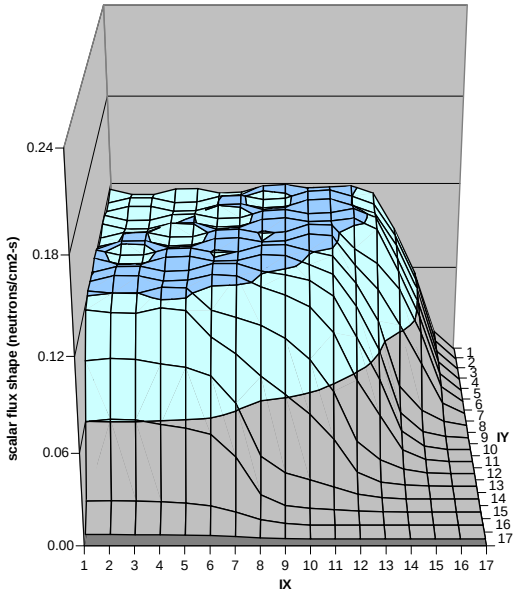

(d) Thermal Flux at 13969 MWD/MTU

Figure 8.8: Fast and Thermal Scalar Flux Shape versus Position in the reactor core at various Exposures (approximately 2/3 cycle, EOC)

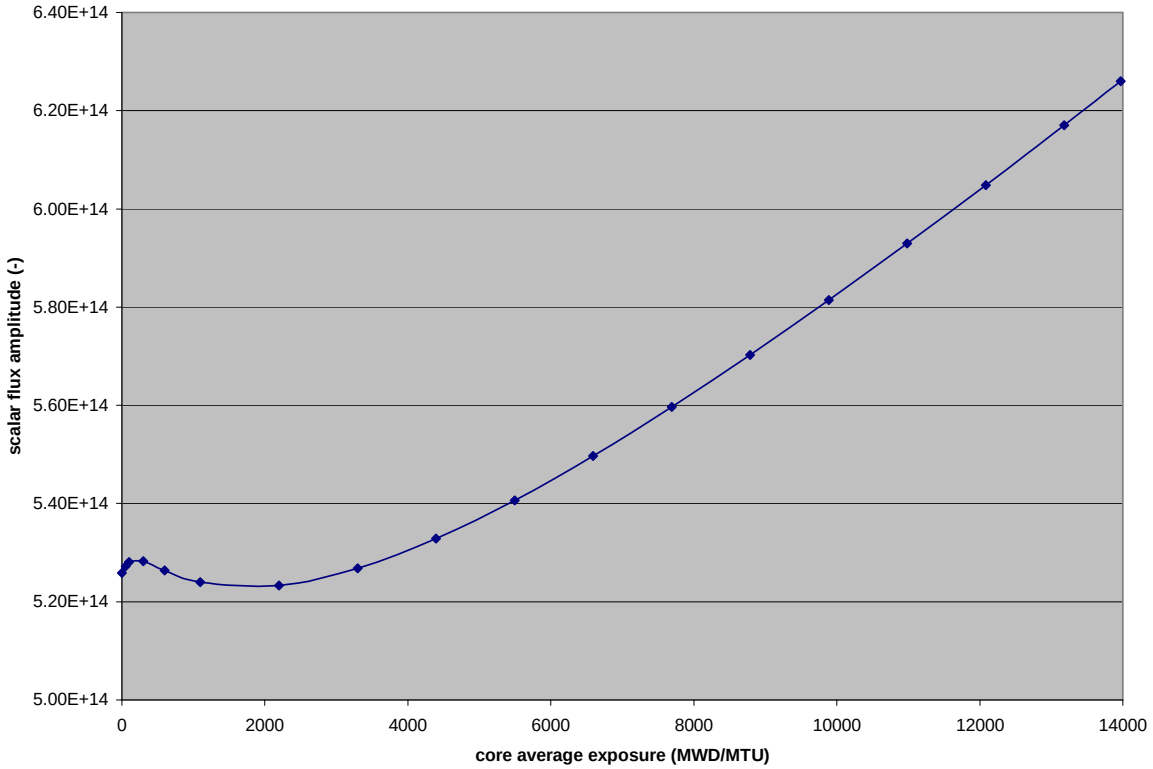

Figure 8.9: The Scalar Flux Amplitude versus Exposure (MWD/MTU), $\vec{\Phi}$.

the results of the perturbation theory. Additionally, the nuclide field provided in Fig. 8.5, complete with transmutation paths, may also prove helpful.

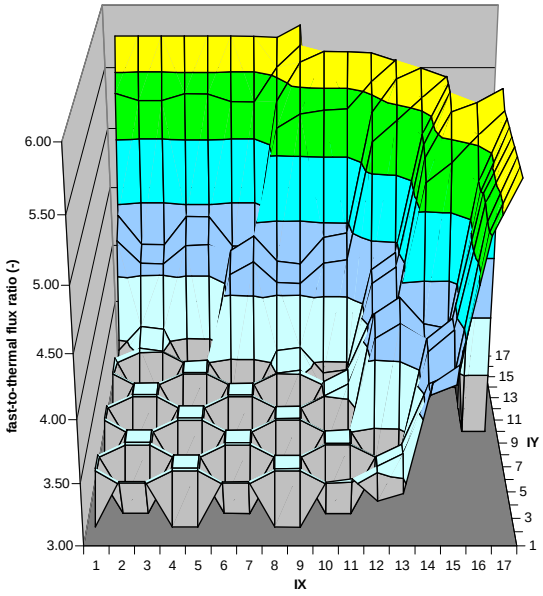

(a) BOC (0 MWD/MTU)

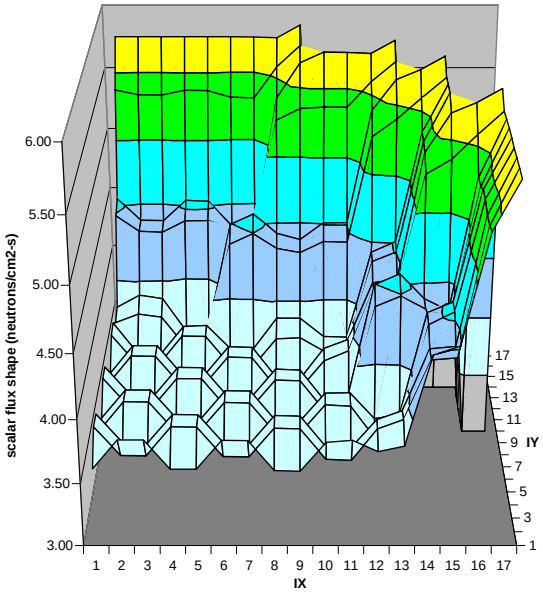

(b) 1/3 cycle (5492 MWD/MTU)

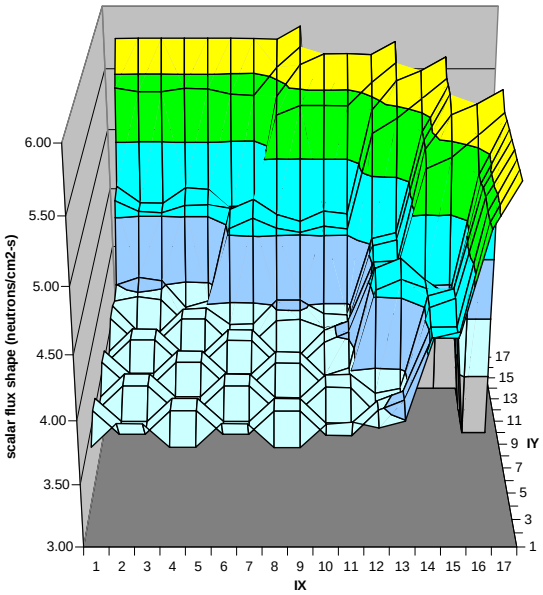

(c) 2/3 cycle (9886 MWD/MTU)

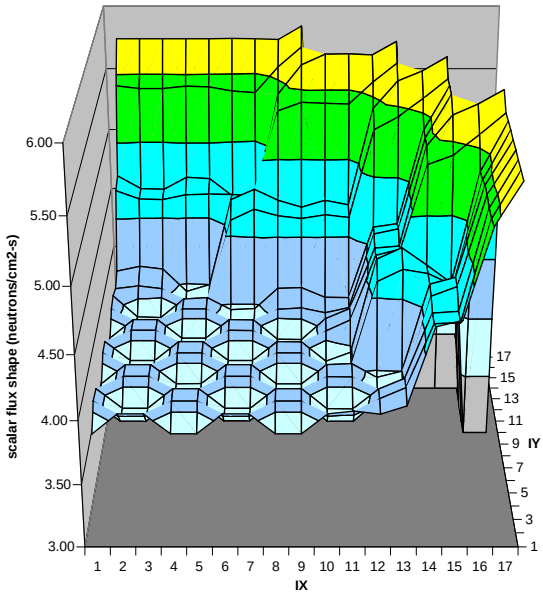

(d) EOC (13969 MWD/MTU)

Figure 8.10: Fast-to-Thermal Flux Ratios versus Position in the reactor core (northeastern symmetric quarter) at various Exposures

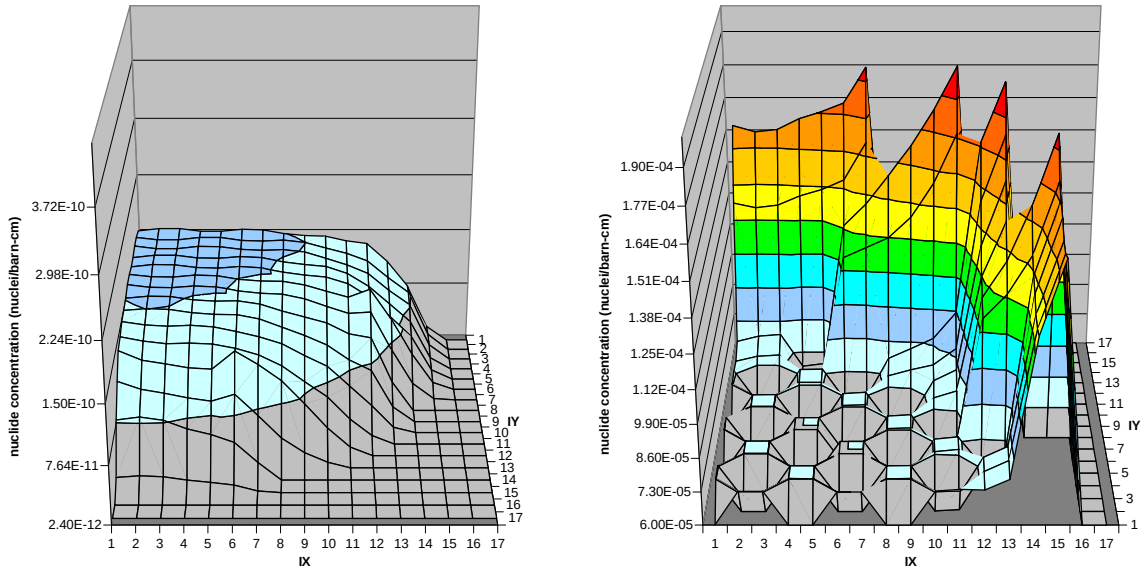

(a) ${}_{234}\mathrm{U}\{\vec{\eta}\}^{18}$ (b) ${}_{235}\mathrm{U}\{\vec{\eta}\}^{18}$

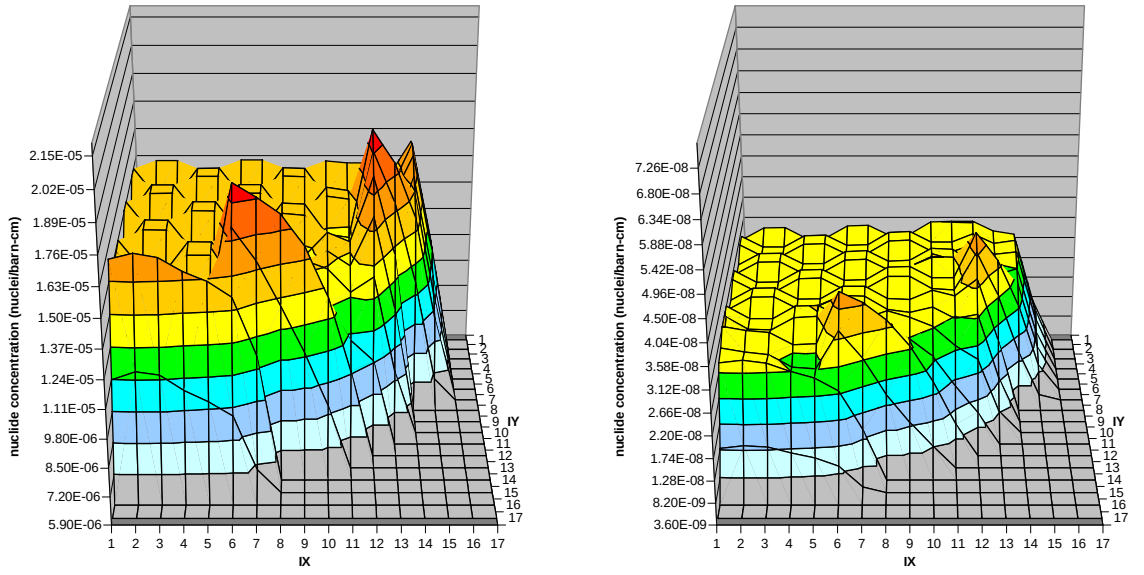

(c) ${}_{236}\mathrm{U}\{\vec{\eta}\}^{18}$ (d) ${}_{237}\mathrm{U}\{\vec{\eta}\}^{18}$

Figure 8.11: Nuclide Concentrations $\left(\frac{\text{nuclei}}{\text{barn}\cdot\text{cm}}\right)$ versus position at EOC (13969 MWD/MTU)

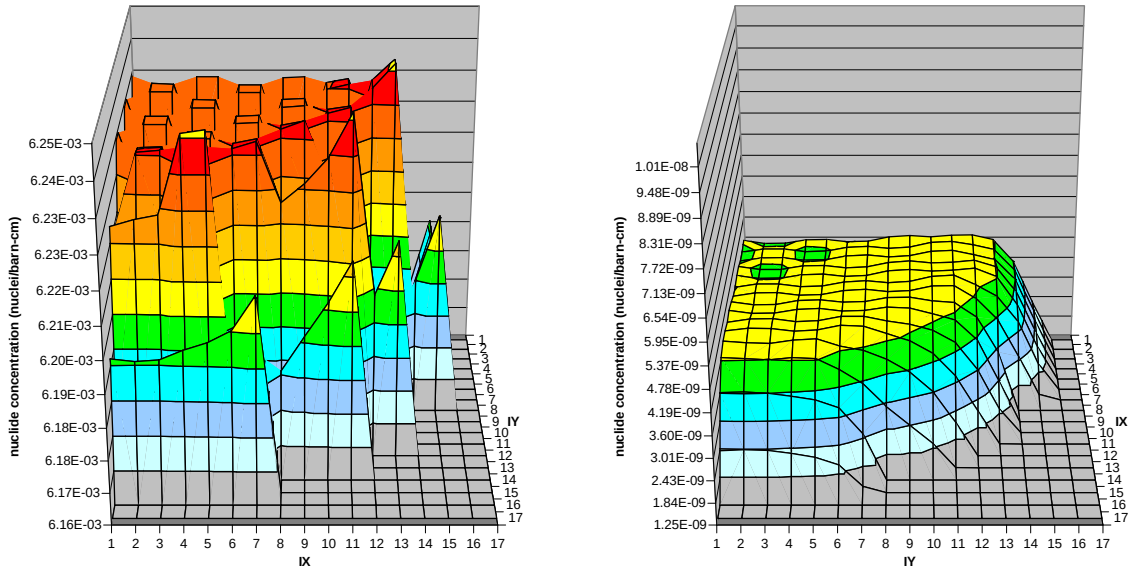

(a) $_{238_{\mathrm{U}}}\{\vec{\eta}\}^{18}$ (b) $_{239_{\mathrm{U}}}\{\vec{\eta}\}^{18}$

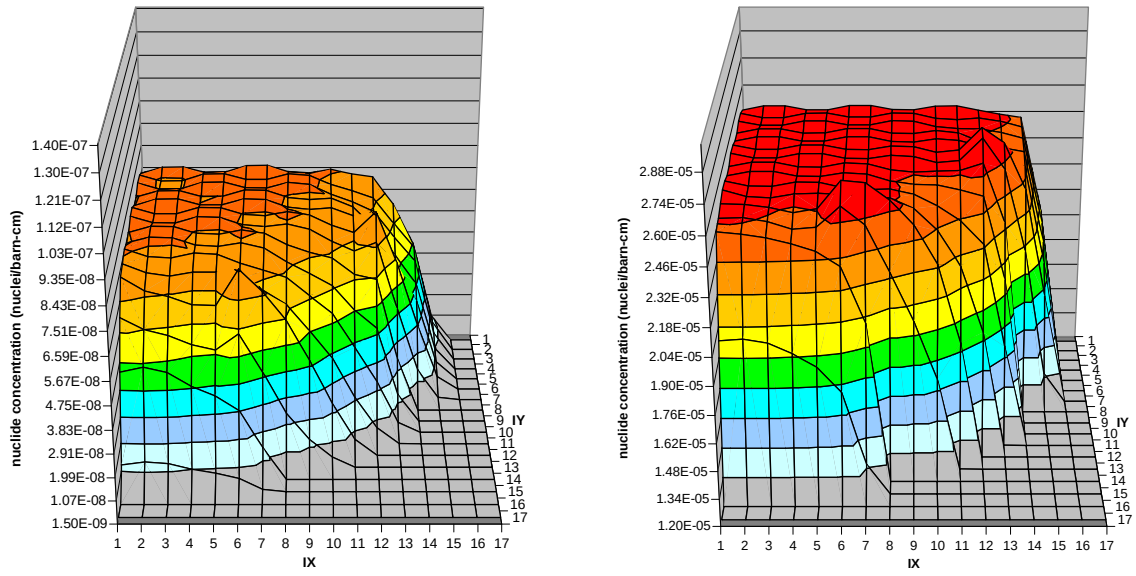

(c) $_{238_{\mathrm{Pu}}}\{\vec{\eta}\}^{18}$ (d) $_{239_{\mathrm{Pu}}}\{\vec{\eta}\}^{18}$

Figure 8.12: Nuclide Concentrations $\left(\frac{\text{nuclei}}{\text{barn}\cdot\text{cm}}\right)$ versus position at EOC (13969 MWD/MTU)

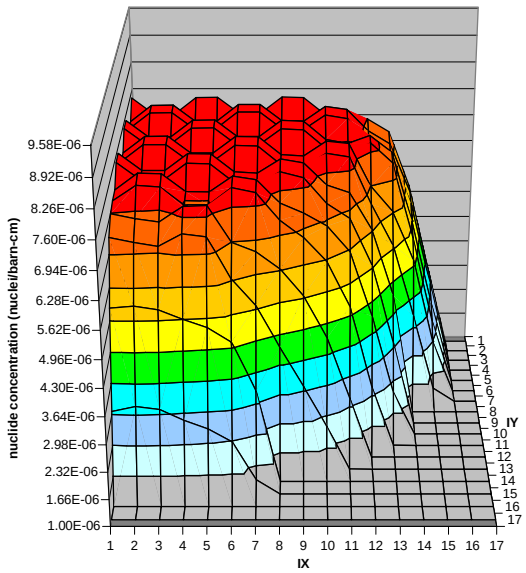

(a) $_{240}\mathrm{Pu}\{\vec{\eta}\}^{18}$

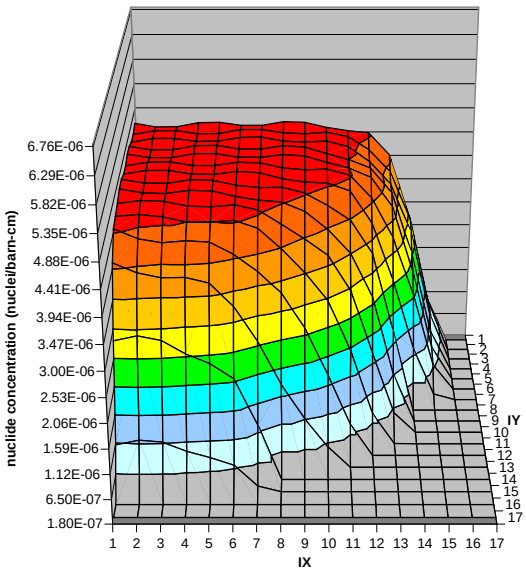

(b) $_{241}\mathrm{Pu}\{\vec{\eta}\}^{18}$

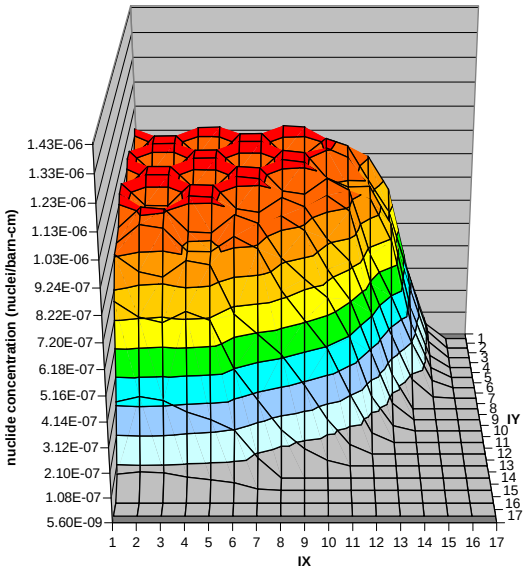

(c) $_{242}\mathrm{Pu}\{\vec{\eta}\}^{18}$

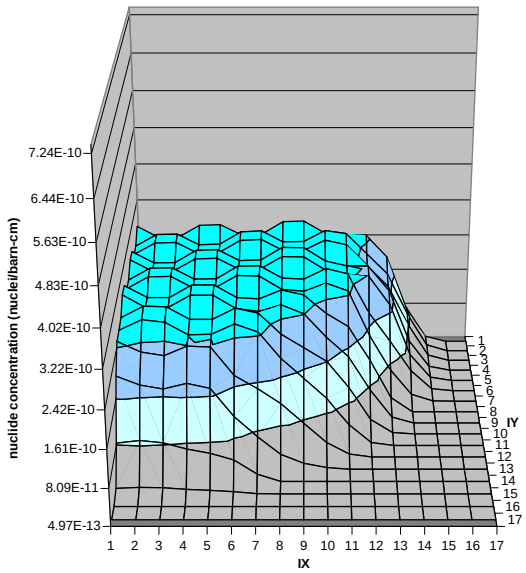

(d) $_{243}\mathrm{Pu}\{\vec{\eta}\}^{18}$

Figure 8.13: Nuclide Concentrations $\left(\frac{\text{nuclei}}{\text{barn}\cdot\text{cm}}\right)$ versus position at EOC (13969 MWD/MTU)

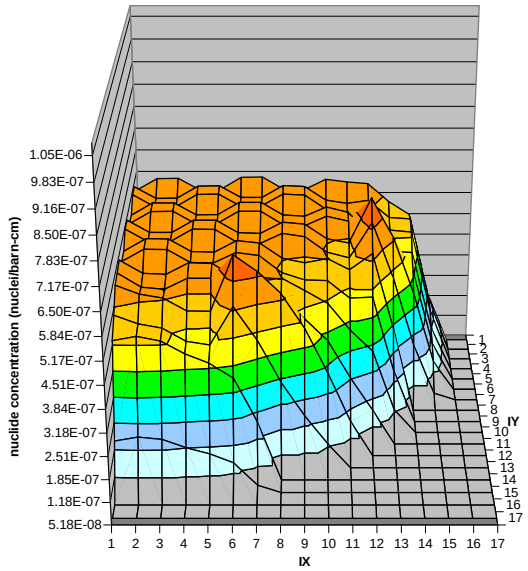

(a) $_{237\mathrm{Np}}\{\vec{\eta}\}^{18}$

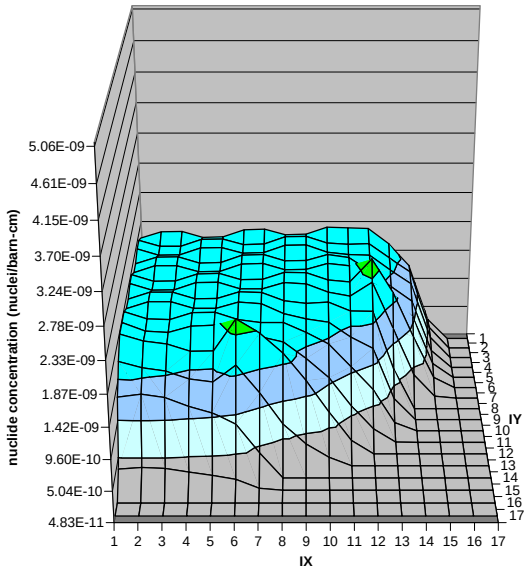

(b) $_{238\mathrm{Np}}\{\vec{\eta}\}^{18}$

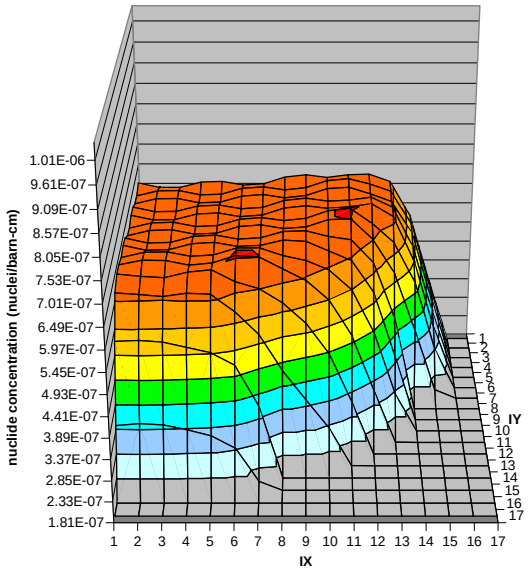

(c) $_{239\mathrm{Np}}\{\vec{\eta}\}^{18}$

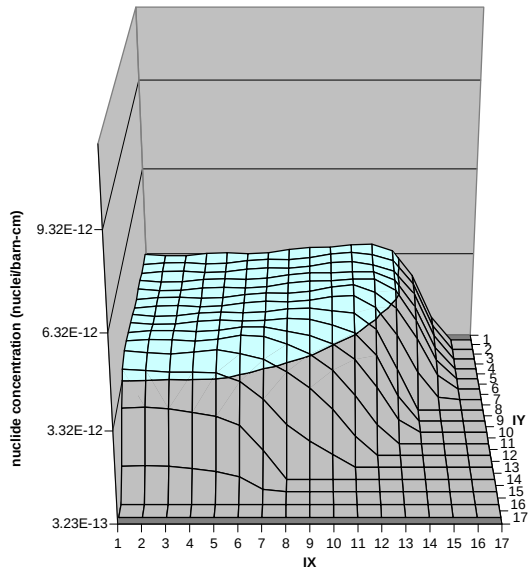

(d) $_{240\mathrm{Np}}\{\vec{\eta}\}^{18}$

Figure 8.14: Nuclide Concentrations $\left(\frac{\text{nuclei}}{\text{barn}\cdot\text{cm}}\right)$ versus position at EOC (13969 MWD/MTU)

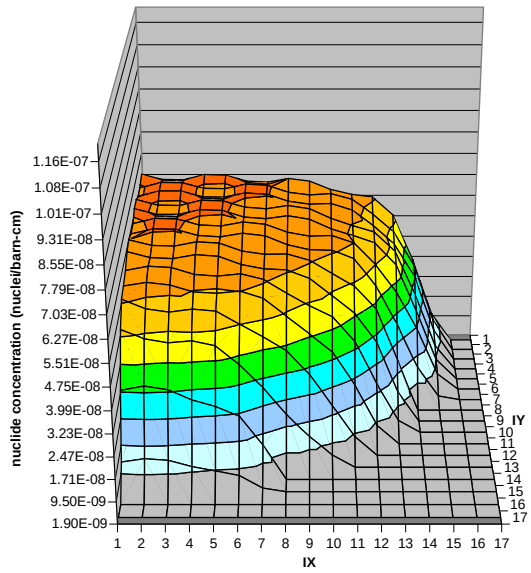

(a) $_{241}\mathrm{Am}\{\vec{\eta}\}^{18}$

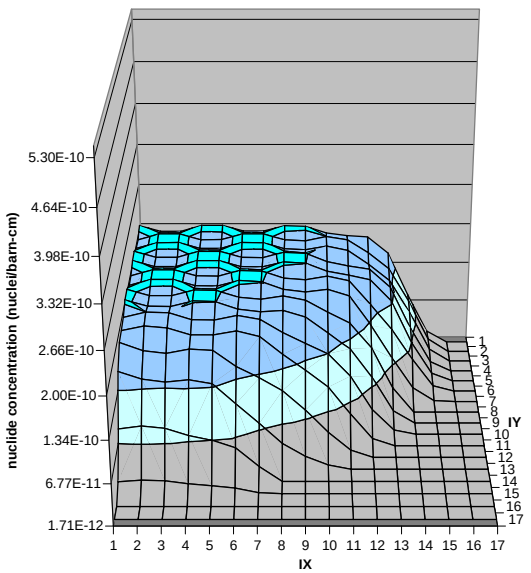

(b) $_{242}\mathrm{Am}\{\vec{\eta}\}^{18}$

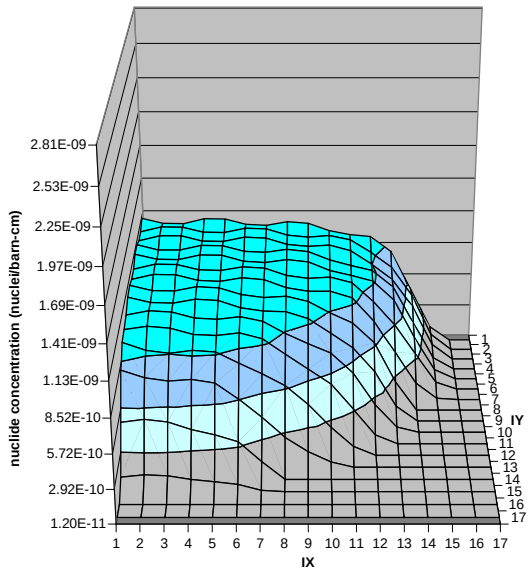

(c) $_{242m}\mathrm{Am}\{\vec{\eta}\}^{18}$

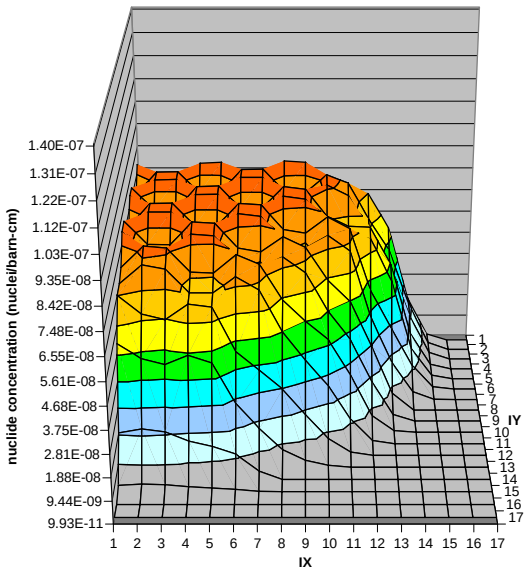

(d) $_{243}\mathrm{Am}\{\vec{\eta}\}^{18}$

Figure 8.15: Nuclide Concentrations $\left(\frac{\text{nuclei}}{\text{barn}\cdot\text{cm}}\right)$ versus position at EOC (13969 MWD/MTU)

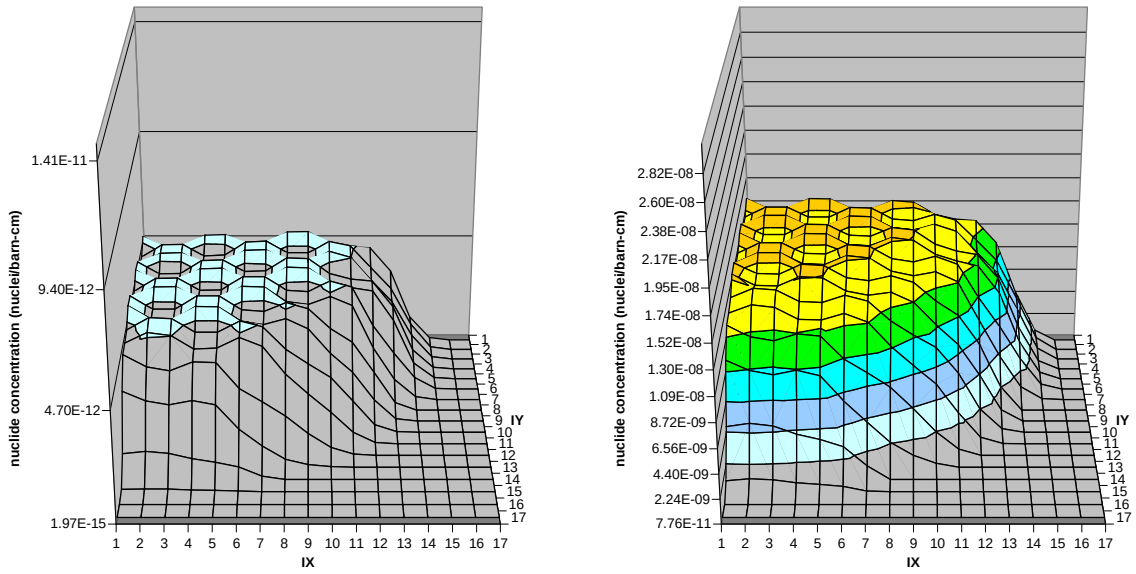

(a) $_{244}\mathrm{Am}\{\vec{\eta}\}^{18}$ (b) $_{242}\mathrm{Cm}\{\vec{\eta}\}^{18}$

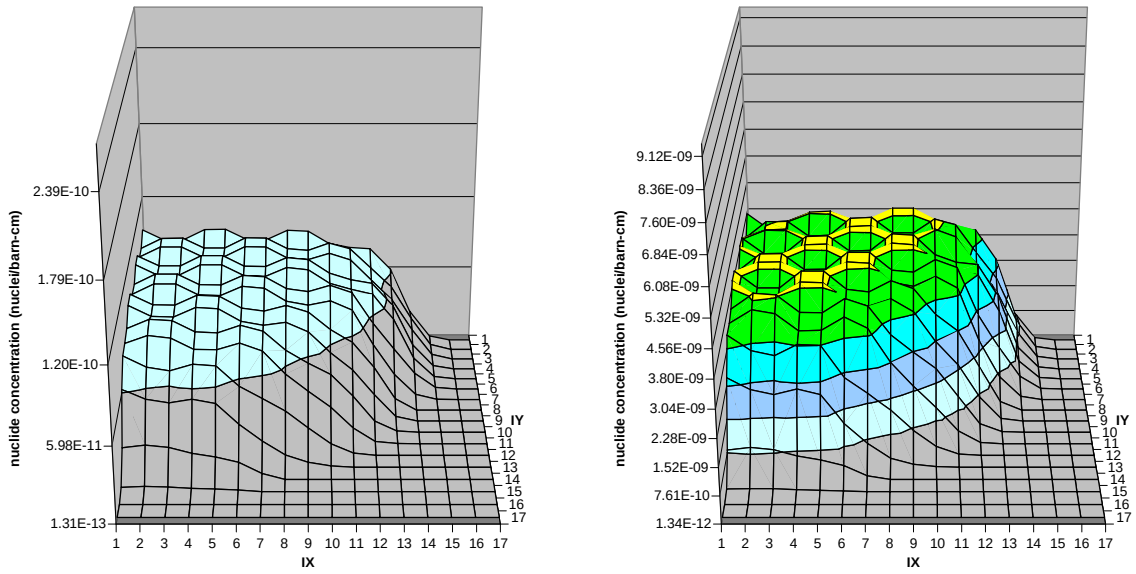

(c) $_{243}\mathrm{Cm}\{\vec{\eta}\}^{18}$ (d) $_{244}\mathrm{Cm}\{\vec{\eta}\}^{18}$

Figure 8.16: Nuclide Concentrations $\left(\frac{\text{nuclei}}{\text{barn}\cdot\text{cm}}\right)$ versus position at EOC (13969 MWD/MTU)

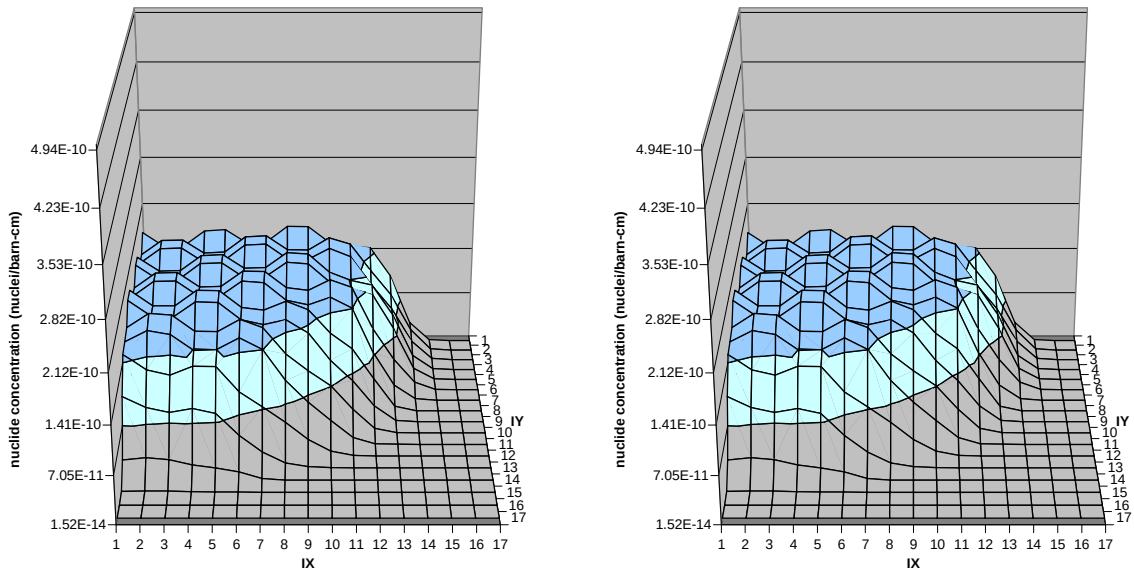

(a) ${}_{245}\mathrm{Cm}\{\vec{\eta}\}^{18}$ (b) ${}_{246}\mathrm{Cm}\{\vec{\eta}\}^{18}$

Figure 8.17: Nuclide Concentrations $\left(\frac{\text{nuclei}}{\text{barn}\cdot\text{cm}}\right)$ versus position at EOC (13969 MWD/MTU)

Core-Average Nuclide Concentrations

The large scale behavior of the nuclide field may be seen in graphs of core-average concentrations of nuclei over time. One can see the steady decrease in fuel nuclide ^{235}U and the accumulation of Np, and Pu in Fig. 8.18. Note that ^{235}U is the main fuel (fission

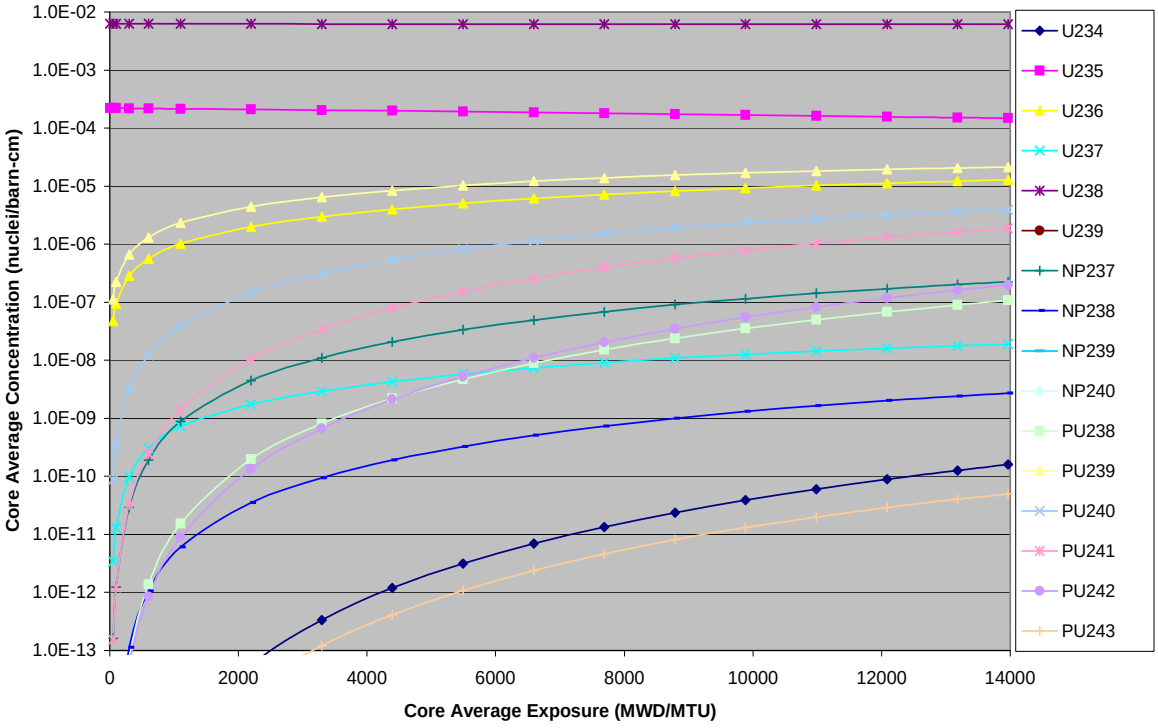

Figure 8.18: Core-Average Concentrations of U, Np, and Pu versus Exposure

neutron producer) but over the cycle, ^{239}Pu become a more and more significant fission neutron producer as fast neutron captures of ^{238}U build up the store of ^{239}Pu in the core. Similarly to fast neutron captures in ^{238}U, fast neutron captures in ^{235}U build up the store of ^{236}U—which explains the similarity between ^{236}U and ^{239}Pu changes in concentration over time. One can see the ^{239}Pu concentration moving toward some equilibrium, as the capture rate that produces it (proportional to the practically static ^{238}U concentration) approaches the fission rate (proportional to the concentration of ^{239}Pu itself) that destroys it.

Average core concentrations of minor actinides Am and Cm are shown in Fig. 8.19. These minor actinides are a relatively small part of the fuel, yet their presence makes disposal

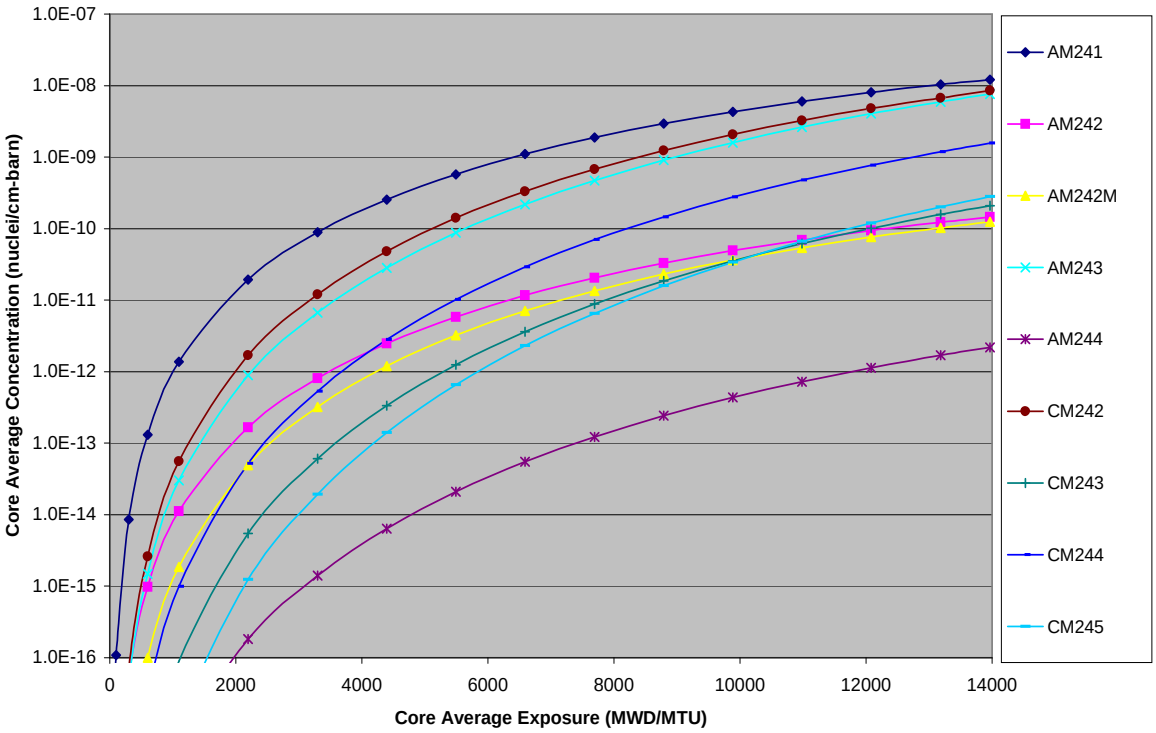

Figure 8.19: Core-Average Concentrations of Am and Cm versus Exposure

of the fuel much more difficult as the minor actinides are long-lived radioactive nuclei, some of which produce a great deal of heat when they decay.

The concentrations of fission products—while not considered in our sensitivity analysis—nonetheless play a role in the core behavior. Although at each time we solve the neutron field equation, we assume the fission products are in equilibrium (their production rate from fissioning nuclei equal their destruction rate—a good assumption) the equilibrium concentrations do change a little over time as the flux spectrum changes and the presence of fissioning nuclei which produce the fission products changes.

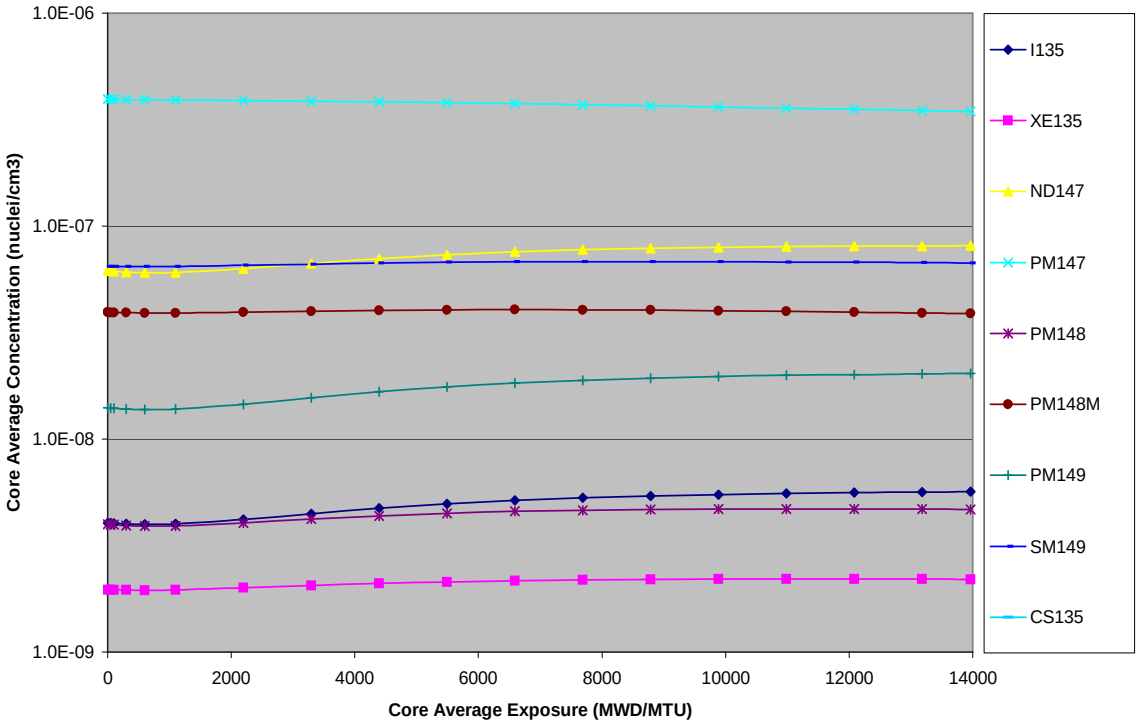

Figure 8.20: The core-average concentrations of fission products versus time.

8.2.2 Core Sensitivity Analysis

Now we proceed to the sensitivity analysis, which we ran using this new version of NESTLE. The main response of interest is EOC nuclide concentrations and their sensitivity to nuclear data perturbations. This gives us information about how the core transmutes nuclei into other nuclei. But to really evaluate various transmutation designs, one must be able to quantify the hazard associated with handling, storing, and disposing of the SNF. The Hazard Index and Total Cancer Dose are two such hazard measures which we will investigate. But first, let us showcase some comparisons of various methods, particularly the DPAR vs. AS, and predictor (P) vs. predictor-corrector (P-C).

Method Comparisons

To compare the P and P-C methods of neutron field coupling with respect to sensitivity analysis, we evaluated the ℓ^2 norm of all response sensitivities calculated with

each method for increasingly refined time meshes, from 18 steps in the most coarse mesh to 180 steps (a mesh refinement factor of 10) in the finest time mesh. The results are shown in Fig. 8.21 and one can see the difference between the two methods seems to be approaching zero, although even at 180 steps there is still some disparity. At the most coarse mesh, the maximum relative difference between the two methods in evaluating a response sensitivity was about 20%. Only in cases where the response sensitivity was very, very small (sensitivity coefficient less than 0.0001), was a difference in sign observed between the response sensitivity predicted by the P and P-C methods.

To compare DPAR vs. AS methodologies, we show how a single response changes with respect to data parameter perturbations. In Fig. 8.22, one can see the ^{245}Cm concentration response with ^{235}U thermal fission cross section perturbation, a response with a very high sensitivity coefficient of -2.53 (see all the key players and their sensitivity coefficients in Table 8.1). The change in ^{245}Cm concentration is nonlinear with respect to ^{235}U thermal fission cross section perturbation, but up to about 5% perturbation in ^{235}U fission cross section, the linear change in response estimated by the AS remains within 1% of the true value predicted by DPAR.

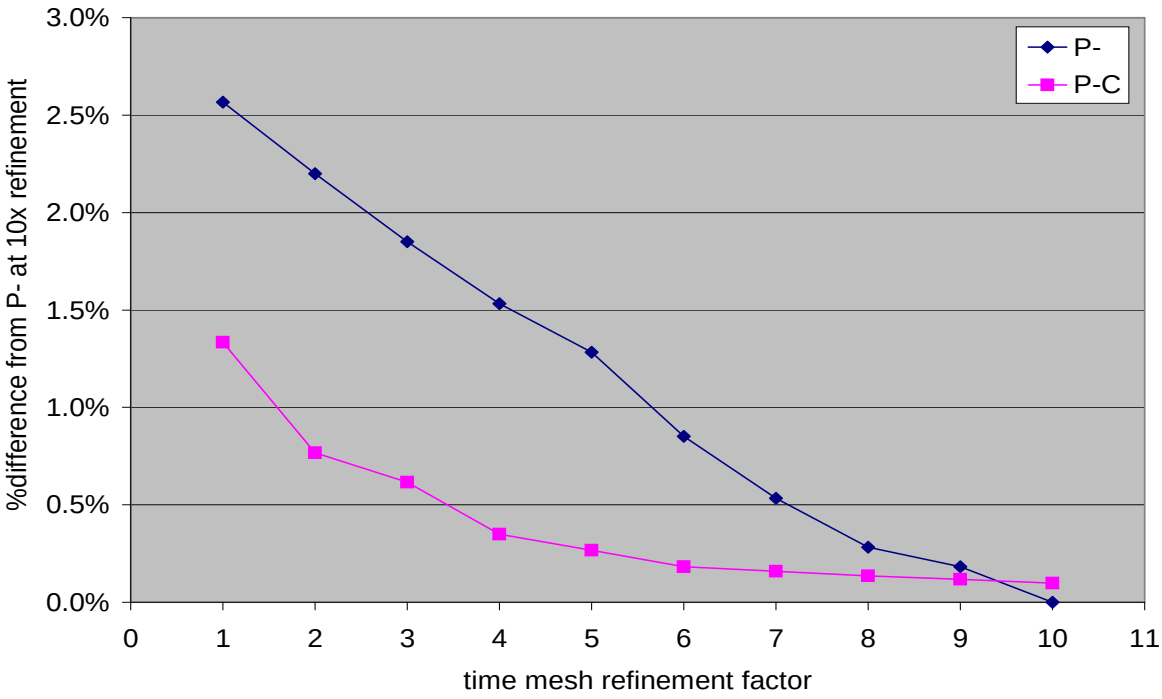

Figure 8.21: Relative change in ℓ^2 norms of all response sensitivities for P and P-C Methods versus time mesh refinement factor.

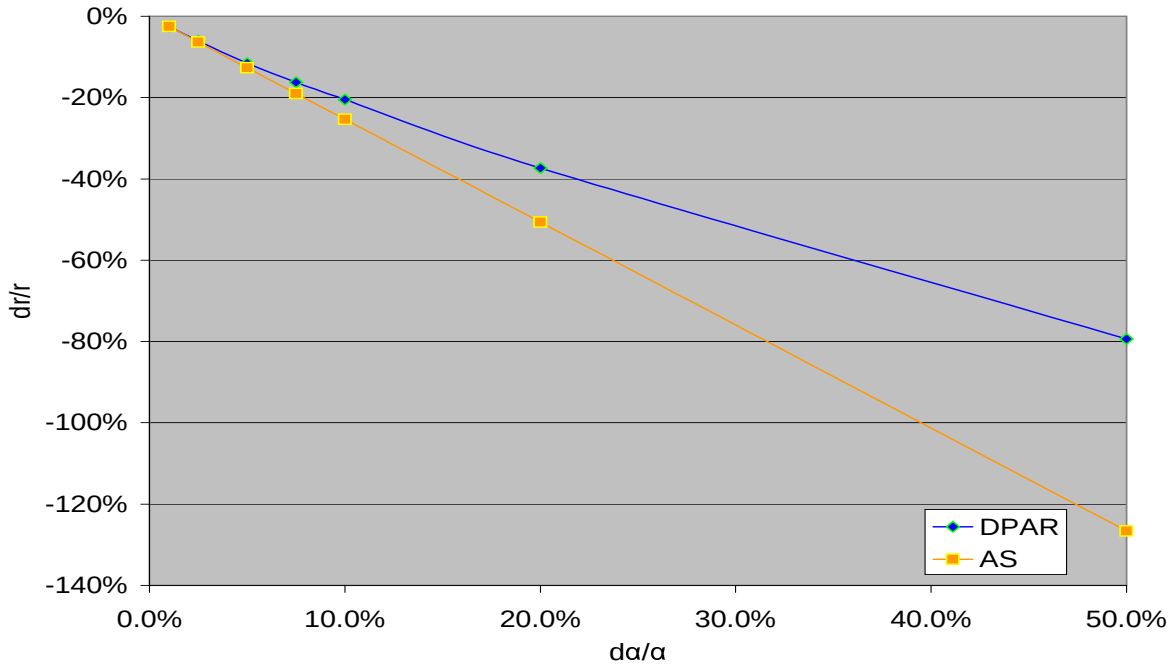

Figure 8.22: Relative change in EOC ^{245}Cm concentration versus relative change in ^{235}U thermal fission cross section.

Hazard Index (HI)

Using our sensitivity analysis tool, we determined the 20 data parameters which influence the HI of the spent fuel at EOC, Fig. 8.23(a)-8.23(b). Note that the HI neglects environmental transport of nuclei from a storage/disposal facility to humans. As is to be expected, fast (n,γ) capture in ^{238}U is the leading data parameter which influences the HI as all minor actinides originate from this transmutation event (see Fig. 8.23(a)). But there is one great way in which we can avoid producing minor actinides—take advantage of the extremely high thermal fission cross section of ^{239}Pu (see Fig. 8.23(b)), which if destroyed by fissioning, cuts off all the minor actinides resulting from capture events in the Pu chain. Unfortunately, "softening" the flux spectrum (increasing the prevalence of thermal energy neutrons) leads to an increase in the HI through thermal (n,γ) capture in ^{238}U—however, per percentage change in cross section, the thermal fission of ^{239}Pu impacts the HI by -6.64% while thermal (n,γ) capture in ^{238}U impacts the HI by only $+4.47\%$, so we would expect a net decrease in the HI from softening the flux spectrum.

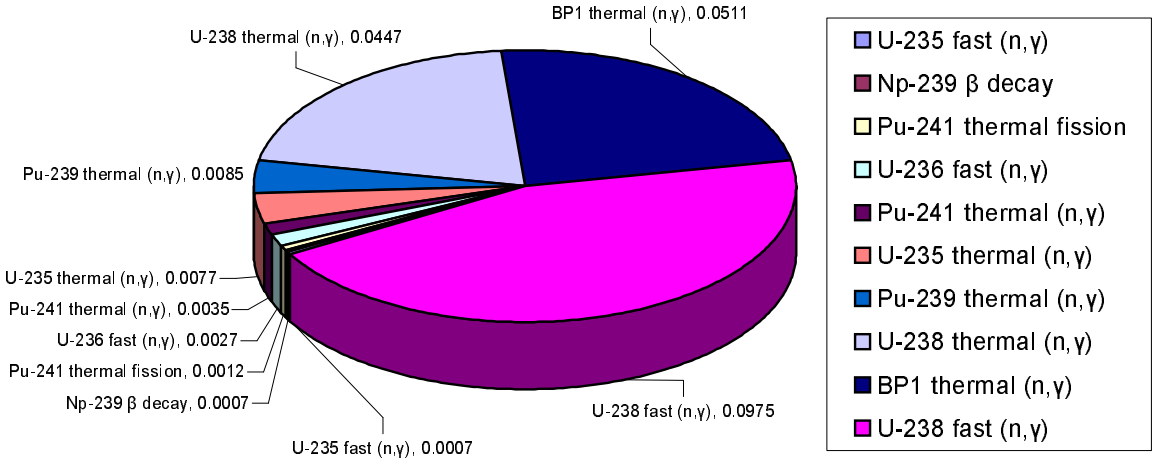

(a) Top 10 Positive Sensitivity Coefficients

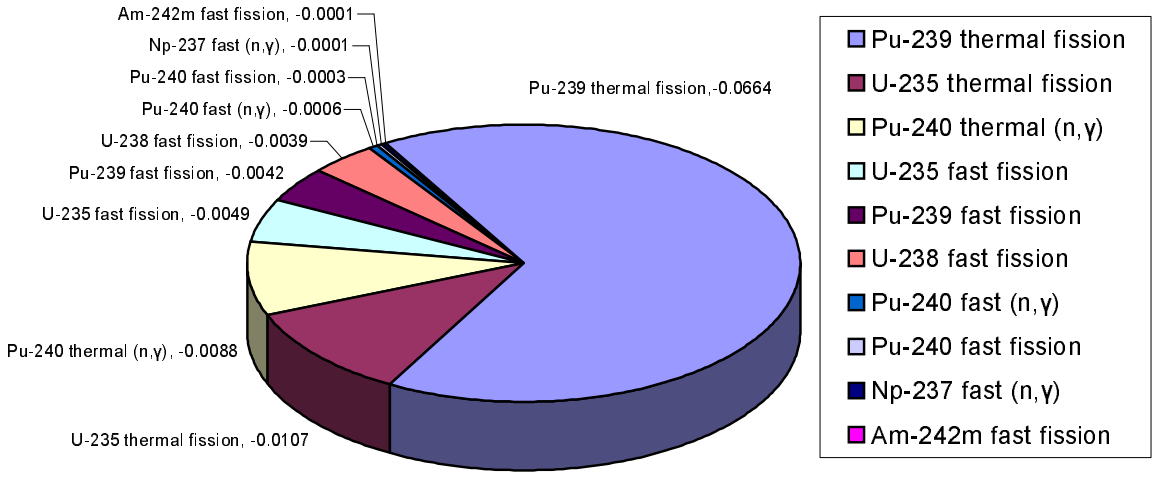

(b) Top 10 Negative Sensitivity Coefficients

Figure 8.23: Sensitivity Coefficients for the Hazard Index (HI) Response

It is a little surprising to learn that the data parameters that most influence the HI are those of the fuel nuclei (^{235}U and ^{239}Pu) and ^{238}U. In the past, the simulation of the reactor core has only been concerned with a handful of nuclei which are pivotal in the UO_2-fuelled thermal reactor system *without* the consideration of transmutation of SNF and/or minimization of some quantification of the SNF hazard. Now as we design AFCI SNF recycling/transmutation schemes (and GEN-IV reactors), and start to consider the change in composition of SNF as an objective (or constraint), it is nice to know that the parameters which appear to most influence the HI are not some obscure minor actinide cross sections with uncertainty $\pm 50\%$.

Total Cancer Dose (TCD)

Using our sensitivity analysis tool, we determined the 20 data parameters that most influence the TCD of SNF, Fig. 8.24(a)-8.24(b). Note that the TCD neglects environmental transport of nuclei from a storage/disposal facility to humans. We see the same basic trends in the TCD as for the HI, but with much higher sensitivity coefficients. The TCD appears to be a much more sensitive quantification of SNF hazard than the HI. Thermal fission cross section for ^{235}U is the parameter which reduces the TCD most dramatically: with a 1% increase in ^{235}U thermal fission cross section, the TCD decreases by 59.45% (see Fig. 8.24(b)!) The (n, γ) capture events dominate the field of parameters which increase the TCD: with a 1% increase in fast (n, γ) capture in ^{238}U, the TCD increases by 47.92% (see Fig. 8.24(a)!) As with the HI, by examining Fig. 8.24(a)-8.24(b), one may notice that softening the flux spectrum could lead to a decrease in the TCD.

Again, we see the fuel nuclei (^{235}U and ^{239}Pu) and ^{238}U are most influential—but in the TCD, as opposed to the HI, we see a greater impact of decay constants with this quantification of SNF hazard.

Nuclide Field Sensitivity

There exist many, many different proposed hazard measures for SNF, but nearly all of them may be formulated just like the HI and TCD: as weighted sums of the concentrations of nuclei. So with sensitivities of EOC concentrations of nuclei, one may easily obtain sensitivities of such hazard measures. Next, the NESTLE code was run to produce a list of

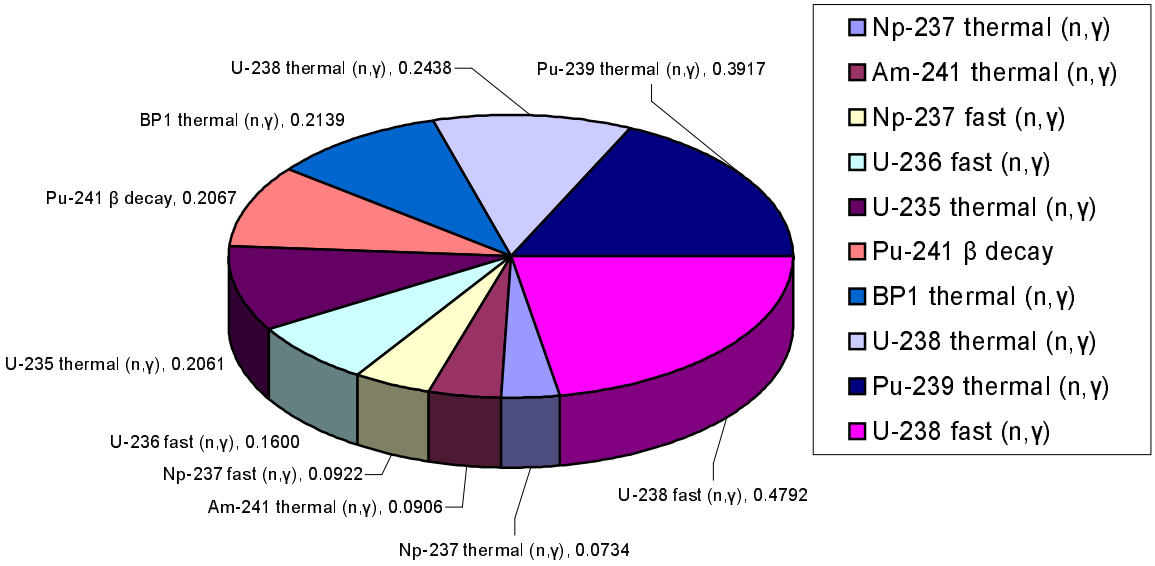

(a) Top 10 Positive Sensitivity Coefficients

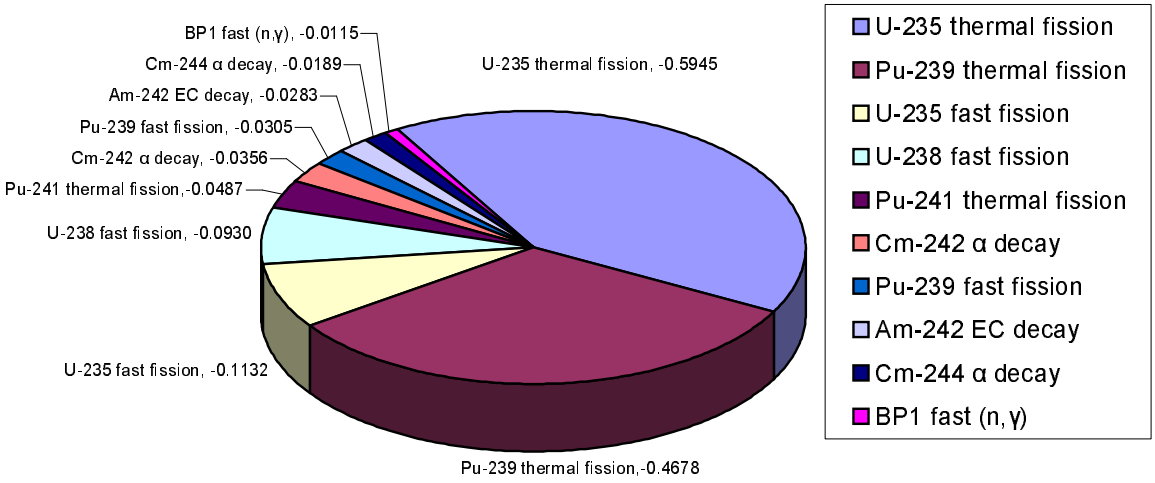

(b) Top 10 Negative Sensitivity Coefficients

Figure 8.24: Sensitivity Coefficients for the Total Cancer Dose (TCD) Response

the 6 most influential data parameters (3 with positive impact/3 with negative impact) on the core-average EOC concentrations of all heavy metal nuclei in Table 8.1. Again, one can notice how sensitive practically all minor actinides are to the ^{235}U fission cross section, at least for our cycle 1, CASE 10 core.

Table 8.1: CASE 10 Response Sensitivities and Sensitivity Coefficients for EOC Nuclide Concentrations

nuclide	**data** m'			$\{\,\delta r_\ell^+\,\}_{m',p}$	r_ℓ^+	$\{\,\Delta\alpha^+\,\}_{m',p}$	$\{\,\alpha^+\,\}_{m'}$	$\{\,\varrho_\ell^+\,\}_{m'}$	$\{\,c_\ell^+\,\}_{m'}$
ℓ	x	k	g	$\frac{\text{nuclei}}{\text{barn}\cdot\text{cm}}$	$\frac{\text{nuclei}}{\text{barn}\cdot\text{cm}}$	(barn)/(-)	(barn)/(-)	$\frac{\text{nuclei}}{\text{barn}^2\cdot\text{cm}}$	$(-)$
^{241}Am	fission	^{235}U	2	-3.60E-10	4.75E-08	2.3860	238.60	-1.51E-10	-0.76
	fission	^{239}Pu	2	-1.68E-10	4.75E-08	6.1700	617.00	-2.72E-11	-0.35
	fission	^{241}Pu	2	-1.27E-10	4.75E-08	6.3520	635.20	-2.00E-11	-0.27
	(n,γ)	^{240}Pu	2	2.64E-10	4.75E-08	9.1590	915.90	2.88E-11	0.56
	(n,γ)	^{239}Pu	2	3.74E-10	4.75E-08	3.4810	348.10	1.07E-10	0.79
	β decay	^{241}Pu	-	4.71E-10	4.75E-08	0.0100	1.00	4.71E-08	0.99
^{242}Am	fission	^{235}U	2	-1.68E-12	1.49E-10	2.3860	238.60	-7.02E-13	-1.12
	β decay	^{242}Am	-	-1.21E-12	1.49E-10	0.0083	0.83	-1.46E-10	-0.81
	fission	^{239}Pu	2	-7.21E-13	1.49E-10	6.1700	617.00	-1.17E-13	-0.48
	(n,γ)	^{240}Pu	2	7.92E-13	1.49E-10	9.1590	915.90	8.64E-14	0.53
	(n,γ)	^{239}Pu	2	1.19E-12	1.49E-10	3.4810	348.10	3.41E-13	0.80
	β decay	^{241}Pu	-	1.48E-12	1.49E-10	0.0100	1.00	1.48E-10	0.99
^{242m}Am	fission	^{235}U	2	-7.54E-12	7.84E-10	2.3860	238.60	-3.16E-12	-0.96
	fission	^{242m}Am	2	-3.24E-12	7.84E-10	17.7640	1776.40	-1.82E-13	-0.41
	fission	^{239}Pu	2	-3.07E-12	7.84E-10	6.1700	617.00	-4.98E-13	-0.39
	(n,γ)	^{240}Pu	2	4.63E-12	7.84E-10	9.1590	915.90	5.06E-13	0.59
	(n,γ)	^{239}Pu	2	6.40E-12	7.84E-10	3.4810	348.10	1.84E-12	0.82
	β decay	^{241}Pu	-	7.78E-12	7.84E-10	0.0100	1.00	7.78E-10	0.99

nuclide	**data** m'			$\{\,\delta r_\ell^+\,\}_{m',p}$	r_ℓ^+	$\{\,\Delta\alpha^+\,\}_{m',p}$	$\{\,\alpha^+\,\}_{m'}$	$\{\,\varrho_\ell^+\,\}_{m'}$	$\{\,c_\ell^+\,\}_{m'}$
ℓ	x	k	g	$\frac{\text{nuclei}}{\text{barn}\cdot\text{cm}}$	$\frac{\text{nuclei}}{\text{barn}\cdot\text{cm}}$	(barn)/(-)	(barn)/(-)	$\frac{\text{nuclei}}{\text{barn}^2\cdot\text{cm}}$	$(-)$
^{243}Am	fission	^{235}U	2	-9.54E-10	5.19E-08	2.3860	238.60	-4.00E-10	-1.84
	fission	^{239}Pu	2	-2.31E-10	5.19E-08	6.1700	617.00	-3.74E-11	-0.44
	(n,γ)	BP1	2	-1.81E-10	5.19E-08	8.0000	800.00	-2.26E-11	-0.35
	(n,γ)	^{239}Pu	2	4.07E-10	5.19E-08	3.4810	348.10	1.17E-10	0.78
	(n,γ)	^{241}Pu	2	4.32E-10	5.19E-08	2.2280	222.80	1.94E-10	0.83
	(n,γ)	^{242}Pu	1	4.50E-10	5.19E-08	0.3650	36.50	1.23E-09	0.87
^{244}Am	fission	^{235}U	2	-7.05E-14	3.34E-12	2.3860	238.60	-2.95E-14	-2.11
	β decay	^{244}Am	-	-3.30E-14	3.34E-12	0.0100	1.00	-3.30E-12	-0.99
	fission	^{239}Pu	2	-2.35E-14	3.34E-12	6.1700	617.00	-3.81E-15	-0.70
	(n,γ)	^{241}Pu	2	2.78E-14	3.34E-12	2.2280	222.80	1.25E-14	0.83
	(n,γ)	^{242}Pu	1	2.89E-14	3.34E-12	0.3650	36.50	7.91E-14	0.86
	(n,γ)	^{239}Pu	2	3.00E-14	3.34E-12	3.4810	348.10	8.63E-15	0.90
^{242}Cm	fission	^{235}U	2	-1.25E-10	9.40E-09	2.3860	238.60	-5.26E-11	-1.34
	fission	^{239}Pu	2	-3.69E-11	9.40E-09	6.1700	617.00	-5.98E-12	-0.39
	(n,γ)	BP1	2	-2.99E-11	9.40E-09	8.0000	800.00	-3.73E-12	-0.32
	(n,γ)	^{240}Pu	2	5.54E-11	9.40E-09	9.1590	915.90	6.04E-12	0.59
	(n,γ)	^{239}Pu	2	7.37E-11	9.40E-09	3.4810	348.10	2.12E-11	0.78
	β decay	^{241}Pu	-	9.32E-11	9.40E-09	0.0100	1.00	9.32E-09	0.99
^{243}Cm	fission	^{235}U	2	-1.11E-12	6.31E-11	2.3860	238.60	-4.65E-13	-1.76
	fission	^{239}Pu	2	-2.82E-13	6.31E-11	6.1700	617.00	-4.57E-14	-0.45
	fission	^{235}U	1	-1.84E-13	6.31E-11	0.0760	7.60	-2.42E-12	-0.29
	(n,γ)	^{242}Cm	1	4.56E-13	6.31E-11	0.0312	3.12	1.46E-11	0.72
	(n,γ)	^{239}Pu	2	5.18E-13	6.31E-11	3.4810	348.10	1.49E-13	0.82
	β decay	^{241}Pu	-	6.26E-13	6.31E-11	0.0100	1.00	6.26E-11	0.99
^{244}Cm	fission	^{235}U	2	-5.54E-11	2.55E-09	2.3860	238.60	-2.32E-11	-2.17
	α decay	^{244}Cm	-	-1.89E-11	2.55E-09	0.0100	1.00	-1.89E-09	-0.74
	fission	^{239}Pu	2	-1.66E-11	2.55E-09	6.1700	617.00	-2.69E-12	-0.65
	(n,γ)	^{241}Pu	2	2.12E-11	2.55E-09	2.2280	222.80	9.53E-12	0.83
	(n,γ)	^{242}Pu	1	2.22E-11	2.55E-09	0.3650	36.50	6.07E-11	0.87
	(n,γ)	^{239}Pu	2	2.25E-11	2.55E-09	3.4810	348.10	6.47E-12	0.88

nuclide	**data** m'			$\{\,\delta r_\ell^+\,\}_{m',p}$	r_ℓ^+	$\{\,\Delta\alpha^+\,\}_{m',p}$	$\{\,\alpha^+\,\}_{m'}$	$\{\,\varrho_\ell^+\,\}_{m'}$	$\{\,c_\ell^+\,\}_{m'}$
ℓ	x	k	g	$\frac{\text{nuclei}}{\text{barn}\cdot\text{cm}}$	$\frac{\text{nuclei}}{\text{barn}\cdot\text{cm}}$	(barn)/(-)	(barn)/(-)	$\frac{\text{nuclei}}{\text{barn}^2\cdot\text{cm}}$	$(-)$
^{245}Cm	fission	^{235}U	2	-2.89E-12	1.14E-10	2.3860	238.60	-1.21E-12	-2.53
	α decay	^{244}Cm	-	-8.07E-13	1.14E-10	0.0100	1.00	-8.07E-11	-0.71
	fission	^{239}Pu	2	-7.87E-13	1.14E-10	6.1700	617.00	-1.28E-13	-0.69
	(n,γ)	^{242}Pu	1	1.00E-12	1.14E-10	0.3650	36.50	2.75E-12	0.88
	(n,γ)	^{239}Pu	2	1.08E-12	1.14E-10	3.4810	348.10	3.09E-13	0.94
	(n,γ)	^{244}Cm	1	1.10E-12	1.14E-10	0.3213	32.13	3.43E-12	0.97
^{237}Np	fission	^{235}U	2	-3.92E-09	4.74E-07	2.3860	238.60	-1.64E-09	-0.83
	fission	^{239}Pu	2	-1.26E-09	4.74E-07	6.1700	617.00	-2.04E-10	-0.26
	fission	^{235}U	1	-6.48E-10	4.74E-07	0.0760	7.60	-8.53E-09	-0.14
	(n,γ)	BP1	2	1.65E-09	4.74E-07	8.0000	800.00	2.07E-10	0.35
	(n,γ)	^{235}U	2	3.70E-09	4.74E-07	0.4290	42.90	8.63E-09	0.78
	(n,γ)	^{236}U	1	4.25E-09	4.74E-07	0.0790	7.90	5.38E-08	0.90
^{238}Np	fission	^{235}U	2	-1.67E-11	1.46E-09	2.3860	238.60	-6.99E-12	-1.15
	β decay	^{238}Np	-	-1.40E-11	1.46E-09	0.0100	1.00	-1.40E-09	-0.96
	fission	^{239}Pu	2	-6.38E-12	1.46E-09	6.1700	617.00	-1.03E-12	-0.44
	(n,γ)	^{237}Np	1	7.38E-12	1.46E-09	0.2407	24.07	3.07E-11	0.51
	(n,γ)	^{235}U	2	1.21E-11	1.46E-09	0.4290	42.90	2.81E-11	0.83
	(n,γ)	^{236}U	1	1.30E-11	1.46E-09	0.0790	7.90	1.65E-10	0.89
^{239}Np	β decay	^{239}Np	-	-5.61E-09	5.66E-07	0.0100	1.00	-5.61E-07	-0.99
	fission	^{235}U	2	-1.43E-09	5.66E-07	2.3860	238.60	-6.01E-10	-0.25
	fission	^{239}Pu	2	-1.42E-09	5.66E-07	6.1700	617.00	-2.31E-10	-0.25
	(n,γ)	^{238}U	2	1.33E-09	5.66E-07	0.0123	1.23	1.08E-07	0.23
	(n,γ)	BP1	2	2.06E-09	5.66E-07	8.0000	800.00	2.58E-10	0.36
	(n,γ)	^{238}U	1	3.21E-09	5.66E-07	0.0085	0.85	3.78E-07	0.57
^{240}Np	β decay	^{239}Np	-	-3.14E-14	3.16E-12	0.0100	1.00	-3.14E-12	-0.99
	β decay	^{240}Np	-	-3.13E-14	3.16E-12	0.0100	1.00	-3.13E-12	-0.99
	fission	^{235}U	2	-1.63E-14	3.16E-12	2.3860	238.60	-6.81E-15	-0.51
	(n,γ)	^{238}U	1	1.45E-14	3.16E-12	0.0085	0.85	1.70E-12	0.46
	(n,γ)	BP1	2	2.43E-14	3.16E-12	8.0000	800.00	3.04E-15	0.77
	(n,γ)	^{239}Np	1	2.73E-14	3.16E-12	0.2634	26.34	1.04E-13	0.86

nuclide	**data** m'			$\{\,\delta r_\ell^+\,\}_{m',p}$	r_ℓ^+	$\{\,\Delta\alpha^+\,\}_{m',p}$	$\{\,\alpha^+\,\}_{m'}$	$\{\,\varrho_\ell^+\,\}_{m'}$	$\{\,c_\ell^+\,\}_{m'}$
ℓ	x	k	g	$\frac{\text{nuclei}}{\text{barn}\cdot\text{cm}}$	$\frac{\text{nuclei}}{\text{barn}\cdot\text{cm}}$	(barn)/(-)	(barn)/(-)	$\frac{\text{nuclei}}{\text{barn}^2\cdot\text{cm}}$	$(-)$
^{238}Pu	fission	^{235}U	2	-7.27E-10	5.88E-08	2.3860	238.60	-3.05E-10	-1.24
	fission	^{239}Pu	2	-1.82E-10	5.88E-08	6.1700	617.00	-2.95E-11	-0.31
	fission	^{235}U	1	-1.28E-10	5.88E-08	0.0760	7.60	-1.68E-09	-0.22
	(n,γ)	^{237}Np	1	2.90E-10	5.88E-08	0.2407	24.07	1.20E-09	0.49
	(n,γ)	^{235}U	2	4.80E-10	5.88E-08	0.4290	42.90	1.12E-09	0.82
	(n,γ)	^{236}U	1	5.03E-10	5.88E-08	0.0790	7.90	6.37E-09	0.85
^{239}Pu	fission	^{239}Pu	2	-1.33E-07	2.39E-05	6.1700	617.00	-2.16E-08	-0.56
	(n,γ)	^{239}Pu	2	-3.40E-08	2.39E-05	3.4810	348.10	-9.75E-09	-0.14
	fission	^{239}Pu	1	-8.37E-09	2.39E-05	0.0980	9.80	-8.54E-08	-0.04
	(n,γ)	^{238}U	2	9.20E-08	2.39E-05	0.0123	1.23	7.48E-06	0.39
	(n,γ)	BP1	2	1.14E-07	2.39E-05	8.0000	800.00	1.42E-08	0.48
	(n,γ)	^{238}U	1	2.02E-07	2.39E-05	0.0085	0.85	2.38E-05	0.85
^{240}Pu	(n,γ)	^{240}Pu	2	-3.42E-08	6.22E-06	9.1590	915.90	-3.73E-09	-0.55
	fission	^{239}Pu	2	-3.21E-08	6.22E-06	6.1700	617.00	-5.21E-09	-0.52
	fission	^{235}U	2	-1.48E-08	6.22E-06	2.3860	238.60	-6.20E-09	-0.24
	(n,γ)	^{238}U	2	1.98E-08	6.22E-06	0.0123	1.23	1.61E-06	0.32
	(n,γ)	^{238}U	1	4.24E-08	6.22E-06	0.0085	0.85	4.99E-06	0.68
	(n,γ)	^{239}Pu	2	4.96E-08	6.22E-06	3.4810	348.10	1.42E-08	0.80
^{241}Pu	fission	^{235}U	2	-2.44E-08	3.74E-06	2.3860	238.60	-1.02E-08	-0.65
	fission	^{239}Pu	2	-1.78E-08	3.74E-06	6.1700	617.00	-2.89E-09	-0.48
	fission	^{241}Pu	2	-1.22E-08	3.74E-06	6.3520	635.20	-1.93E-09	-0.33
	(n,γ)	^{238}U	1	1.74E-08	3.74E-06	0.0085	0.85	2.04E-06	0.46
	(n,γ)	^{240}Pu	2	1.75E-08	3.74E-06	9.1590	915.90	1.91E-09	0.47
	(n,γ)	^{239}Pu	2	2.94E-08	3.74E-06	3.4810	348.10	8.45E-09	0.79
^{242}Pu	fission	^{235}U	2	-9.19E-09	6.67E-07	2.3860	238.60	-3.85E-09	-1.38
	(n,γ)	BP1	2	-3.84E-09	6.67E-07	8.0000	800.00	-4.80E-10	-0.58
	fission	^{239}Pu	2	-2.58E-09	6.67E-07	6.1700	617.00	-4.19E-10	-0.39
	(n,γ)	^{240}Pu	2	3.47E-09	6.67E-07	9.1590	915.90	3.79E-10	0.52
	(n,γ)	^{239}Pu	2	4.84E-09	6.67E-07	3.4810	348.10	1.39E-09	0.73
	(n,γ)	^{241}Pu	2	5.47E-09	6.67E-07	2.2280	222.80	2.45E-09	0.82

nuclide	**data** m'			$\{\,\delta r_\ell^+\,\}_{m',p}$	r_ℓ^+	$\{\,\Delta\alpha^+\,\}_{m',p}$	$\{\,\alpha^+\,\}_{m'}$	$\{\,\varrho_\ell^+\,\}_{m'}$	$\{\,c_\ell^+\,\}_{m'}$
ℓ	x	k	g	$\frac{\text{nuclei}}{\text{barn}\cdot\text{cm}}$	$\frac{\text{nuclei}}{\text{barn}\cdot\text{cm}}$	(barn)/(-)	(barn)/(-)	$\frac{\text{nuclei}}{\text{barn}^2\cdot\text{cm}}$	$(-)$
^{243}Pu	fission	^{235}U	2	-3.20E-12	1.94E-10	2.3860	238.60	-1.34E-12	-1.65
	β decay	^{243}Pu	-	-1.92E-12	1.94E-10	0.0100	1.00	-1.92E-10	-0.99
	fission	^{239}Pu	2	-1.25E-12	1.94E-10	6.1700	617.00	-2.02E-13	-0.64
	(n,γ)	^{241}Pu	2	1.60E-12	1.94E-10	2.2280	222.80	7.18E-13	0.82
	(n,γ)	^{239}Pu	2	1.63E-12	1.94E-10	3.4810	348.10	4.68E-13	0.84
	(n,γ)	^{242}Pu	1	1.66E-12	1.94E-10	0.3650	36.50	4.55E-12	0.85
^{234}U	fission	^{235}U	2	-1.46E-12	1.13E-10	2.3860	238.60	-6.13E-13	-1.29
	fission	^{235}U	1	-2.63E-13	1.13E-10	0.0760	7.60	-3.45E-12	-0.23
	fission	^{239}Pu	2	-2.28E-13	1.13E-10	6.1700	617.00	-3.70E-14	-0.20
	(n,γ)	^{235}U	2	9.47E-13	1.13E-10	0.4290	42.90	2.21E-12	0.84
	(n,γ)	^{236}U	1	9.85E-13	1.13E-10	0.0790	7.90	1.25E-11	0.87
	α decay	^{238}Pu	-	1.13E-12	1.13E-10	0.0100	1.00	1.13E-10	1.00
^{235}U	fission	^{235}U	2	-8.89E-08	9.01E-05	2.3860	238.60	-3.73E-08	-0.10
	(n,γ)	^{235}U	2	-7.60E-08	9.01E-05	0.4290	42.90	-1.77E-07	-0.08
	(n,γ)	^{235}U	1	-3.24E-08	9.01E-05	0.0420	4.20	-7.71E-07	-0.04
	(n,γ)	^{238}U	2	5.50E-08	9.01E-05	0.0123	1.23	4.47E-06	0.06
	fission	^{239}Pu	2	9.62E-08	9.01E-05	6.1700	617.00	1.56E-08	0.11
	(n,γ)	^{238}U	1	1.15E-07	9.01E-05	0.0085	0.85	1.36E-05	0.13
^{236}U	fission	^{235}U	2	-7.47E-08	1.38E-05	2.3860	238.60	-3.13E-08	-0.54
	fission	^{239}Pu	2	-1.72E-08	1.38E-05	6.1700	617.00	-2.79E-09	-0.13
	(n,γ)	^{238}U	1	-1.66E-08	1.38E-05	0.0085	0.85	-1.96E-06	-0.12
	(n,γ)	BP1	2	8.36E-09	1.38E-05	8.0000	800.00	1.04E-09	0.06
	(n,γ)	^{235}U	1	3.66E-08	1.38E-05	0.0420	4.20	8.71E-07	0.27
	(n,γ)	^{235}U	2	9.56E-08	1.38E-05	0.4290	42.90	2.23E-07	0.69
^{237}U	β decay	^{237}U	-	-2.54E-10	2.65E-08	0.0100	1.00	-2.54E-08	-0.96
	fission	^{235}U	2	-2.05E-10	2.65E-08	2.3860	238.60	-8.61E-11	-0.77
	fission	^{239}Pu	2	-1.01E-10	2.65E-08	6.1700	617.00	-1.63E-11	-0.38
	(n,γ)	BP1	2	1.45E-10	2.65E-08	8.0000	800.00	1.81E-11	0.55
	(n,γ)	^{235}U	2	2.01E-10	2.65E-08	0.4290	42.90	4.69E-10	0.76
	(n,γ)	^{236}U	1	2.35E-10	2.65E-08	0.0790	7.90	2.97E-09	0.89

nuclide	**data** m'			$\{\,\delta r_\ell^+\,\}_{m',p}$	r_ℓ^+	$\{\,\Delta\alpha^+\,\}_{m',p}$	$\{\,\alpha^+\,\}_{m'}$	$\{\,\varrho_\ell^+\,\}_{m'}$	$\{\,c_\ell^+\,\}_{m'}$
ℓ	x	k	g	$\frac{\text{nuclei}}{\text{barn}\cdot\text{cm}}$	$\frac{\text{nuclei}}{\text{barn}\cdot\text{cm}}$	(barn)/(-)	(barn)/(-)	$\frac{\text{nuclei}}{\text{barn}^2\cdot\text{cm}}$	$(-)$
^{238}U	(n,γ)	^{238}U	1	-3.80E-07	6.21E-03	0.0085	0.85	-4.47E-05	-0.01
	(n,γ)	^{238}U	2	-1.77E-07	6.21E-03	0.0123	1.23	-1.44E-05	0.00
	(n,γ)	BP1	2	-1.37E-07	6.21E-03	8.0000	800.00	-1.72E-08	0.00
	fission	^{235}U	1	4.73E-08	6.21E-03	0.0760	7.60	6.22E-07	0.00
	fission	^{239}Pu	2	1.05E-07	6.21E-03	6.1700	617.00	1.71E-08	0.00
	fission	^{235}U	2	2.28E-07	6.21E-03	2.3860	238.60	9.55E-08	0.00
^{239}U	β decay	^{239}U	-	-3.88E-11	3.92E-09	0.0100	1.00	-3.88E-09	-0.99
	fission	^{235}U	2	-9.96E-12	3.92E-09	2.3860	238.60	-4.18E-12	-0.25
	fission	^{239}Pu	2	-9.89E-12	3.92E-09	6.1700	617.00	-1.60E-12	-0.25
	(n,γ)	^{238}U	2	9.19E-12	3.92E-09	0.0123	1.23	7.47E-10	0.23
	(n,γ)	BP1	2	1.43E-11	3.92E-09	8.0000	800.00	1.79E-12	0.37
	(n,γ)	^{238}U	1	2.22E-11	3.92E-09	0.0085	0.85	2.62E-09	0.57

Chapter 9

Conclusion

The research presented in this paper had the objectives of

1. implementing a generalized nuclide field solver in the reactor physics code NESTLE, capable of handling an arbitrary field of nuclei and an arbitrary number of user-defined transmutation paths describing the change of one nuclide to another,

2. implementing sensitivity analysis methods in NESTLE capable of predicting changes in EOC nuclide inventory due to perturbations in input data (nuclear data and initial nuclide concentrations),

3. and providing a sample of EOC nuclide inventory analysis using the tool we developed.

Addressing the first goal, we designed and implemented a generalized nuclide field solver capable of handling an arbitrary field of user-defined nuclei with an arbitrary number of user-defined transmutation paths. Each nuclide defined may have neutron capture cross section $\sigma_{(n,\gamma)}$, neutron production cross section $\sigma_{(n,2n)}$, neutron capture and nucleus excitation cross section $\sigma_{(n,*)}$, and fission cross section σ_f which NESTLE then uses in its nuclide and flux calculations. All decay paths, decay constants, and branch ratios are user input. For the resulting system of ODEs, we have developed two solvers capable of calculating time-dependent nuclide concentrations $\vec{\eta}(t)$: a 2^{nd} order Rosenbrock method and a matrix exponential method. The 2^{nd} order Rosenbrock method is a stiff ODE solver, and in practice, a field of nuclei will exhibit stiff behavior if the time constants associated

with different transmutation paths vary dramatically (e.g. One path has a time constant indicating a slow change, like 1E-05 s^{-1}, and another has a time constant indicating a fast change, like -2E-01 s^{-1}.) We have benchmarked our nuclide field solution methods against a small set of other methods and found the agreement to be very good.

Addressing the second goal, we developed and implemented a sensitivity analysis and uncertainty propagation method in North Carolina State University's reactor physics code, NESTLE. For this work, we read many references on perturbation theory, before proceeding with a physical adjoint formulation of the system of adjoint equations. In the end, we decided not to add a sparse linear system solver to NESTLE, believing a perturbation theory independent of the method of nuclide field ODE discretization was a nice feature, as despite any changes in the future to NESTLE's nuclide and neutron field solvers, the tool we have developed will still be applicable. The AS we developed through differential methods is the same as the "depletion perturbation theory" developed through variational methods presented in [6] for a predictor neutron/nuclide field coupling method. In this work we extended the AS formulation to include capability to analyze sensitivities when using the predictor-corrector neutron/nuclide field coupling method. As a result, NESTLE user now has the ability to use first order perturbation theory to evaluate response sensitivities $\vec{r}_\alpha$ when input data $\vec{\alpha}$ is perturbed. We envision typical uses of this tool may be

- propagating uncertainties in nuclide concentrations using the AS and input data covariance matrices and/or
- identifying the data parameters which influence a response the most using the AS, then use DPAR to check the results.

The AS is well-suited to targeting a specific response and efficiently determining all the parameters which impact that response. When exact changes in many responses with respect to few parameters are desired, then DPAR is probably the best way to proceed.

Addressing the third goal, we performed calculations on the EOC nuclide inventory for a cycle 1 PWR 2D core slice, and found some good news: at least for cycle 1 cores (and probably extended to the first cycle for fresh fuel) it appears that the cross sections for ^{235}U, ^{238}U, and ^{239}Pu are the dominant parameters which influence EOC inventory of most nuclei and spent nuclear fuel (SNF) hazard measures, the Hazard Index (HI) and the Total Cancer Dose (TCD).

The tools developed in this research and implemented in reactor physics code NESTLE, represent a significant upgrade in the research capabilities of the code, helping to support the need for better design and evaluation tools for reactor-based transmutation systems (as well as Generation IV reactor systems). However, NESTLE has received other significant upgrades in the course of the work, in the hope that the more accessible a code is, the better it can become. The upgrades NESTLE has received as a result of this research are summarized below.

1. Conversion of 90% of the NESTLE source code from fixed-form FORTRAN77 to free-form FORTRAN95. The reasons were

   1. free-form FORTRAN95 produces cleaner, more readable source code
   2. this is the FORTRAN known by most students—thus future students who work on the code do not need to experience the FORTRAN77 "learning curve", and
   3. many implicitly parallel intrinsic functions/subroutines exist in FORTRAN95—by using them, the parallel efficiency of NESTLE has been greatly increased.

2. To facilitate the general chains of nuclei and transmutation paths, a more versatile input scheme was needed. After searching and not finding an appropriate package to handle this, the `IO` module was created to handle input/output in a command-plus-arguments format. With `IO`

   1. data may be written and read as text for user input/output or debugging *or* binary for internal saving of data for use at a later time (in our case, as the forward system solutions are generated, they are written to binary files and later when the AS calculations are performed, forward system data is loaded as needed) and
   2. one may initiate restarts or initialization seamlessly.

3. To aid future development, the NESTLE code was restructured to

   1. remove the "container array" storage method for all arrays of problem-dependent size and instead use dynamically allocatable arrays contained in appropriately-named variable modules and

2. remove hard-coded dependence of the code on specific algorithms so now one can easily add another nuclide solver, flux solver, interpolation algorithm, etc. by just inserting a couple lines in the part of the code with the other procedures which perform the same operation.

Future work in the realm of sensitivity analysis and uncertainty propagation with NESTLE would be to incorporate additional responses into the code and develop methods to solve adjoint equations for thermal hydraulics (T/H) feedback and nodal expansion method (NEM) current correction terms. Also, the capability to determine end-of-life (EOL) versus end-of-cycle (EOC) isotopic concentrations, implying multi-cycle depletions, without the need to obtain EOC spatial isotopic concentration distributions, remains a challenge to be addressed.

Bibliography

[1] Argonne National Lab. *Benchmark Source Book ANL76.* 1976.

[2] Electric Power Research Center at North Carolina State University. *NESTLE Version 5.2.1: Few-Group Neutron Diffusion Equation Solver Utilizing The Nodal Expansion Method for Eigenvalue, Adjoint, Fixed-Source Steady-State and Transient Problems*, July 2003.

[3] H. H. Rosenbrock. Some general implicit processes for the numerical solution of differential equations. *Computer Journal*, 5:329–330, 1963. (in Russian).

[4] D. Y. Anistratov and V. Y. Gol'din. A two-stage difference scheme with complex coefficients for solving systems of the first order nonlinear ODE's. *Mathematical Modelling*, 4(2):45–50, 1992. (in Russian).

[5] Cleve Moler and Charles Van Loan. Nineteen dubious ways to compute the exponential of a matrix, twenty-five years later. *Society for Industrial and Applied Mathematics*, 45(1):3–49, 2003.

[6] M. L. Williams. Development of depletion perturbation theory for coupled neutron/nuclide fields. *Nuclear Science and Engineering*, 70:20–36, 1979.

[7] Richard Bellman. *Introduction to Matrix Analysis.* McGraw-Hill Book Company, Inc., 1960.

[8] Richard L. Burder and J. Douglas Faires. *Numerical Analysis.* Wadsworth Group, 7 edition, 2001.

[9] D. S. Gujev and P.D. Shirkov. Rosenbrock schemes with complex coefficients for stiff differential equations. *Preprint of National Center for Mathematical Modelling*, 47, 1991.

[10] K.F. Eckerman and J.C. Ryman. Federal guidance report no. 12. Technical report, U.S. Environmental Protection Agency, 1993.

[11] Weston M. Stacy. *Nuclear Reactor Physics*. John Wiley & Sons, Inc., 2001.

[12] D. G. Cacuci. *Sensitivity and Uncertainty Analysis Theory*, volume 1. CRC Press, 2000.

[13] James J. Duderstadt and Louis J. Hamilton. *Nuclear Reactor Analysis*. John Wiley & Sons, Inc., 1976.

[14] M[ark] L. Williams. *CRC Handbook of Nuclear Reactors Calculations*, volume III, section Perturbation Theory for Nuclear Reactor Analysis, pages 53–188. CRC Press, 1987.

[15] D. G. Cacuci, C. F. Weber, E. M. Oblow, and J. H. Marable. Sensitivity theory for general systems of nonlinear equations. *Nuclear Science and Engineering*, 75:88–110, 1980.

[16] G. Marchuk. *Adjoint equations and perturbation algorthms in nonlinear problems*. CRC Press, 1996.

[17] L. A. Belblidia, J. M. Kallfelz, and D. G. Cacuci. Generalized perturbation theory with derivative operators for power density investigations in nuclear reactors. *Nuclear Science and Engineering*, 84:206–225, 1983.

[18] James J. Duderstadt and William R. Martin. *Transport Theory*, chapter Variational Methods, pages 378–389. John Wiley & Sons, 1966.

[19] R. B. Sidje. EXPOKIT. A Software Package for Computing Matrix Exponentials. *ACM Trans. Math. Softw.*, 24(1):130–156.

[20] Argonne National Lab. *ANL Benchmark Sourcebook*.